EUROPEAN Journal of Medicine

Has been issued since 2013.
E-ISSN 2310-3434
2019. 7(2). Issued 2 times a year

Journal is indexed by: **CAS Source Index** (USA), **CiteFactor** (Canada), **CrossRef** (UK), **EBSCOhost Electronic Jornals Service** (USA), **Electronic scientific library** (Russia), **Open Academic Journals Index** (Russia), **ResearchBib** (Japan), **Sherpa Romeo** (Spain).

All manuscripts are peer reviewed by experts in the respective field. Authors of the manuscripts bear responsibility for their content, credibility and reliability.

Editorial board doesn't expect the manuscripts' authors to always agree with its opinion.

Postal Address: 1367/4, Stara Vajnorska str., Bratislava – Nove Mesto, Slovakia, 831 04

Website: http://ejournal5.com/
E-mail: aphr.sro@gmail.com

Founder and Editor: Academic Publishing House Researcher s.r.o.

Release date 16.12.19.
Format 21 × 29,7/4.

Headset Georgia.

Order № 20.

European Journal of Medicine

2019

Is. 2

C O N T E N T S

Articles

Published in the Slovak Republic
European Journal of Medicine
Has been issued since 2013.
E-ISSN: 2310-3434
2019, 7(2): 68-91

DOI: 10.13187/ejm.2019.2.68
www.ejournal5.com

Articles

Multi-Beam Interference Patterns of Living Sarcoma Cells may be Approximated by a Fractal Julia Set and Rieman Spheres or Fatou Components Decoded as a Siegel Discs

Alexander Bolkhovitinov [a], Viktor Krukowskikh [a], Serge Pankratov [a]

[a] INEPCP (2014, 2016), Moscow, Russian Federation

Abstract

It's well known, that the morphology of a carcinoma cells was studied many a time and oft (on repeated occasions) from the second part of the XX century. But mathematical approximations of such sarcoma cell structures are not very good on the grounds of non-regular semi-chaotic elements in morphogenesis and morphology of cancer cells. Many approximations in sarcoma oncology works are not applying for cell morphology as is, despite the fact of good morphological representation of sarcoma cells in different microscopic and specific-staining methods. Our work is a first work where the multi-beam interference patterns of living sarcoma cells are approximated by a fractal Julia set and Fatou components known as a Siegel discs.

Keywords: sarcoma, oncomorphology, interference microscopy, multi-beam interference, Fatou components, Siegel discs, Riman spheres, Julia set.

1. Introduction

1. Why the carcinoma cell is optimal object for analytical morphology?

It's well known, that the morphology of a carcinoma cells was studied many a time and oft (on repeated occasions) from the second part of the XX century. They were analyzed not only in static, but also in dynamic (kinetic) reaction conditions, which may be applied as potential therapeutic agents, including a respiration and morphology of sarcoma cells exposed to liquid nitrogen (Hodapp et al., 1952).

We can separate physical or physiotherapeutic and chemical or chemotherapeutic agents (Prince, 1962) of this reaction studies into multiple dimensions of multi-descriptor scores (or manifolds):

I. channelome-mediated agent pulls (Civitelli et al., 1992);

II. second messenger pulls (for example, cyclic adenosine monophosphate = 3',5'-cyclic adenosine monophosphate, which is equivalent to cAMP, cyclic AMP, in abbreviations) (Mitchell et al., 1978));

III. cytoskeleton-associated agent pulls (for example – ABP-assisted pulls [Actin-Binding Protein], in particular – vinculin* phosphorylation pulls (Kellie et al., 1986);

* By definitions: 1) vinculin is a membrane-cytoskeletal protein in focal adhesion plaques that is involved in linkage of integrin adhesion molecules to the actin cytoskeleton; 2) vinculin is a cytoskeletal protein associated with cell-cell and cell-matrix junctions, where it is thought to function as one of several interacting proteins involved in anchoring F-actin to the membrane; 3) vinculin is actin binding protein localized in focal

IV. dose dependent effect pulls (for some agents, such as sodium butyrate), including inhibition of proliferation pulls, differentiation induction and repression induction (repression of gene expression) pulls (Altenburg et al., 1976);

V. sarcoma growth factors and their derivatives or mimetics (Keski-Oja et al., 1980; Tokuyama and Tokuyama, 1989);

VI. pulls of clonal factors (Earle, 1975);

VII. mitotropic and nucleotropic agents (Seegers et al., 1992);

VIII. virological agent pulls (Smidová et al., 1968; Altenburg et al., 1976);

IX. pulls of oncogenic agents *sensu stricto* (Chaturvedi, 2013);

X. snake venom cytotoxin pulls (Pate et al., 1969).

But mathematical approximations of such sarcoma cell structures are not very good on the grounds of non-regular semi-chaotic elements in morphogenesis and morphology of cancer cells. Many approximations in sarcoma oncology works are not applying for cell morphology as is (Svoboda and Hasek, 1956), despite the fact of good morphological representation of sarcoma cells in different microscopic and specific-staining methods. In different years for sarcoma oncology studies many different microscopic and specific-staining methods was applied. Among them were noted:

A. electron microscopy (Gandzii, 1956; Yasuzumi et al., 1960; Luse, 1960; Driessens et al., 1964; Kubo et al., 1969; Courington and Vogt, 1967; Rice et al., 1973; Waldo, 1979; Kukuté and Smirnova, 1981; Choux et al., 1981; Kanaya et al., 1985; Husain and Nguyen, 1995; Marquart, 2006)

B. combined electron and light microscopy (Weinberger and Banfield, 1965; Fabrizio and Cottrell, 1972; Fj et al., 1975; Varela and Diazflores, 1977; Waldo et al., 1983; Akerman, 1988; Åkerman et al., 1988; Beziat et al, 1989);

C. comparative scanning electron microscopy and transmission electron microscopy (Llombart-Bosch and Peydro-Olaya, 1983)

D. mass determination of sarcoma virus virions by scanning transmission electron microscopy (Vogt and Simon, 1999);

E. cryo-electron microscopy (Briggs et al., 2006);

F. immunoelectron microscopy (Aoki et al., 1973; Houston, 1974; Hiraki et al., 1974; Kawauchi, 1995; Becker et al., 1991);

G. comparative electron microscopic and immunohistochemical studies (Mukai et al., 1983; Oord et al., 1986; Welch, et al., 1986; Nonomura et al., 1988; Nanomuna, 1988; Pettinato et al., 1989; Nishio et al., 2003);

H. comparative light-scattering spectroscopy and electron microscopy for determination of hydrodynamic radiuses of viruses in sarcoma cells (Salmeen et al., 1976;

I. electron microscopy of viruses in sarcoma cells (Nishimi et al., 1961; Hanaichi et al., 1975; Orenstein et al., 1997; Said et al., 1997);

J. electron microscopy of nucleic acids of sarcoma cells (Guntaka et al., 1976; Murti et al., 1981);

K. conventional or light microscopy (Siegler, 1970; Ackerman, 1979; Amazon and Rywlin, 1979; Tsokos et al., 1988);

L. correlation studies between microscopy data, magnetic resonance imaging data and positron emission tomography data [or two-photon emission tomography data, which are equivalents] (Plowman et al., 2016);

M. phase contrast microscopy (Ludford and Smiles, 1950; Kato and Makino, 1962; Veselý and Pluta, 1972);

N. florescence microscopy (Dorfman, 1962), including epiluminescent microscopy (Krischer et al., 1999);

O. ultraviolet microscopy (Roe and King, 1950; Zhudina and Shalumovich, 1969;

P. in vivo reflectance confocal microscopy (Grazziotin et al., 2010; Paganelli et al., 2018);

Q. structured illumination microscopy (Fu et al., 2016);

adhesions and cell-cell junctions; 4) vinculin is tyrosine phosphorylated in platelets spread on fibrinogen and that the phosphorylation is Src kinases dependent.

R. interference microsopy and quantitative cytology / cytopathology based on this technique, including multiple-beam interference microscopy and similar analytical protocols (Mellors et al., 1953).

2. Why interference microscopy is optimal micro-technique for analytical morphology?

Unfortunately, despite this fact (particularly, despite the quantitative character of multiple-beam interference microscopy, consequently, the quantitative character of interference cytometric and cytopathological data), as a general rule interference microscopy are not usable as a wild-field histological method for carcinoma cell morphology visualization, detection and quantification. It is not very good simplification of research protocols and microdiagnostic approaches, because the photometric methods for the measurement of the organic mass of cells, cell components (including sets of chromosomes) by multiple beam interference microscopy are not only possible, but also they are very effective (Melors, 1953, 1954)!

Multiple-beam interference microscopy was developed initially not only as a technique for material science and metallography (Faust, 1952), but from the third quarter of the XX century they was applied predominantly for metal structure analysis (Tolansky, 1970; Richardson, 1972) and (much later) for liquid crystal measurements, based on the phase retardation principles (Chernyaev et al., 2008). Multiple-beam interference microscopy was reborn in 2000th, when multiple beam interference confocal microscopy was designed and implemented in cell biology laboratories (Joshi and Medina, 2000; Joshi and Medina, 2000b), including biophysical departments, where some effects of an electric field on the motility of cells was examined by multiple-beam interference microscopy techniques (Joshi et al., 2001). Detection, dynamical imaging and kinetics of sub-micron organelles of specialized cells (for example – chondrocytes) were implemented by multiple beam interference microscopy in 2004 (Joshi et al., 2004). Diffential interference phase contrast microscopy using multiple beam shearing interferometry for bio-imaging was applied in 2006 (Roy et al., 2006). Capturing and sorting of multiple cells by polarization-controlled three-beam interference was realized in 2016 (Hou et al., 2016). But such methods were not applied for carcinoma cells.

3. What kind of interference microscopy is optimal for the target cells?

Everyone would very much like to eliminate this omission, because methods of interference microscopy and by interference phase microscopy of cancer cells were developed from 1960th (Sandritter et al., 1960; Hirst, 1961) and very good developed to date or by now (in frames of spatial light interference microscopy (Majeed et al., 2015, 2016), differential interference contrast microscopy assisted by nanoparticles (Sun et al., 2008, 2010), reflection interference contrast microscopy (Matsuzaki et al, 2016)). It is a very specialized branch of the general trend of interference microscopy of living cells, provided in different techniques, such as:

1) digital holographic interferention microscopy (Kizilova et al., 2010);
2) spatial light interference microscopy (Babacan et al., 2011; Popescu and Wang, 2012), including deconvolved spatial light interference microscopy for live cell imaging (Haldar et al., 2011);
3) interference reflection microscopy (Gingell and Todd, 1979; Verschueren, 1985), including quantitative reflection interference contrast microscopy or RICM (Schindl et al., 1995; Usson et al., 1997; Holt et al., 2008; Limozin and Sengupta, 2009);
4) fluorescence interference-contrast microscopy (Braun and Fromherz, 1997);
5) phase-shifting interference microscopy (Dunn and Zicha, 1993);
6) correlational mapping between interference-reflexion and indirect-immunofluorescence microscopy photoregistrograms (Wehland et al., 1979);
7) laser interference microscopy with volumetric and cytorefractometric measurements (Yusipovich et al., 2011) and coherent phase microscopy (Tychinsky and Tikhonov, 2010a; Tychinsky and Tikhonov, 2010b);
8) phase-modulation laser interference microscopy (Brazhe et al., 2008);
9) interference microscopy under double-wavelet analysis (Sosnovtseva et al., 2005);
10) dual-interference-channel quantitative-phase microscopy (Shaked et al., 2009);
11) scanning angle interference microscopy (Paszek et al., 2012);

12) Nomarski differential interference contrast microscopy (Geissinger and Bond, 1971; Geissinger and Duitschaever, 1971) and other (for example – Pluto DIC) differential interference contrast microscopy techniques (Falimirski et al., 2007);

13) total internal reflection aqueous fluorescence overcomes a basic ambiguity of interference reflection microscopy (Todd et al., 1988); etc.

4. Why multiple beam interference microscopy is informative source?

It's known, that the multiple beam interference may be used for discrete signal transmission with small noise levels (Bhardwaj et al., 2017; Hibino and Takatsuji, 2002). Multiple-beam interference effects in Fabry-Perot interferometer with small wedge between mirrors, deriving expressions for light beams path, were researched in 1970th not only in USA, but also in USSR (Koniukhov, 1971). Mechano-optical transductors / sensors based on multiple-beam interference were introduced for optical waveguide measurements in XXI century (El-Diastry, 2001), but their physical and technical principles were developed in XX century, where the Barakat group was started the project on the GRIN optical waveguides (Barakat et al., 1985, 1988, 2001), despite the fact, that the first Barakat works for multiple beam interference studies were published in 1960th (Barakat and Abouzakhm, 1985; Barakat et al., 1965). Earliest works on multiple beam interference fringes and their applications were published from 1940th to 1960th (Tolansky, 1945; Brossel, 1946; Tolansky and Barakat, 1950; Bruce, 1951; Glauert, 1951; Smith, F. D. 1952; Tolansky and Emara, 1955; Hargreaves, 1963; Burnett, 1965; Herriott, 1965, 1966; Fulinska, 1966). Some very beautiful works were published in 1970th (Roberge and Boivin, 1971; Koppelmann, 1972, 1974; Koppelmann and Vosskuhl, 1973) and 1980th (El-Dehemy et al., 1981; Baumbach et al, 1989). Fist articles by Tolansky were republished in 1990th – 2000th in "SPIE milestone series" (Tolansky, 1991, 2000). Many interesting applications for multiple beam interference fringes were provided in 1990th – 2000th (Shao-po, 1999; Tadmor et al., 2003; Abdelsalam et al., 2010; Hamza et al., 2010; El-Hennawi et al., 2012).

2. Relevance

Different types of cells may be measured and quantitative or semi-quantitative visualized by different methods of interference microscopy (Mellors, 1953; Barer and Joseph, 1957; Dunn, Zicha, 1994). Examples include:

- calculation of lignin concentration and porosity of cell-wall regions by interference microscopy (Boutelje, 1972; Donaldson, 1985);
- dry mass and cell area measurements (Goldacre et al., 1957; Lee at al., 1960);
- cell-substrate interactions in amoeboid locomotion (King et al., 1983);
- interaction between intracellular vacuoles and the cell surface (Gingell, 1982);
- growth cone interactions with cell and substrate adhesion molecules of cells (Drazba et al., 1997);
- visualization of red cell membranes (Miller and Dvorak, 1973);
- bacterial cell identification in DIC interference contrast microscopy in label-free conditions (Obara et al., 2013);
- radiation dose effect analysis (Lee and Richards, 1964);
- comparative analysis of epithelial cells (Pappelis et al., 1976);
- real time 3D and "4D" imaging of cells (Salmon et al., 1998; Li et al., 2007; Tsunoda et al., 2008), from yeast cells to cancer cels.

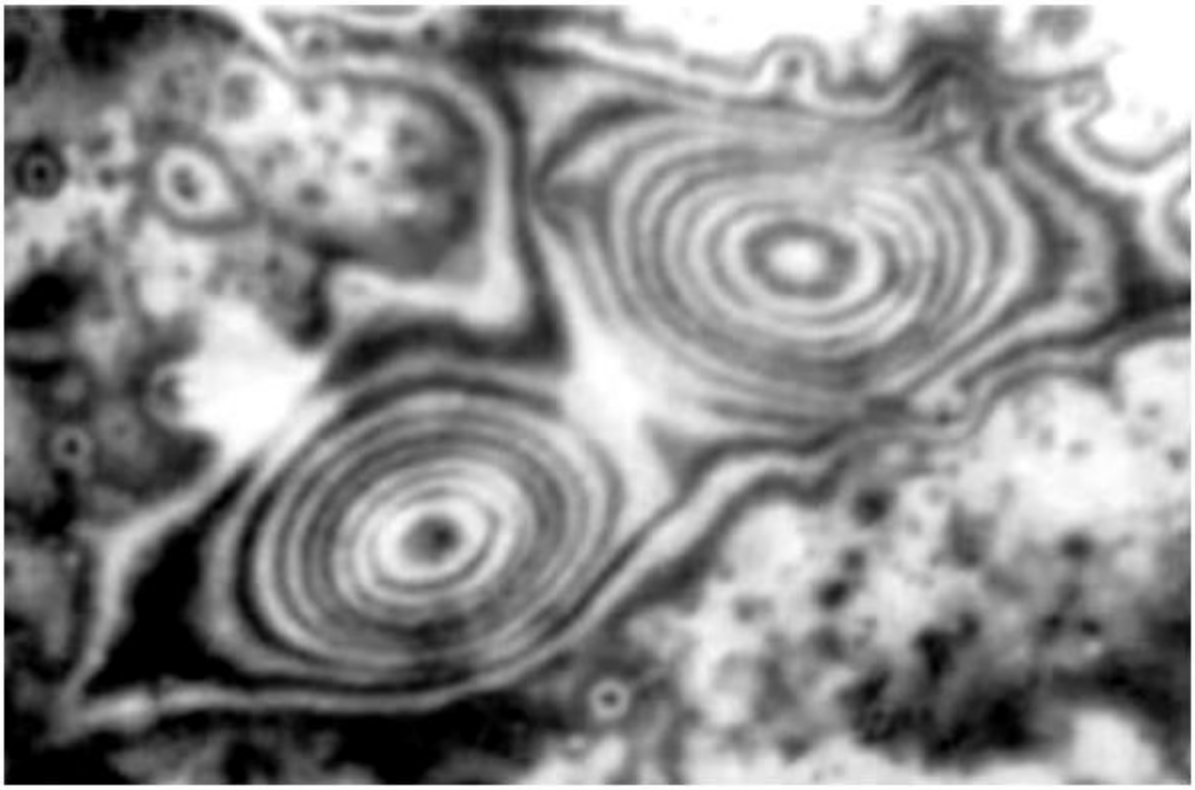

Fig. 1. Multiple beam interference image of living sarcoma cells in a tissue culture

3. Materials and methods

It has been known that biological membranes as thin films are characterized by multiple-beam interference and, consequently, can be directly detected using multiple-beam interference microscopy. Multiple beam interference microscopy patterns of membranous cellular structures with different surface tension levels are different from the standard optical images of these objects. This follows at once from physical considerations. Thin-film interference occurs when the incident light waves reflected by the upper and lower boundaries of the membrane cell film interfere with one another to form a new wave.

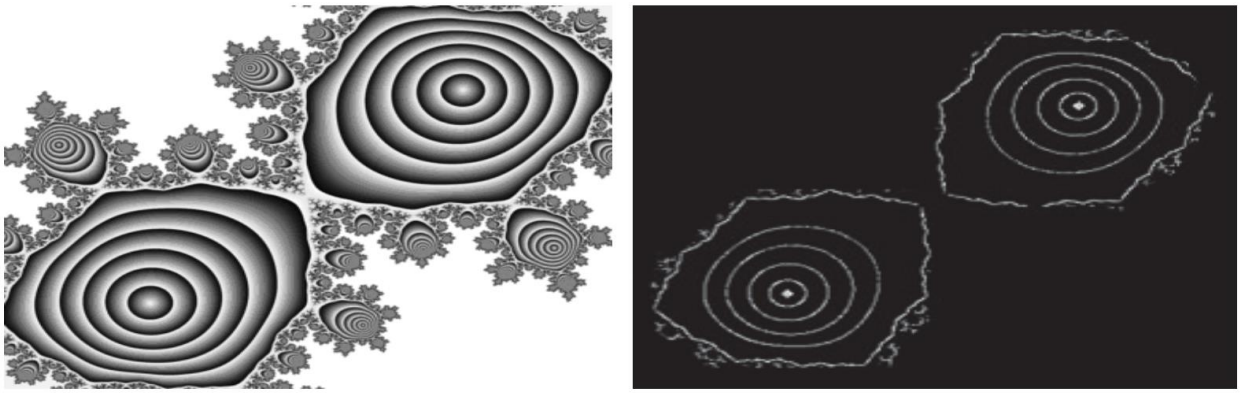

A B

Fig. 2. A fractal Julia set with a Siegel disc (A) and a filled Julia set for the golden mean rotation number with the the Siegel disc and some orbits inside (B)

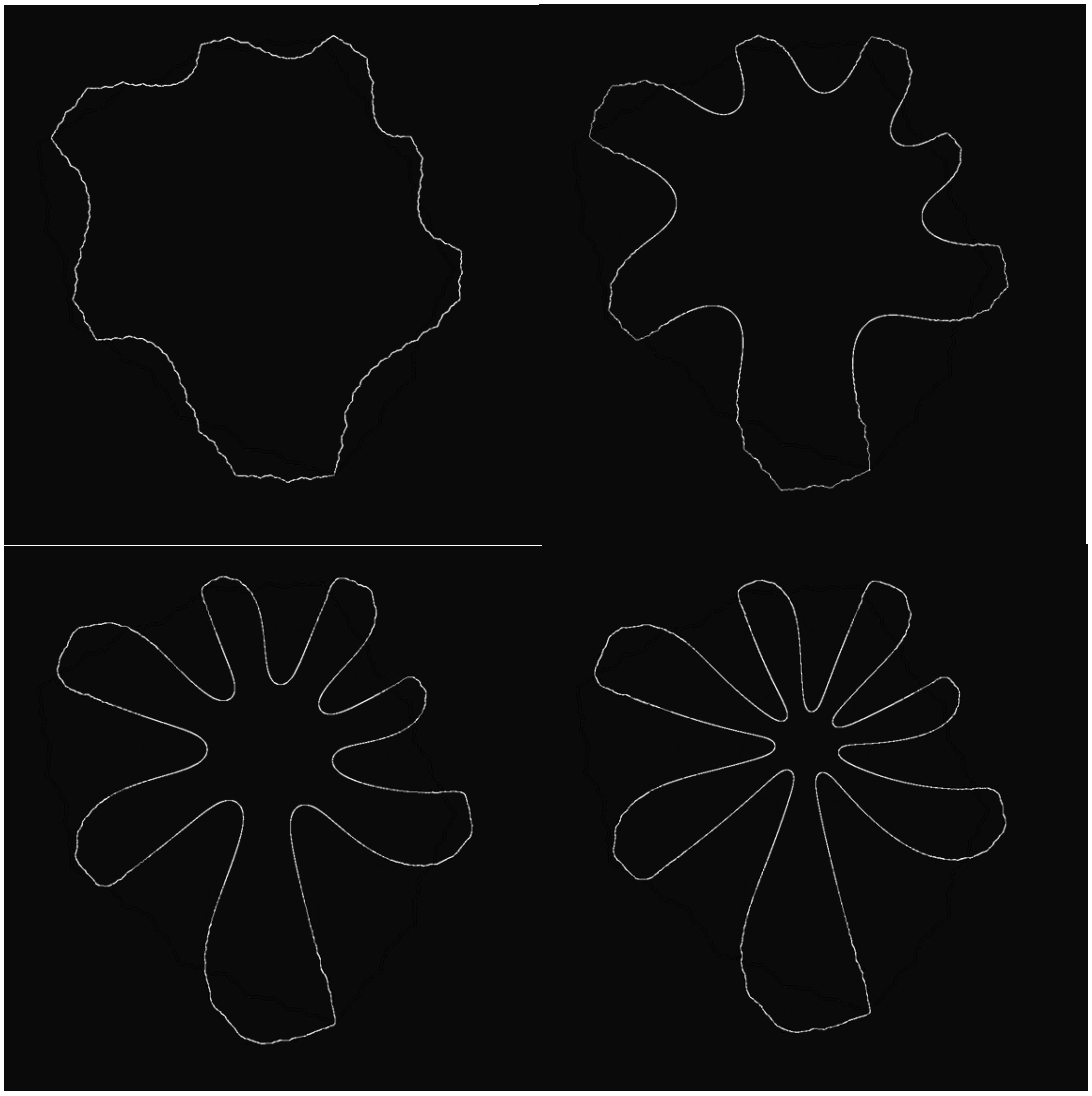

Fig. 3. Infolding Siegel disc near 2/7

4. Results

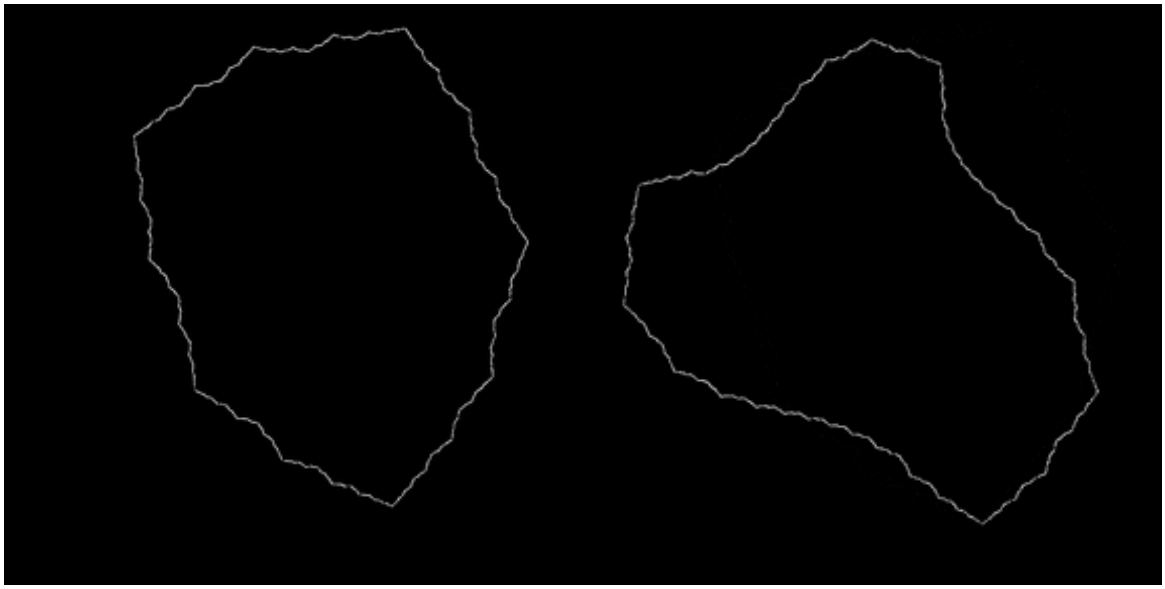

Fig. 4. Infolding Siegel disc near 1/3. One can see virtual Siegel disc

This is sketched in Fig. 1 representing a multiple beam interference image of living sarcoma cells in a tissue culture in air (magnification: 1.000). Optically identical regions are presented as light and dark elliptical zones which together form a topographic map of the cell. The cell thickness, shape and intramembranous volume can be easily calculated from the interference pattern.

In accordance with the modern standards the above method may seem to provide insufficient resolution and low information. However, there are still no mathematical approximations of intermembrane interference patterns, different from the ones derivable from the first physical principles. We propose here to apply Julia sets and Fatou components, such as Herman ring and Siegel disc for approximating carcinoma cells. The definition of Siegel disc is provided in the Table 1. Fig. 2 (compare with Fig. 1) shows an example of such an approach application, representing the early iterations of a fractal Julia set with a Siegel disc and an "isosurface-like" ("equipotential line – like") visualization of this filled Julia set for the golden mean rotation number with the Siegel disc and some orbits inside. It can be seen that Fig. 2 satisfactory simulates the morphology from Fig. 1. Thus, there is an appropriate approximation for this morphology due to the membranous properties of the cell represented here formally using Fatou components. A similar visualization can be obtained using the Herman ring, but this is beyond the scope of this report for the lack of space. The morphology of cells with filopodia also may6 be approximated by Siegel disc formalism, including dynamic representation (see Fig. 3 – “Infolding Siegel disc near 2/7” and Fig. 4 – “Infolding Siegel disc near 1/3”).

Table 1. Definition of Siegel disc

Definition of Siegel disks

Setting

$0 \in U$ open subset of $\mathbb{C}$
$f : U \to \mathbb{C}$ holomorphic

f defines a dynamical system: $z_{n+1} = f(z_n)$

$f(0) = 0$ (the origin is a fixed point)
the multiplier $f'(0)$ has modulus one: $f'(0) = e^{2i\pi\theta}$
the multiplier is aperiodic: $\theta \notin \mathbb{Q}$

This is called an
irrationally indifferent fixed point of a complex one dimensional holomorphic dynamical system.

What would it mean to behave like a rotation? That near 0,

- f is analytically conjugated to $R_\theta : z \mapsto e^{2i\pi\theta}z$? (meaning $\exists\phi$ analytic bijection defined near 0 mapping 0 to 0 and $\phi \circ f \circ \phi^{-1} = R_\theta$)
- f is topologically conjugated to R_θ? (now ϕ is only required to be a homeomorphism)
- the orbits stay bounded? (Lyapunov stability)

It turns out that all three are equivalent. We say that f is *linearizable*.

The quantity θ is unique and is called the *rotation number*.

https://www.math.univ-toulouse.fr/~cheritat/Exposes/Rome.pdf

5. Supplements: Possible program codes from the open access I-net sources

The Julia set is the set of complex numbers z that do not diverge under the following iteration:

z=z2+cz=z2+c

Where c is a constant complex number.

Different values of z reach infinity at different rates. A colourful fractal is produced by colouring the complex plane based on the number of iterations required to reach infinity.

```
function colour = julia(c, total_iterations, image_size, limits)
% Calculates julia set by iterating z = z^2 + c, where z and c are complex,
% and recording when z reaches infinity.
%
% Inputs:
%
% c                 Fixed complex number, of form a + bi
% total_iterations  Number of iterations of z = z^2 + c
% image_size        2D vector with number of complex coordinates in
```

```
%                    x and y directions
%   limits           Vector with 4 elements: min x, max x, min y, max y
%
%   Outputs:
%
%   colour           Matrix of doubles, with size equal to image_size.
%                    Plotting this matrix will produce a julia set


im_step = (limits(4) - limits(3)) / (image_size(2) - 1);
re_step = (limits(2) - limits(1)) / (image_size(1) - 1);

reals = limits(1) : re_step : limits(2);          % Real numbers
imags = limits(3) : im_step : limits(4);          % Imaginary numbers
z = bsxfun(@plus, reals(:), (imags(:) * 1i)');     % Complex coordinates
colour = inf(size(z));                            % Colour of Julia set

for iteration = 1:total_iterations
   index = isinf(z);
   % Only perform calculation on the z values that are less than infinity
   z(~index) = z(~index).^2 + c;
   % Colour depends on number of iterations to reach infinity
   colour(index & isinf(colour)) = iteration;
end

colour = colour'; % Transpose so that plot will have reals on the x axis

end
```

https://codereview.stackexchange.com/questions/145752/function-for-plotting-julia-set

```
function Julia(c,k,v)

% JULIA(C,K,V) draws the Julia set with the following parameters:
% c is a complex number used in the map f(z) = z² + c.
% k gives the number of iterations
% v determines the number of points on the x-axis.

% JULIA uses c = 0.2+0.65i, k = 14, v = 500.

% This file was generated by students as a partial fulfillment
% for the requirements of the course "Fractals", Winter term
% 2004/2005, Stuttgart University.

% Author : Sylvia Frey
% Date   : Nov 2004
% Version: 1.1

% default settings
if nargin < 3
   c = 0.2+0.65i;
   k = 14;
   v = 500;
end

% radius of the circle beyond which every point diverges
r = max(abs(c),2);
```

```
% divide the x-axis
d = linspace(-r,r,v);

% create the matrix A containing complex numbers
A = ones(v,1)*d+i*(ones(v,1)*d)';

% create the point matrix
B = zeros(v,v);

% iteration
for s = 1:k
   B = B+(abs(A)<=r);
   % the map
   A = A.*A+ones(v,v).*c;
end;

% plot settings
imagesc(B);
colormap(jet);

hold off;
axis equal;
axis off;
```

http://m2matlabdb.ma.tum.de/download.jsp?MC_ID=5&SC_ID=13&MP_ID=283

Julia(c,k,v) draws the Julia set with the following parameters:
c is a complex number used in the map f(z) = z^2 + c.
k gives the number of iterations.
v determines the number of points on the x-axis.

Julia uses c = 0.2+0.65i, k = 14, v = 500.

This file was generated by students as a partial fulfillment
for the requirements of the course "Fractals",
Winter term 2004/2005, Stuttgart University.

Visualize Julia Sets using Matlab

```
function myjulia(Zmax,c,N)
% Generate and visualize quadratic Julia Sets
% More information about Julia Sets can be found here:
% http://en.wikipedia.org/wiki/Julia_set
% this code is for the assignment of the "Introduction to Matlab" offered
by MITOPENCOURSEWARE
% Coded by http://scriptdemo.blogspot.com

if (nargin==1)
  Ndemo=Zmax; clear Zmax
  switch Ndemo
  case {1}
     myjulia(1,-0.297491+i*0.641051,100);
     return;
  case {2}
     myjulia(0.35,-0.297491+i*0.641051,250);
     return;
  otherwise
    disp('Not defined demo type!')
    help myjulia;
    return
  end
```

```
elseif (nargin~=3)
  help myjulia;
  return
end

% generate the basic matrix
NM=500;
[Z,tmpy]=meshgrid(linspace(-Zmax,Zmax,NM),zeros(1,NM));
Z=Z+i*Z'; clear tmpy

% compute the escape velocity
myM=reshape(escapeVelocity(Z(:),c,N),NM,NM);

% visualize the results
imagesc(atan(0.1*myM)); figurenicer;axis xy;

function n=escapeVelocity(z0,c,N)
n=z0*0;
NLen=length(z0);
IndZ=1:length(z0);
IndZ=IndZ';
for ni=1:N
    IndLT=find(abs(z0)<2);
    IndGE=find(abs(z0)>=2);
    n(IndZ(IndGE))=ni;
    if (length(IndLT)>0)
      z0(IndLT)=z0(IndLT).*z0(IndLT)+c;
    end
    z0(IndGE)=[];
    IndZ(IndGE)=[];
end
if ~isempty(IndZ)
  n(IndZ)=N;
end
```

Basin of attraction to infinity = exterior of filled-in Julia set and The Divergence Scheme = Escape Time Method (ETM)

First read definitions

Here one computes *forward iterations* of a complex point Z_o:

Here is function which computes the *last iteration*, that is the first iteration that lands in the target set (for example leaves a circle around the origin with a given *escape radius* ER) for the iteration of the complex quadratic polynomial above. It is a iteration (integer) for which (abs(Z)>ER). It can also be improved [2]

C version (here ER2=ER*ER) using double floating point numbers (without complex type numbers):

```
int GiveLastIteration(double Zx, double Zy, double Cx, double Cy, int IterationMax, int ER2)
{
 double Zx2, Zy2; /* Zx2=Zx*Zx;  Zy2=Zy*Zy  */
 int i=0;
 Zx2=Zx*Zx;
 Zy2=Zy*Zy;
 while (i<IterationMax && (Zx2+Zy2<ER2) ) /* ER2=ER*ER */
 {
```

```
  Zy=2*Zx*Zy + Cy;
  Zx=Zx2-Zy2 +Cx;
  Zx2=Zx*Zx;
  Zy2=Zy*Zy;
  i+=1;
 }
 return i;
}
```

C with complex type from GSL :[3]

```
#include <gsl/gsl_complex.h>
#include <gsl/gsl_complex_math.h>
#include <stdio.h>
// gcc -L/usr/lib -lgsl -lgslcblas -lm t.c
// function fc(z) = z*z+c

gsl_complex f(gsl_complex z, gsl_complex c) {
  return gsl_complex_add(c, gsl_complex_mul(z,z));
}

int main () {
  gsl_complex c = gsl_complex_rect(0.123, 0.125);
  gsl_complex z = gsl_complex_rect(0.0, 0.0);
  int i;
  for (i = 0; i < 10; i++) {
    z = f(z, c);
    double zx = GSL_REAL(z);
    double zy = GSL_IMAG(z);
    printf("Real: %f4 Imag: %f4\n", zx, zy);
  }
  return 0;
}
```

C++ versions:

```
 int GiveLastIteration(complex C,complex Z , int imax, int ER)
  {
   int i; // iteration number
   for(i=0;i<=imax-1;i++) // forward iteration
    {
     Z=Z*Z+C; // overloading of operators
     if(abs(Z)>ER) break;
    }
   return i;
 }
#include <complex> // C++ complex library

// bailout2 = bailout * bailout
// this function is based on function esctime from mndlbrot.cpp
// from program mandel ver. 5.3 by Wolf Jung
// http://www.mndynamics.com/indexp.html

int escape_time(complex<double> Z, complex<double> C , int iter_max,  double bailout2)
{
```

```
  // z= x+ y*i   z0=0
  long double x =Z.real(), y =Z.imag(),  u ,  v ;
  int iter; // iteration
  for ( iter = 0; iter <= iter_max-1; iter++)
  { u = x*x;
    v = y*y;
    if ( u + v <= bailout2 )
      {
        y = 2 * x * y + C.imag();
        x = u - v + C.real();
      } // if
    else break;
  } // for
  return iter;
} // escape_time
```

[4]

Delphi version (using user defined complex type, cabs and f functions)

```
function GiveLastIteration(z,c:Complex;ER:real;iMax:integer):integer;
  var i:integer;
  begin
  i:=0;
  while (cabs(z)<ER) and (i<iMax) do
    begin
      z:= f(z,c);
      inc(i);
    end;
  result := i;
end;
```

where :

```
type complex = record x, y: real; end;

function cabs(z:complex):real;
begin
  cabs:=sqrt(z.x*z.x+z.y*z.y)
end;

function f(z,c:complex):complex; // complex quadratic polynomial
  var tmp:complex;
begin
  tmp.x := (z.x*z.x) - (z.y*z.y) + c.x;
  tmp.y := 2*z.x*z.y + c.y ;
  result := tmp;

end;
```

Delphi version without explicit definition of complex numbers :

```
function GiveLastIteration(zx0,zy0,cx,cy,ER2:extended;iMax:integer):integer;
  // iteration of z=zx+zy*i under fc(z)=z*z+c
  // where c=cx+cy*i
  // until abs(z)<ER  ( ER2=ER*ER )  or i>=iMax
```

```
  var i:integer;
     zx,zy,
     zx2,zy2:extended;
  begin
  zx:=zx0;
  zy:=zy0;
  zx2:=zx*zx;
  zy2:=zy*zy;

  i:=0;
  while (zx2+zy2<ER2) and (i<iMax) do
   begin
     zy:=2*zx*zy + cy;
     zx:=zx2-zy2 +cx;
     zx2:=zx*zx;
     zy2:=zy*zy;
     //
     inc(i);
   end;
  result := i;
end;
```

Euler version by R. Grothmann (with small change : from z^2-c to z^2+c) [5]

```
function iter (z,c,n=100) ...

h=z;
loop 1 to n;
h=h^2 + c;
if totalmax(abs(h))>1e20; m=#; break; endif;
end;
return {h,m};
endfunction
```

Lisp version
This version uses complex numbers. It makes the code short but is also inefficien.

```
((DEFUN GIVELASTITERATION (Z_0 _C IMAX ESCAPE_RADIUS)
  (SETQ Z Z_0)
  (SETQ I 0)
  (LOOP WHILE (AND (< I IMAX) (< (ABS Z) ESCAPE_RADIUS)) DO
    (INCF I)
    (SETQ Z (+ (* Z Z) _C)))
   I)
```

Maxima version :

```
/* easy to read but very slow version, uses complex type numbers */
GiveLastIteration(z,c):=
 block([i:0],
  while abs(z)<ER and i<iMax
     do (z:z*z + c,i:i+1),
  i)$
/* faster version, without use of complex type numbers,
   compare with c version, ER2=ER*ER */
```

```
GiveLastIter(zx,zy,cx,cy,ER2,iMax):=
block(
 [i:0,zx2,zy2],
 zx2:zx*zx,
 zy2:zy*zy,
 while (zx2+zy2<ER2) and i<iMax do
 (
  zy:2*zx*zy + cy,
  zx:zx2-zy2 +cx,
  zx2:zx*zx,
  zy2:zy*zy,
  i:i+1
 ),
 return(i)
);
```

Boolean Escape time [edit]

Algorithm: for every point z of dynamical plane (z-plane) compute iteration number (last iteration) for which magnitude of z is greater than escape radius. If last_iteration=max_iteration then point is in filled-in Julia set, else it is in its complement (attractive basin of infinity). Here one has 2 options, so it is named boolean algorithm.

```
if (LastIteration==IterationMax)
   then color=BLACK;   /* bounded orbits = Filled-in Julia set */
   else color=WHITE;  /* unbounded orbits = exterior of Filled-in Julia set  */
```

In theory this method is for drawing Filled-in Julia set and its complement (exterior), but when c is Misiurewicz point (Filled-in Julia set has no interior) this method draws nothing. For example for c=i . It means that it is good for drawing interior of Filled-in Julia set.

ASCII graphic*[edit]*

```
; common lisp
(loop for y from -2 to 2 by 0.05 do
    (loop for x from -2 to 2 by 0.025 do
                (let* ((z (complex x y))
                (c (complex -1 0))
                (iMax 20)
                        (i 0))

                (loop       while (< i iMax ) do
                            (setq z (+ (* z z) c))
                            (incf i)
                            (when (> (abs z) 2) (return i)))


        (if (= i iMax) (princ (code-char 42)) (princ (code-char 32)))))
    (format t "~%"))
```

Source: https://en.wikibooks.org/wiki/Fractals/Iterations_in_the_complex_plane/Julia_set

References

Abdelsalam et al., 2010 – *Abdelsalam, D.G., Shaalan, M.S., Eloker, M.M.* (2010). Surface microtopography measurement of a standard flat surface by multiple-beam interference fringes at reflection. *Optics and Lasers in Engineering*, 48(5): 543-547.

Ackerman, 1979 – *Ackerman, A.B.* (1979). Subtle clues to diagnosis by conventional microscopy: The patch stage of Kaposi's sarcoma. *The American Journal of Dermatopathology*, 1(2): 165-172.

Åkerman et al., 1988 – *Åkerman, M., Alvegård, T., Eliasson, J., Garwicz, S., Mandahl, N., Rydholm, A., Willén, H.* (1988). A case of Ewing's sarcoma diagnosed by fine needle aspiration: Light microscopy, electron microscopy and chromosomal analysis. *Acta Orthopaedica Scandinavica*, 59(5): 589-592.

Altenburg et al., 1976 – *Altenburg, B.C., Via, D.P., Steiner, S.H.* (1976). Modification of the phenotype of murine sarcoma virus-transformed cells by sodium butyrate: effects on morphology and cytoskeletal elements. *Experimental cell research*, 102(2): 223-231.

Amazon, Rywlin, 1979 – *Amazon, K., Rywlin, A.M.* (1979). Subtle clues to diagnosis by conventional microscopy: Lymph node involvement in Kaposi's sarcoma. *The American Journal of Dermatopathology*, 1(2): 173-176.

Aoki et al., 1973 – *Aoki, T., Stephenson, J.R., Aaronson, S.A.* (1973). Demonstration of a cell-surface antigen associated with murine sarcoma virus by immunoelectron microscopy. *Proceedings of the National Academy of Sciences*, 70(3): 742-746.

Babacan et al., 2011 – *Babacan, S.D., Wang, Z., Do, M., Popescu, G.* (2011). Cell imaging beyond the diffraction limit using sparse deconvolution spatial light interference microscopy. *Biomedical optics express*, 2(7): 1815-1827.

Barakat, Abouzakhm, 1965 – *Barakat, N., Abouzakhm, F.G. (*1965). Phase modulation of the first beam in reflected multiple beam interference fringes. *Optica Acta: International Journal of Optics*, 12(4): 321-332.

Barakat et al., 1965 – *Barakat, N., Farghaly, A.S., Abd-El-Azim, A.* (1965). Studies on multiple beam interference fringes formed on high order planes of localization: intensity distribution and the fringe shift between successive planes of localization. *Optica Acta: International Journal of Optics*, 12(2): 205-212.

Barakat et al., 1985 – *Barakat, N., Hamza, A.A., Goneid, A.S.* (1985). Multiple-beam interference fringes applied to GRIN optical waveguides to determine fiber characteristics. *Applied optics*, *24*(24), 4383-4386.

Barakat et al., 1988 – Barakat, N., El-Hennawi, H. A., & El-Diasti, F. (1988). Multiple-beam interference fringes applied to GRIN optical waveguides to examine fiber formation. *Applied optics*, 27(24): 5090-5094.

Barakat et al., 2001 – *Barakat, N., El-Hennawi, H.A., El-Ghafar, E. A., El-Ghandoor, H., Hassan, R., El-Diasty, F.* (2001). Three-dimensional refractive index profile of a GRIN optical waveguide using multiple beam interference fringes. *Optics communications*, 191(1-2): 39-47.

Barer, Joseph, 1957 – *Barer, R., Joseph, S.* (1957). Phase-contrast and interference microscopy in the study of cell structure. *Symp. Soc. exp. Biol.*, 10: 160-184.

Baumbach et al., 1989 – *Baumbach, P., Rassow, B., Wesemann, W.* (1989). Absolute ocular fundus dimensions measured by multiple-beam interference fringes. *Investigative ophthalmology & visual science*, 30(11): 2314-2319.

Becker et al., 1991 – *Becker, J., Schuppan, D., Rabanus, J. P., Gelderblom, H. R., Reichart, P.* (1991). Immunoelectron microscopy shows an atypical pattern and a quantitative shift of collagens type I, III and VI in oral Kaposi's sarcoma of AIDS. *Virchows Archiv A*, 419(3): 237-244.

Beziat et al., 1989 – *Beziat, J.L., Tabone, E., Bailly, C., Gerard, J.P.* (1989). Osteogenic sarcoma of the tongue: case report with light and electron microscopy studies and review of the literature. *Journal of Oral and Maxillofacial Surgery*, 47(5): 524-528.

Bhardwaj et al., 2017 – *Bhardwaj, R., Saxena, S.B., Sharma, P., Jaiswal, V.K., Mehrotra, R.* (2017). Experimental realisation of parallel optical logic gates and combinational logic using multiple beam interference. *Optik – International Journal for Light and Electron Optics*, 128: 253-263.

Boutelje, 1972 – *Boutelje, B.* (1972). Calculation of lignin concentration and porosity of cell-wall regions by interference microscopy. *Svensk Papperstidning-Nordisk Cellulosa*, 75(16): 683.

Braun, Fromherz, 1997 – *Braun, D., Fromherz, P.* (1997). Fluorescence interference-contrast microscopy of cell adhesion on oxidized silicon. *Applied Physics A: Materials Science & Processing*, 65(4): 341-348.

Brazhe et al., 2008 – *Brazhe, A.R., Brazhe, N.A., Maksimov, G.V., Ignatyev, P.S., Rubin, A.B., Mosekilde, E., Sosnovtseva, O.V.* (2008). Phase-modulation laser interference microscopy: an advance in cell imaging and dynamics study. *Journal of biomedical optics*, 13(3): 034004.

Briggs et al., 2006 – *Briggs, J.A., Johnson, M.C., Simon, M.N., Fuller, S.D., Vogt, V.M.* (2006). Cryo-electron microscopy reveals conserved and divergent features of gag packing in immature particles of Rous sarcoma virus and human immunodeficiency virus. *Journal of molecular biology*, 355(1): 157-168.

Brossel, 1946 – *Brossel, J.* (1946). Asymmetrical Broadening with Multiple-Beam Interference Fringes. *Nature*, 157(3993): 623.

Bruce, 1951 – *Bruce, C.F.* (1951). Transmission-like Multiple-Beam Reflexion Interference Fringes. *Nature*, 167(4245): 398.

Burnett, 1965 – *Burnett, C.* (1965). Instructional use of multiple-beam located interference fringes. *American Journal of Physics*, 33(1): 67.

Chaturvedi, 2013 – *Chaturvedi, A.* (2013). Molecular dissection of the mechanism utilized by the EWS/FLI oncogene to influence the morphology and behavior of Ewing sarcoma cells (Doctoral dissertation, The University of Utah).

Chernyaev et al., 2008 – *Chernyaev, I., Suvorova, A., Podgornov, F., Haase, W.* (2008). Influence of the multiple beam interference on phase retardation of liquid crystal cells. *Molecular Crystals and Liquid Crystals*, 488(1): 219-230.

Choux et al., 1981 – *Choux, R., Pluot, M., Faugere, M. C., Rodriguez, M., Hassoun, J., Caulet, T.* (1981). Clear cell sarcoma of the tendons and aponeuroses. A study of 2 cases using electron microscopy. *La semaine des hopitaux: organe fonde par l'Association d'enseignement medical des hopitaux de Paris*, 57(9-10): 479-482.

Civitelli et al., 1992 – *Civitelli, R., Fujimori, A., Bernier, S.M., Warlow, P.M., Goltzman, D., Hruska, K.A., Avioli, L.V.* (1992). Heterogeneous intracellular free calcium responses to parathyroid hormone correlate with morphology and receptor distribution in osteogenic sarcoma cells. *Endocrinology*, 130(4): 2392-2400.

Courington and Vogt, 1967 – *Courington, D., Vogt, P.K.* (1967). Electron microscopy of chick fibroblasts infected by defective Rous sarcoma virus and its helper. *Journal of virology*, *1*(2): 400-414.

Donaldson, 1985 – *Donaldson, L.A.* (1985). Critical assessment of interference microscopy as a technique for measuring lignin distribution in cell walls. *NZJ For. Sci*, 15: 349-360.

Dorfman, 1962 – *Dorfman, R.F.* (1962). Enzyme histochemistry and fluorescence microscopy of Kaposi's sarcoma, malignant hemangioendothelioma, and postmastectomy lymphangiosarcoma. *S. Afr. med. J*, 36: 989-990.

Drazba et al., 1997 – *Drazba, J., Liljelund, P., Smith, C., Payne, R., Lemmon, V.* (1997). Growth cone interactions with purified cell and substrate adhesion molecules visualized by interference reflection microscopy. *Developmental brain research*, 100(2): 183-197.

Driessens et al., 1964 – *Driessens, J., Dupont, A., Demaille, A., Puvion, E.* (1964). Cytological study by electron microscopy of the rat jensen sarcoma. *Comptes rendus des seances de la Societe de biologie et de ses filiales*, 158: 559.

Dunn, Zicha, 1993 – *Dunn, G.A., Zicha, D.* (1993). Phase-shifting interference microscopy applied to the analysis of cell behaviour. *Symposia of the Society for Experimental Biology*, 47: 91-106.

Dunn, Zicha, 1994 – *Dunn, G.A., Zicha, D.* (1994). Using interference microscopy to study cell behaviour. *Handbook of Cell Biology*, 25-33.

Earle, 1975 – *Earle, W.R.* (1975). The Development of Variations in Transplantability and Morphology Within a Clone of Mouse Fibroblasts Transformed to Sarcoma-Producing Cells In *Vitro1. Readings in Mammalian Cell Culture*: 185.

El-Dehemy et al., 1981 – *El-Dehemy, K.A., El-Nicklawy, M.M., Hassan, A.F., Nasr, E.A.* (1981). Studies on the visibility and intensity distribution of multiple-beam interference fringes. *Acta Physica Polonica: A*, 60: 389.

El-Diastry, 2001 – *El-Diasty, F.* (2001). Theory and measurement of Young's modulus radial profiles of bent single-mode optical fibers with the multiple-beam interference technique. *JOSA A*, 18(5): 1171-1175.

El-Hennawi et al., 2012 – *El-Hennawi, H.A., El-Diasty, F., El-Ghandoor, H., Soliman, M.A.* (2012). Multiple-beam interference fringes applied to investigate the index profile of the optical fiber dip. *Optical and Quantum Electronics*, 43(1-5): 35-48.

Fabrizio, Cottrell, 1972 – *Fabrizio, A., Cottrell, J.* (1972, January). Light and electron-microscopy studies of fabrizio hamster reticulum-cell sarcoma. *American Journal of Patholog,* 66(3): A98.

Falimirski et al., 2007 – *Falimirski, M., Syed, A., Prybilla, D.* (2007). Immunocompetence of the severely injured spleen verified by differential interference contrast microscopy: the red blood cell pit test. *Journal of Trauma and Acute Care Surgery*, 63(5): 1087-1092.

Faust, 1952 – *Faust, R.C.* (1952). Multiple-beam interference microscopy. *Proc. R. Soc. Lond. A*, 211(1105): 240-254.

Fj et al., 1975 – *Fj, P.M., Cañadell, J.M., Herranz, P., Imizcoz, J.L., Vázquez, J.J.* (1975). Chordoid sarcoma of the femur. Electronic and optical microscopy study of a case. *Revista de medicina de la Universidad de Navarra*, 19(1): 133-141.

Fu et al., 2016 – *Fu, H.L., Mueller, J.L., Whitley, M.., Cardona, D.M., Willett, R.M., Kirsch, D.G., Brown J.Q., Ramanujam, N.* (2016). Structured illumination microscopy and a quantitative image analysis for the detection of positive margins in a pre-clinical genetically engineered mouse model of sarcoma. *PloS one*, 11(1): e0147006.

Fulinska, 1966 – *Fulinska, K.F.* (1966). Effect of the Asymmetry of the Interference Layer on the Contrast of Fizeau Fringes Produced by Multiple-Beam Interference in Reflected Light. *Optics and Spectroscopy*, 20: 495.

Gandzii, 1956 – *Gandzii, G.* (1956). Electron microscopy of cells from tissue cultures of chicken sarcoma. *Voprosy onkologii*, 2(2): 205-211.

Geissinger, Bond, 1971 – *Geissinger, H.D., Bond, E.F.* (1971). Nomarski differential interference contrast microscopy and scanning electron microscopy of tissue sections and fibroblast cell culture monolayers. *Mikroskopie*, 27(1): 32.

Geissinger, Duitschaever, 1971 – *Geissinger, H.D., Duitschaever, C.L.* (1971). Nomarski differential-interference contrast microscopy in transillumination : Its use on unstained or stained sections, smears, and wet mounts, or on fluorochromed sections and cell-culture monolayers. *Journal of Microscopy*, 94(2): 107-124.

Gingell, Todd, 1979 – *Gingell, D., Todd, I.* (1979). Interference reflection microscopy. A quantitative theory for image interpretation and its application to cell-substratum separation measurement. *Biophysical Journal*, 26(3): 507-526.

Gingell, 1982 – *Gingell, D, Todd, I., Owens, N.* (1982). Interaction between intracellular vacuoles and the cell surface analysed by finite aperture theory interference reflection microscopy. *Journal of cell science*, 54(1): 287-298.

Glauert, 1951 – *Glauert, A.M.* (1951). Superposition Effects in Multiple-Beam Interference Fringes. *Nature*, 168: 861-862.

Goldacre et al., 1957 – *Goldacre, R.J., Easty, D.M., Ambrose, E.J.* (1957). A cell compressor for the measurement of mass and concentration by interference microscopy. *Nature*, 180(4600): 1487.

Grazziotin et al., 2010 – *Grazziotin, T.C., Cota, C., Buffon, R.B., Pinto, L.A., Latini, A., Ardigò, M.* (2010). Preliminary evaluation of in vivo reflectance confocal microscopy features of Kaposi's sarcoma. *Dermatology*, *220*(4), 346-354.

Guntaka et al., 1976 – *Guntaka, R.V., Richards, O.C., Shank, P.R., Kung, H.J., Davidson, N., Pritsch, E., Bishop M.J., Varmus, H.E.* (1976). Covalently closed circular DNA of avian sarcoma virus: purification from nuclei of infected quail tumor cells and measurement by electron microscopy and gel electrophoresis. *Journal of molecular biology*, 106(2): 337-357.

Haldar et al., 2011 – *Haldar, J.P., Wang, Z., Popescu, G., Liang, Z.P.* (2011). Deconvolved spatial light interference microscopy for live cell imaging. *Ieee Transactions on Biomedical Engineering*, 58(9): 2489-2497.

Hamza et al., 2010 – *Hamza, A.A., Sokkar, T.Z.N., El-Farahaty, K.A., Raslan, M.I.* (2010). Reconstruction of refractive indices distribution in 3D using a single pattern of multiple-beam interference fringes for online investigation of necking phenomenon. *Polymer Testing*, *29*(8): 1031-1040.

Hanaichi et al., 1975 – *Hanaichi, T., Kanotanaka, K., Tanaka, T.* (1975). Properties of a rat-adapted murine sarcoma-virus (moloney)-size determination by electron-microscopy. *Journal of Electron Microscopy*, 24(3): 204-204.

Hargreaves, 1963 – *Hargreaves, C.M.D.* (1963). Multiple-beam 'Transmission-like'Fizeau Fringes in the Reflexion Interference System. *Nature*, 197(4870): 890.

Herriott, 1965 – *Herriott, D.R.* (1965). Multiple-beam interference fringes at large plate spacing. *Journal of the Optical Society of America,* 55(5): 614.

Herriott, 1966 – *Herriott, D.R.* (1966). Long-path multiple-wavelength multiple-beam interference fringes. *Journal of the Optical Society of America,* 56(6): 719-721.

Hibino, Takatsuji, 2002 – *Hibino, K., Takatsuji, T.* (2002). Suppression of multiple-beam interference noise in testing an optical-parallel plate by wavelength-scanning interferometry. *Optical review*, 9(2): 60-65.

Hiraki et al., 1974 – *Hiraki, S., Chan, J.C., Hales, R.L., Dmochowski, L.* (1974). An immunoelectron microscopy study of Soehner-Dmochowski murine sarcoma virus following passage in rats and hamsters. *Cancer research*, 34(11): 2906-2910.

Hirst, 1961 – *Hirst, D.V.* (1961). Office examination of fresh cancer cells by interference phase microscopy. *American Journal of Obstetrics & Gynecology*, 81(1): 138-139.

Hodapp et al., 1952 – *Hodapp, E.L., Wade, N.J., Menz, L.J.* (1952). Survival, respiration and morphology of sarcoma-37 cells exposed to liquid nitrogen. *Proceedings of the Society for Experimental Biology and Medicine*, 81(2): 468-474.

Holt et al., 2008 – *Holt, M.R., Calle, Y., Sutton, D.H., Critchley, D.R., Jones, G.E., Dunn, G.A.* (2008). Quantifying cell–matrix adhesion dynamics in living cells using interference reflection microscopy. *Journal of microscopy*, *232*(1): 73-81.

Hou et al., 2016 – *Hou, Y., Wang, Z., Hu, Y., Li, D., Qiu, R.* (2016). Capture and sorting of multiple cells by polarization-controlled three-beam interference. *Journal of Optics*, 18(3): 035401.

Houston, 1974 – *Houston, T.* (1974). An Immunoelectron Microscopy Study of Soehner-Dmochowski Murine Sarcoma Virus following Passage in Rats and Hamsters'. *Cancer Research*, 34(2906â): 2910.

Husain, Nguyen, 1995 – *Husain, M., Nguyen, G.K.* (1995). Alveolar soft part sarcoma. Report of a case diagnosed by needle aspiration cytology and electron microscopy. *Acta cytologica*, 39(5): 951-954.

Joshi, Medina, 2000a – *Joshi, N.V., Medina, H.* (2000). Multiple beam interference confocal microscopy: tool for morphological investigation of a living spermatozoon. *Microscopy and Microanalysis*, 6(5): 471-477.

Joshi, Medina, 2000b – *Joshi, N.V., Medina, H.* (2000, May). Multiple beam interference confocal microscopy: a tool for morphological investigation of living cells and tissues. *Three-Dimensional and Multidimensional Microscopy: Image Acquisition Processing VII,* 3919: 86-92. International Society for Optics and Photonics.

Joshi et al., 2001 – *Joshi, N.V., Medina, H., Tucci, P.* (2001). Effect of an electric field on the motility of Entamoeba histolytica examined by multiple-beam interference microscopy. *Experimental parasitology*, 97(4): 179-185.

Joshi et al., 2004 – *Joshi N.V., Medina H., Barboza J.M., Colantuoni G., Quintero M.* (2004). Detection, imaging, and kinetics of sub-micron organelles of chondrocytes by multiple beam interference microscopy. *Three-Dimensional and Multidimensional Microscopy: Image Acquisition and Processing XI.* – International Society for Optics and Photonics, 5324: 145-151.

Kanaya et al., 1985 – *Kanaya, K., Baba, N., Kitagawa, Y., Mukai, M.* (1985). The digital structural analysis of human alveolar soft part sarcoma obtained by electron microscopy. *Micron and microscopica acta*, 16(1): 17-32.

Kato, Makino, 1962 – *Kato, H., Makino, S.* (1962, January). Phase microscopy study on effects of temperature and chemicals upon locomotion of tumor cells of MTK-sarcoma III of a rat. *Japanese Journal of Genetics,* 37(5): 393.

Kawauchi, 1995 – *Kawauchi, S.* (1995). The Utility of Immunoelectron Microscopy in Diagnosis of Small Round Cell Sarcoma of Soft Tissue. *Journal of Japanese Orthopaedic Association*, 69: S1001-S1001.

Kellie et al., 1986 – *Kellie, S., Patel, B., Mitchell, A., Critchley, D.R., Wigglesworth, N.M., Wyke, J.A.* (1986). Comparison of the relative importance of tyrosine-specific vinculin

phosphorylation and the loss of surface-associated fibronectin in the morphology of cells transformed by Rous sarcoma virus. *Journal of cell science*, 82(1): 129-142.

Keski-Oja et al., 1980 – *Keski-Oja, J., De Larco, J.E., Rapp, U.R., Todaro, G.J.* (1980). Murine sarcoma growth factors affect the growth and morphology of cultured mouse epithelial cells. *Journal of cellular physiology*, 104(1): 41-46.

King et al., 1983 – *King, C.A., Preston, T.M., Miller, R.H.* (1983). Cell-substrate interactions in amoeboid locomotion — A matched reflexion interference and transmission electron microscopy study. *Cell biology international reports*, 7(8): 641-649.

Kizilova et al., 2010 – *Kizilova, N.N., Tishko, T.V., Tishko, D.V.* (2010). Analysis of erythrocyte shape using digital holographic interferention microscopy. *3rd Eurasian Congress on Medical Physics and Engineering 'Medical Physics*, pp. 260-262.

Koniukhov, 1971 – *Koniukhov, V.* (1971). [Theory of a Fabry-Perot interferometer with a small wedge between the mirrors]. *Zhurnal Prikladnoi Spektroskopii*, 14: 212-215.

Koppelmann, Vosskuhl, 1973 – *Koppelmann, G., Vosskuhl, W.* (1973). Intensity distributions in multiple-beam fizeau interference fringes. 2. Experiments for normal incidence. *Optik*, 37(2): 164-174.

Koppelmann, 1972 – *Koppelmann, G.* (1972). Intensity distribution in multiple-beam fizeau interference fringes. 1. *Optik*, 36(4): 474.

Koppelmann, 1974 – *Koppelmann, G.* (1974). Intensity distributions in multiple-beam fizeau interference fringes. 3. Similarity relations for non-normal incidence. *Optik*, 40(1): 89-100.

Krischer et al., 1999 – *Krischer, J., Braun, R. P., Toutous-Trellu, L., Saurat, J. H., Pechere, M.* (1999). Kaposi's sarcoma: a new approach of lesional follow-up using epiluminescent light microscopy. *Dermatology (Basel, Switzerland)*, 198(4): 420-422.

Kubo et al., 1969 – *Kubo, T.* (1969). Clear cell sarcoma of patellar tendon studied by electron microscopy. *Cancer*, 24(5): 948-953.

Kukuté, Smirnova, 1981 – *Kukuté, B.G., Smirnova, E.A.* (1981). Electron microscopy in the differential diagnosis of uterine sarcoma. *Arkh. Pat.*, 43(7): 23-28.

Lee and Richards, 1964 – *Lee, H., Richards, V.* (1964). Relationship between radiation dose and giant cells in the surviving cell population of mouse marrow as determined by interference microscopy. *Nature*, 204(4959): 656.

Lee at al., 1960 – *Lee, H., Richards, V., Klausner, C.* (1960). Dry mass and cell area changes in Ehrlich mouse ascites carcinoma cells after complement-fixation reaction measured by interference microscopy. *Cancer research*, 20(10): 1415-1421.

Li et al., 2007 – *Li, H.W., McCloskey, M., He, Y., Yeung, E.S.* (2007). Real-time dynamics of label-free single mast cell granules revealed by differential interference contrast microscopy. *Analytical and bioanalytical chemistry*, 387(1): 63-69.

Limozin, Sengupta, 2009 – *Limozin, L., Sengupta, K.* (2009). Quantitative reflection interference contrast microscopy (RICM) in soft matter and cell adhesion. *ChemPhysChem*, 10(16): 2752-2768.

Llombart-Bosch, Peydro-Olaya, 1983 – *Llombart-Bosch, A., Peydro-Olaya, A.* (1983). Scanning and transmission electron microscopy of Ewing's sarcoma of bone (typical and atypical variants). *Virchows Archiv A*, 398(3): 329-346.

Ludford, Smiles, 1950 – *Ludford, R.J., Smiles, J.* (1950). Cytological characteristics of fibroblasts and sarcoma cells demonstrable by phase-contrast microscopy. *Journal of Microscopy*, 70(2): 186-193.

Luse, 1960 – *Luse, S.A.* (1960). A synovial sarcoma studied by electron microscopy. *Cancer*, *13*(2): 312-322.

Majeed et al., 2015 – *Majeed, H., Kandel, M. E., Han, K., Luo, Z., Macias, V., Tangella, K.V., Balla A., Popescu, G.* (2015). Breast cancer diagnosis using spatial light interference microscopy. *Journal of biomedical optics*, 20(11): 111210.

Majeed et al., 2016 – *Majeed, H., Nguyen, T., Macias, V., Tangella, K., Kajdacsy-Balla, A., Do, M., Popescu, G.* (2016). Towards Automated Histopathology of Breast Cancer Using Spatial Light Interference Microscopy (SLIM). *Laboratory Investigation*, 96: 55A-56A.

Marquart, 2006 – *Marquart, K.H.* (2006). Electron microscopy reveals fungal cells within tumor tissue from two African patients with AIDS-associated Kaposi sarcoma. *Ultrastructural pathology*, 30(3): 187-192.

Matsuzaki et al, 2016 – *Matsuzaki, T., Ito, K., Masuda, K., Kakinuma, E., Sakamoto, R., Iketaki, K., Tanii, T.* (2016). Quantitative evaluation of cancer cell adhesion to self-assembled monolayer-patterned substrates by reflection interference contrast microscopy. *The Journal of Physical Chemistry B*, 120(7): 1221-1227.

Mellors et al., 1953 – *Mellors R.C., Kupfer A., Hollender A.* (1953). Quantitative cytology and cytopathology. Measurement of the thickness, the volume, the hydrous mass, and the anhydrous mass of living cells by interference microscopy. *Cancer*. 1953 Mar; 6(2): 372-84.

Mellors, 1953 – *Mellors, R.C.* (1953). The quantitative analysis of the cell by interference and ultraviolet microscopy. *Texas reports on biology and medicine*, 11(4): 693-708.

Melors, 1953 – *Mellors, R.C.* (1953). Multiple beam interference microscopy and quantitative cytology. *Journal of the Optical Society of America*, 43(4): 326-326.

Melors, 1954 – *Mellors, R.C.* (1954). Photographic methods for the measurement of the organic mass of cells and cell components (including sets of chromosomes) by multiple beam interference microscopy. *Journal of Histochemistry & Cytochemistry*, 2(6): 482-483.

Miller, Dvorak, 1973 – *Miller, L.H., Dvorak, J.A.* (1973). Visualization of red cell membranes of lysed malaria-infected cells by differential interference microscopy. *Journal of Parasitology*, 59(1): 202-3.

Mitchell et al., 1978 – *Mitchell, W., Schuffman, S., Korinek, J., Moses, H.* (1978). Effect of cyclic-AMP on growth properties and surface morphology of XC sarcoma-cells in vitro. Preprint.

Mukai et al., 1983 – *Mukai, M., Iri, H., Nakajima, T., Hirose, S., Torikata, C., Kageyama, K., Ueno, N., Murakami, K.* (1983). Alveolar soft-part sarcoma. A review on its histogenesis and further studies based on electron microscopy, immunohistochemistry, and biochemistry. *The American journal of surgical pathology*, 7(7): 679-689.

Murti et al., 1981 – *Murti, K.G., Bondurant, M., Tereba, A.L.L.A.N.* (1981). Secondary structural features in the 70S RNAs of Moloney murine leukemia and Rous sarcoma viruses as observed by electron microscopy. *Journal of virology*, 37(1): 411-419.

Nanomuna, 1988 – *Nanomuna, A.* (1988). Primary artery sarcoma. Report of two cases and studied by immunohistochemistry and electric microscopy and a review of 110 cases in the literature. *Acta Pathol Jpn*, 38: 883-896.

Nishimi et al., 1961 – *Nishiumi, Y., Okano, H., Imai, T.* (1961). Inoculation of chicken sarcoma virus into chicken thymus. An electron microscopy. *Proceedings of the Society for Experimental Biology and Medicine*, 107(1): 88-90.

Nishio et al., 2003 – *Nishio, J., Iwasaki, H., Sakashita, N., Haraoka, S., Isayama, T., Naito, M., ..., Kikuchi, M.* (2003). Undifferentiated (embryonal) sarcoma of the liver in middle-aged adults: smooth muscle differentiation determined by immunohistochemistry and electron microscopy. *Human pathology*, 34(3): 246-252.

Nonomura et al., 1988 – *Nonomura, A., Kurumaya, H., Kono, N., Nakanuma, Y., Ohta, G., Terahata, S., ... , Nishino, T.* (1988). Primary pulmonary artery sarcoma. Report of two autopsy cases studied by immunohistochemistry and electron microscopy, and review of 110 cases reported in the literature. *Pathology International*, 38(7): 883-896.

Obara et al., 2013 – *Obara, B., Roberts, M.A., Armitage, J.P., Grau, V.* (2013). Bacterial cell identification in differential interference contrast microscopy images. *BMC bioinformatics*, 14(1): 134.

Oord et al., 1986 – *Oord, J., Wolf-Peeters, C., Vos, R., Thomas, J., Desmet, V.J.* (1986). Sarcoma arising from interdigitating reticulum cells: report of a case, studied with light and electron microscopy, and enzyme-and immunohistochemistry. *Histopathology*, 10(5): 509-523.

Orenstein et al., 1997 – *Orenstein, J.M., Alkan, S., Blauvelt, A., Jeang, K.T., Weinstein, M.D., Ganem, D., Herndier, B.* (1997). Visualization of human herpesvirus type 8 in Kaposi's sarcoma by light and transmission electron microscopy. *AIDS*, 11(5): F35-F45.

Paganelli et al., 2018 – *Paganelli, A., Bassoli, S., Roncati, L., Bigi, L., Ciardo, S., Pellacani, G.* (2018). Pseudo-Kaposi sarcoma: report of a case investigated by dermoscopy, reflectance confocal microscopy and optical coherence tomography. *Journal of the European Academy of Dermatology and Venereology*.

Pappelis et al., 1976 – *Pappelis, C.K., Slobin, J., Detwiler, H.D., Pappelis, A.J., Pappelis, G.A.* (1976). Comparison of buccal and nasal epithelial cells using a new cell development index and quantitative interference microscopy. *Acta cytologica*, 20(4): 372-374.

Paszek et al., 2012 – *Paszek, M.J., DuFort, C.C., Rubashkin, M.G., Davidson, M.W., Thorn, K.S., Liphardt, J.T., Weaver, V.M.* (2012). Scanning angle interference microscopy reveals cell dynamics at the nanoscale. *Nature methods*, 9(8): 825.

Pate et al., 1969 – *Patel, T.N., Braganca, B.M., Bellare, R.A.* (1969). Changes produced by cobra venom cytotoxin on the morphology of Yoshida sarcoma cells. *Experimental cell research*, 57(2-3): 289-297.

Pettinato et al., 1989 – *Pettinato, G., De, A. C., Insabato, L., Ferbo, U., Di, A. B., Marino, G.M.* (1989). Reactive glioma in intracranial sarcoma ('sarcoglioma'). Histology, electron microscopy and immunohistochemistry of two additional cases. *Applied pathology*, 7(3): 192-200.

Plowman et al., 2016 – *Plowman, R.S., Cassell, I., Ritland, F., Bonatus, T., Jorgensen, S.A., Towbin, A.J., Towbin, R.* (2016). Indolent synovial sarcoma in adolescent male: MR, PET, microscopy, and arthroscopy correlation. Applied Radiology – The Journal of Practical Medical Imaging and Management. [Electronic resource]. URL: https://appliedradiology.com/articles/indolent-synovial-sarcoma-in-adolescent-male-mr-pet-microscopy-and-arthroscopy-correlation

Popescu and Wang, 2012 – *Popescu, Gabriel, Zhuo Wang* (2012). Spatial light interference microscopy and fourier transform light scattering for cell and tissue characterization. U.S. Patent No. 8,184,298. 22 May 2012.

Prince, 1962 – *Prince, A.M.* (1962). Factors influencing the determination of cellular morphology in cells infected with Rous sarcoma virus. *Virology*, 18(4): 524-534.

Rice et al., 1973 – *Rice, R.W., Cabot, A., Johnston, A.D.* (1973). The application of electron microscopy to the diagnostic differentiation of Ewing's sarcoma and reticulum cell sarcoma of bone. *Clinical orthopaedics and related research*, 91: 174-185.

Richardson, 1972 – *Richardson, J.H.* (1972). Multiple-beam interference microscopy of metals by S. Tolansky. *Journal of Applied Crystallography*, 5(6): 442-442.

Roberge, Boivin, 1971 – *Roberge, R., Boivin, A.* (1971). Multiple-beam interference fringes formed by a spherical thin shell. *Journal of the Optical Society of America*, 61(11): 1561.

Roe, King, 1950 – *Roe, E.M.F., King, R.G.* (1950). Ultra-Violet Microscopy of Tumour and Virus of Rouse Fowl Sarcoma. *Phot. J.*, 90: 94.

Roy et al., 2006 – *Roy, M., Matsuda, K., Grover, C., Baldock, C.* (2006). Diffential Interference Phase Contrast Microscopy Using Multiple Beam Shearing Interferometry for Bio-imaging. *Australasian Physical & Engineering Sciences in Medicine*, 29(1): 157.

Said et al., 1997 – *Said, J.W., Chien, K., Tasaka, T., Koeffler, H. P.* (1997). Ultrastructural characterization of human herpesvirus 8 (Kaposi's sarcoma-associated herpesvirus) in Kaposi's sarcoma lesions: electron microscopy permits distinction from cytomegalovirus (CMV). *The Journal of Pathology: A Journal of the Pathological Society of Great Britain and Ireland*, 182(3): 273-281.

Salmeen et al., 1976 – *Salmeen, I.R.V.I.N.G., Rimai, L.A.J.O.S., Luftig, R.B., Libes, L., Retzel, E.R.N.E.S.T., Rich, M., McCormick, J.J.* (1976). Hydrodynamic diameters of murine mammary, Rous sarcoma, and feline leukemia RNA tumor viruses: studies by laser beat frequency light-scattering spectroscopy and electron microscopy. *Journal of virology*, 17(2): 584-596.

Salmon et al., 1998 – *Salmon, E.D., Yeh, E., Shaw, S., Skibbens, B., Bloom, K.* (1998). High-resolution video and digital-enhanced differential interference contrast light microscopy of cell division in budding yeast. *Methods in enzymology*, 298: 317-331.

Sandritter et al., 1960 – *Sandritter, W., Schiemer, H., Alt, W.* (1960). Interference microscopy in cytology and cancer research. *Klinische Wochenschrift*, 38: 590-595.

Schindl et al., 1995 – *Schindl, M., Wallraff, E., Deubzer, B., Witke, W., Gerisch, G., Sackmann, E.* (1995). Cell-substrate interactions and locomotion of Dictyostelium wild-type and mutants defective in three cytoskeletal proteins: a study using quantitative reflection interference contrast microscopy. *Biophysical Journal*, 68(3): 1177-1190.

Seegers et al., 1992 – *Seegers, J.C., Els, H.J.* (1992). Effects of gamma-linolenic acid on mitosis and nuclear morphology in osteogenic sarcoma cells. South African medical journal = Suid-Afrikaanse tydskrif vir geneeskunde, 81(9): 467-472.

Shaked et al., 2009 – *Shaked, N.T., Rinehart, M.T., Wax, A.* (2009). Dual-interference-channel quantitative-phase microscopy of live cell dynamics. *Optics letters*, 34(6): 767-769.

Shao-po, 1999 – *Shao-po, Z.* (1999). Experiment of multiple-beam equal inclination interference fringes. *Optical Technique*, (5): 82-90.

Siegler, 1970 – *Siegler, R.* (1970). Pathogenesis of virus-induced murine sarcoma. I. Light microscopy. *Journal of the National Cancer Institute*, 45(1): 135-147.

Smidová et al., 1968 – *Smidová, V., Ujházy, V., Matoska, J., Smida, J.* (1968). In vitro passages of hamster tumour cells induced with Schmidt-Ruppin strain of Rous sarcoma viruse: their oncogenicity, morphology and karyology. *Neoplasma*, 15(6): 597-605.

Smith, 1952 – *Smith, F.D.* (1952). Bright multiple beam interference fringes in reflection. *Journal of the Optical Society of America*, 42(11): 877-877.

Sosnovtseva et al., 2005 – *Sosnovtseva O.V., Pavlov A.N., Brazhe N.A., Brazhe A.R., Erokhova L.A., Maksimov G.V., Mosekilde E.* (2005). Interference microscopy under double-wavelet analysis: a new approach to studying cell dynamics. *Physical review letters*, 94(21): 218103.

Sun et al., 2008 – *Sun, W., Fang, N., Trewyn, B. G., Tsunoda, M., Slowing, I. I., Lin, V. S., Yeung, E. S.* (2008). Endocytosis of a single mesoporous silica nanoparticle into a human lung cancer cell observed by differential interference contrast microscopy. *Analytical and Bioanalytical Chemistry*, 391(6): 2119.

Sun et al., 2010 – *Sun, W., Fang, N., Trewyn, B. G., Tsunoda, M., Slowing, I. I., Lin, V. S., Yeung, E.S.* (2010). Endocytosis of single mesoporous silica nanoparticle into living human lung cancer cell (a549) observed by differential interference contrast microscopy. *Developing new optical imaging techniques for single particle and molecule tracking in live cells*, 38.

Svoboda, Hasek, 1956 – *Svoboda J., Hasek M.* (1956). Influencing the transplantability of the virus of Rous sarcoma by immunological approximation in turkeys. *Folia biol., Praha*, *2*: 256-284.

Tadmor et al., 2003 – *Tadmor, R., Chen, N., Israelachvili, J.N.* (2003). Thickness and refractive index measurements using multiple beam interference fringes (FECO). *Journal of colloid and interface science*, 264(2): 548-553.

Todd et al., 1988 – *Todd, I., Mellor, J. S., Gingell, D.* (1988). Mapping cell-glass contacts of Dictyostelium amoebae by total internal reflection aqueous fluorescence overcomes a basic ambiguity of interference reflection microscopy. *Journal of cell science*, 89(1): 107-114.

Tokuyama, Tokuyama, 1989 – *Tokuyama, H., Tokuyama, Y.* (1989). Bovine colostric transforming growth factor-β-like peptide that induces growth inhibition and changes in morphology of human osteogenic sarcoma cells (MG-63). *Cell Biology International Reports*, 13(3): 251-258.

Tolansky, Barakat, 1950 – *Tolansky, S., Barakat, N.* (1950). New Localized Multiple-Beam Interference Fringes formed with Curved Thin Sheets. *Proceedings of the Physical Society. Section B*, 63(8): 545.

Tolansky, Emara, 1955 – *Tolansky, S., Emara, S.H.* (1955). Precision multiple-beam interference fringes with high lateral microscopic resolution. *JOSA*, 45(10): 792-795.

Tolansky, 1945 – *Tolansky, S.* (1945). XXXI New contributions to interferometry. Part V. New multiple beam white light interference fringes and their applications. *The London, Edinburgh, and Dublin Philosophical Magazine and Journal of Science*, 36(255): 225-236.

Tolansky, 1970 – *Tolansky, S.* (1970). Multiple-beam interference microscopy of metals. Academic Press Inc. Ltd. Berkele, 147 p.

Tolansky, 1991 – *Tolansky, S.* (1991). New contributions to interferometry. V, New multiple beam white light interference fringes and their applications. *SPIE milestone series*, 28: 163-175.

Tolansky, 2000 – *Tolansky, S.* (2000). New Multiple Beam White Light Interference Fringes and their Applications. *SPIE milestone series*, 163: 246-255.

Tsokos et al., 1988 – *Tsokos, M., Miser, J., Horowitz, M., Kinsella, T., Balis, F., Triche, T.* (1988). Primitive round cell-sarcoma of bone-a group of tumors resembling ewings-sarcoma by light-microscopy, but with distinctive ultrastructural appearance. *Laboratory Investigation*, 58(1): A96.

Tsunoda et al., 2008 – *Tsunoda, M., Isailovic, D., Yeung, E.S.* (2008). Real-time three-dimensional imaging of cell division by differential interference contrast microscopy. *Journal of Microscopy*, 232(2): 207-211.

Tychinsky, Tikhonov, 2010 – *Tychinsky, V.P., Tikhonov, A.N.* (2010). Interference microscopy in cell biophysics. 1. Principles and methodological aspects of coherent phase microscopy. *Cell biochemistry and biophysics*, 58(3): 107-116.

Tychinsky, Tikhonov, 2010b – *Tychinsky, V.P., Tikhonov, A.N.* (2010). Interference microscopy in cell biophysics. 2. Visualization of individual cells and energy-transducing organelles. *Cell biochemistry and biophysics*, 58(3): 117-128.

Usson et al., 1997 – *Usson, Y., Guignandon, A., Laroche, N., Lafage-Proust, M. H., Vico, L.* (1997). Quantitation of cell-matrix adhesion using confocal image analysis of focal contact associated proteins and interference reflection microscopy. *Cytometry*, 28(4): 298-304.

Varela, Diazflores, 1977 – *Varela, J., Diazflores, L.* (1977). Epithelioid sarcoma-light and electron-microscopy observations. *Morfologia Normal y Patologica Seccion B – Anatomia Patologica*, 1(1): 117-121.

Verschueren, 1985 – *Verschueren, H.* (1985). Interference reflection microscopy in cell biology: methodology and applications. *Journal of Cell Science*, 75(1): 279-301.

Veselý, Pluta, 1972 – *Veselý, P., Pluta, M.* (1972). Indication of the surface location of refractive motile spots wreathing the central area of some tissue culture cells (rat Rous sarcoma cells, stereoscopic phase contrast microscopy). *Folia biologica*, 18(5): 374-375.

Vogt, Simon, 1999 – *Vogt, V.M., Simon, M.N.* (1999). Mass determination of Rous sarcoma virus virions by scanning transmission electron microscopy. *Journal of virology*, 73(8): 7050-7055.

Waldo et al., 1983 – *Waldo, E., Sidhu, G. S., Stahl, R., Zolla-Pazner, S.* (1983). Histiocytoid hemangioma with features of angiolymphoid hyperplasia and Kaposi's sarcoma. A study by light microscopy, electron microscopy, and immunologic techniques. *The American journal of dermatopathology*, 5(6): 525-538.

Waldo, 1979 – *Waldo, E.* (1979). Subtle clues to diagnosis by electron microscopy: Kaposi's sarcoma. *The American Journal of Dermatopathology*, 1(2): 177-182.

Wehland et al., 1979 – *Wehland, J., Osborn, M., Weber, K.* (1979). Cell-to-substratum contacts in living cells: a direct correlation between interference-reflexion and indirect-immuno-fluorescence microscopy using antibodies against actin and alpha-actinin. *Journal of cell science*, 37(1): 257-273.

Weinberger, Banfield, 1965 – *Weinberger, M.A., Banfield, W.G.* (1965). Fine structure of a transplantable reticulum cell sarcoma. I. Light and electron microscopy of viable and necrotic tumor cells. *Journal of the National Cancer Institute*, 34(4): 459-479.

Welch, et al., 1986 – *Welch, P., Grossi, C., Carroll, A., Dunham, W., Royal, S., Wilson, E., Crist, W.* (1986). Granulocytic sarcoma with an indolent course and destructive skeletal disease. Tumor characterization with immunologic markers, electron microscopy, cytochemistry, and cytogenetic studies. *Cancer*, 57(5): 1005-1010.

Yasuzumi et al., 1960 – *Yasuzumi, G., Sugihara, R., Nakano, S., Kise, T., Takeuchi, H.* (1960). Submicroscopic structure of cell necrobiosis of Yoshida sarcoma as revealed by electron microscopy. *Cancer research*, 20(3 Part 1): 339-343.

Yusipovich et al., 2011 – *Yusipovich, A.I., Zagubizhenko, M.V., Levin, G.G., Platonova, A., Parshina, E.Y., Grygorzcyk, R., Maksimov, G.V., Rubin, A.B., Orlov, S.N.* (2011). Laser interference microscopy of amphibian erythrocytes: impact of cell volume and refractive index. *Journal of microscopy*, 244(3): 223-229.

Zhudina, Shalumovich, 1969 – *Zhudina, A.I., Shalumovich, V.N.* (1969). Determination of nucleic acids in cells infected by Rous sarcoma virus by means of ultraviolet microscopy. *Voprosy onkologii*, 15(9): 74-79.

Published in the Slovak Republic
European Journal of Medicine
Has been issued since 2013.
E-ISSN: 2310-3434
2019, 7(2): 92-98

DOI: 10.13187/ejm.2019.2.92
www.ejournal5.com

Effects of Electromagnetic Fields over DNA Hydrogen Bonds of Hamsters with Implanted *Graffi* Tumor

Ignat Ignatov [a, *], Christos Drossinakis [b], Reneta Toshkova [c], Elisaveta Zvetkova [c], Iliana Yaneva [d], Georgi Gluhchev [c]

[a] Scientific Research Center of Medical Biophysics (SRCMB), Sofia, Bulgaria
[b] IAWG – INTERNATIONALE Akademie für Wissenschaftliche Geistheilung, Frankfurt Höchst, Germany
[c] Bulgarian Academy of Science (BAS), Sofia, Bulgaria
[d] National Center of Public Health and Analyses, Ministry of Health, Bulgaria

Abstract

Studies were conducted with model systems of bio influence (Drossinakis' method) with electromagnetic (e.m.) fields and infrared thermal field (ITF) (Ignatov et al., 2013). The purpose of research is to analyze effects over DNA. Analysis of effects over water and physiological saline is carried out in the report. Results are achieved with blood serum of hamsters and physiological processes in hamsters with tumors. The water analyses have been conducted with Nonequilibrium Energy Spectrum (NES) and Differential Nonequilibrium Energy Spectrum (DNES) methods (Antonov, 1992; Ignatov, 1998). Experiments were carried out about the influence on tumor cells of mice in water. Reduction of DNES spectrum according to the control sample of cells in healthy animals was observed. (Antonov, 1992). Reduction is also observed in DNES spectrum in blood serum of people having oncological diseases, compared to the one of healthy people (Ignatov, 2012).

Such a reduction is most prevalent in (-0.1387 eV; 8.95 μm; 1117 cm^{-1}). In research of the effects of e.m. fields in water and blood serum from hamsters the range is (-0.08 – -0.14 eV) (8.9 – 15.5μm) (645–1129 cm^{-1}). Research is conducted for the effects over *Graffi* tumor that was implanted in hamsters (Toshkova et al., 2019). Studies are conducted with pH and oxidation redox potential (ORP) effects of e.m. fields over physiological saline (Gluhchev et al., 2019).

Keywords: Infrared thermal field (ITF), electromagnetic fields (e.m. fields), experimental *Graffi* solid tumor, energy spectrum, NES and DNES methods.

1. Introduction

In conducted studies with blood serum from animals and humans parameters of electromagnetic hydrogen bonds were analyzed. The hydrogen bonds are electromagnetic among bipolar molecules, where the hydrogen is connected to an atom with large electronegativity, such as nitrogen (N) and oxygen (O). Hydrogen bonds in DNA are shown in Fig. 1a. In Fig. 1b donor-acceptor interaction is presented. Hydrogen bonds in water are shown in Fig. 1c.

* Corresponding author
E-mail addresses: mbioph@dir.bg (I. Ignatov)

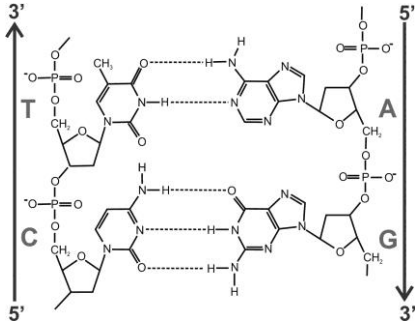

Fig. 1a. Hydrogen bonds among H and N or O in DNA

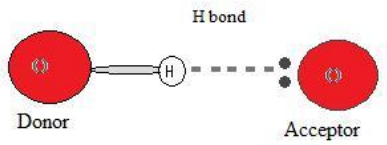

Fig. 1b. Donor-acceptor interaction of hydrogen bonds among H and N, F or O

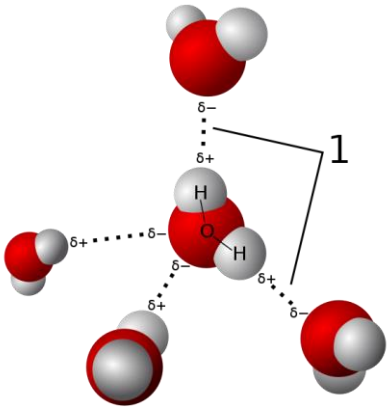

Fig. 1c. Hydrogen bonds among water molecules

The water is a medium of all life processes. The molecules of DNA in the cells are in the form of double helix. The pentose phosphate skeleton of both chains is placed outwards, and the nitrogenous bases are pointed towards the inside of the spiral, and are connected to each other with weak hydrogen bonds.

The multiple, although weak hydrogen bonds, provide stability to the molecule of DNA. The oxygen and nitrogen are electronegative atoms in the nitrogenous bases. Each separate nucleotide contains phosphate, deoxyribose saccharide as well as one of the four nitrogenous bases separated into two categories – purine and pyrimidine. The purine bases adenine (A) and guanine (G) are larger and contain two aromatic rings. The pyrimidine bases are cytosine (C) and thymine (T).

Research shows that the range of e.m. interaction of hydrogen bonds in DNA varies from 1 to 10 THz (10^{12}Hz)(30 –300 μm)(33.4 – 333.6 cm^{-1}) (Tang et al., 2018). Studies of the DNA changes in neoplastic diseases are conducted in such a range (Calvin et al., 2012). The authors investigate within the range 21 до 37 THz (8.9 –15.5μm) (645–1129 cm^{-1}) of effects over cancer cells, as the radiation of e.m. waves is in such a range (Ignatov et al., 2013).

The change of pH and oxidation-reduction potential (ORP) has been examined physiological saline (Ignatov et al., 2019). During the influence with e.m. waves is researched the survival rate of hamsters with tumors, as well as the change in tumor size. The DNA damage contributes to ageing and cancer, as the result depends on the type and number of lesions (injury) in DNA. The cancer related diseases are one of the main reasons for changes in DNA (Hoeijmakers, 2009). During the influence with e.m. fields change of erythrocytes and the animal hair of hamsters is observed (Toshkova et al., 2019).

2. Materials and methods

2.1. Experimental animals

Hamsters, breed "Golden Syrian", aged 2-4 months with weight around 90-100 g were used in the trials. The animals were grown in standard conditions in individual plastic cages with free access to food and water.

2. 2. Experimental tumor model

Tumor cells (1-2.10^6) from the experimental *Graffi* solid tumor are transplanted subcutaneously in the back of hamsters. Between days 7 and 15 after the transplantation tumor appears, grows progressively and the hamsters die around 30-35 days. In this tumor model 100 % tumor transplantation and 100 % mortality are observed. No spontaneous tumor's regression takes place. (Toshkova, 1995).

2.3. Influence by electromagnetic and infrared thermal fields

This type of influence is delivered by Christos Drossinakis who holds the hamsters in the hands for a couple of minutes.

2.4. Hematology examination

Blood smears from experimental Graffi tumour-bearing and control hamsters are prepared, stained by May-Gruenwald Giemsa method and examined light-microscopically.

2.5. Ethical aspects

All experiments were conducted in accordance with the European convention for protection of vertebrate animals, used for experimental and other scientific purposes (OJ L 222) and approved from the National Veterinary Medical Office.

2.6. NES and DNES Spectral Analyses

The device for DNES spectral analysis based on an optical principle was designed by A. Antonov. For this, a hermetic camera for evaporation of water drops under stable temperature (+22–24 ^{o}C) conditions was used. The water drops were placed on a water-proof transparent pad, which consisted of thin maylar folio and a glass plate. The light was monochromatic with filter for yellow color with wavelength at λ = 580±7 nm. The device measures the angle of evaporation of water drops from 72.3^o to 0°.

The DNES-spectrum was measured in the range of -0.08– -0.1387 eV or λ = 8.9–13.8 μm using a specially designed computer program. The main estimation criterion in these studies was the average energy ($\Delta E_{H...O}$) of hydrogen O...H-bonds between H_2O molecules in water samples and hamster serum blood.

3. Results

3.1. Influence of e.m. waves over hydrogen bonds in water medium. Hydrogen bonds in DNA

In the Fig. 2 the four monomers building DNA – deoxyadenosine, deoxycytidine, deoxyguanosine, deoxythymidine are presented. The hydrogen bonds are marked with arrows. DNA is located in water medium, and effects of e.m. fields over hydrogen bonds oxygen-hydrogen were being investigated.

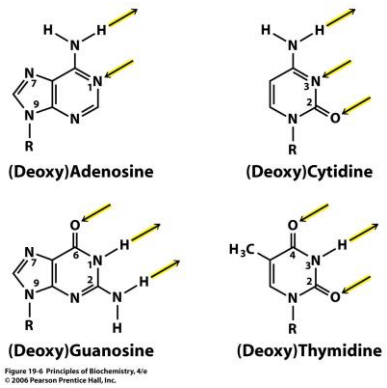

Fig. 2. Four monomers, which are created DNA – deoxyadenosine, deoxycytidine, deoxyguanosine, deoxythymidine

3.2. Electromagnetic parameters with DNES method during influence with electromagnetic fields over blood serum of hamsters with tumor

The average energy ($E_{H...O}$) of hydrogen H...O-bonds among individual H_2O molecules in 1 % solution of Sample of blood serum of hamsters with cancer after influence of Drossinakis is measured at E=-0.1285 eV. The result for the Control sample in 1 % solution of blood serum of hamsters with cancer is E=-0.1214 eV. The results obtained with the NES method are recalculated with the DNES method as a difference of the NES (Sample) minus the NES (Control Sample) equalled the DNES spectrum of 1 % solution of blood serum from hamsters with cancer.

Δf(E) = f (sample 1) – f (control sample 3)

Thus, the result for 1 % solution of blood serum from hamster recalculated with the DNES method is ΔE=-0.0071±0.0011 eV. The result shows the increasing of the values of the energy of hydrogen bonds in 1% solution of blood serum of hamsters with tumore after influence of Drossinakis regarding control sample blood serum of hamsters with tumors.

Fig. 3 displays DNES spectrum of 1% solution of blood serum of hamsters with tumors with influence from e.m. fields, and control group of hamsters with tumors. At the x-axis are reported the values of energy (-E) of hydrogen bonds. A portion of these bonds is in DNA. The function of distribution by energies for DNES df (E) в eV^{-1} is given at the y-axis. The positive values of the spectrum indicate effects over the tumor cells. Biological studies reveal improvement of the life status of tumor cells compared to the condition of healthy ones. It comes as a result of the improved replication of DNA.

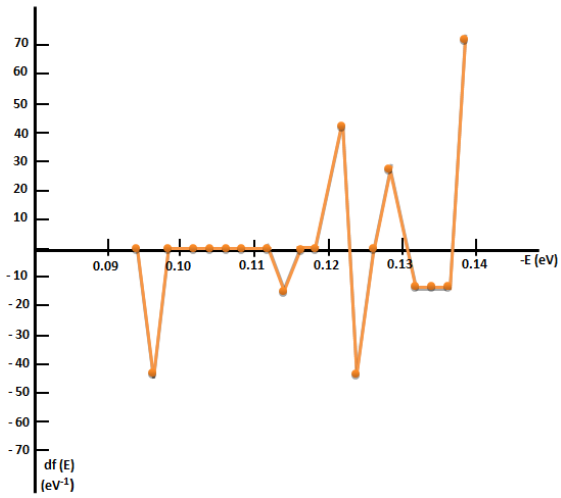

Fig. 3. DNES of 1 % solution of blood serum of hamsters with tumors with influence of e.m. fields as difference from the control group of hamsters with tumors

3.3. Biological parameters

Following biometric parameters have been measured for the evaluation of bioinfluence on the tumor: transplantability, tumor size (mm), lethality/mortality rate and survival rate. Their measurement revealed significant differences between the experimental and control group.

3.3.1. Life span of hamsters

Hamsters that have undergone bioinfluence have had low mortality. Until the 35th day, mortality was 0, at day 40- 40%, at day 45 was 80 %, and at day 50 it was 100%. At the same time the lethality was 50 % on the 30th day and reached 100% on the 38th day in the control group. Thus the average survival rate of hamsters with therapy was 43.6±5.8 days and for control group- without therapy – 31.75±6.8 days, which was 12 days longer than the controls.

Also, some delay in tumor transplantability and growth was registered. The conclusion we can draw from the obtained results is that bioinfluence therapy (in this scheme of application and duration) in hamsters with developed tumor doesn't stop the tumor growth, but delayed its progression, decreased lethality and prolonged average survival time.

3.3.2. Hematological research

Cytological differences in the erythrocyte /RBCs-/ morphology and differentiation were noticed in the blood smears of hamsters from control group vs bio-influenced hamsters with implanted myeloid tumours of *Graffi*. The observed differences probably indicate positive effects of the near infrared bio-influence on the erythropoiesis of *Graffi* tumour-bearing hamsters, that may lead to improvement of the anemia-syndrome – obligatory developed in this and/or in other experimental models of myeloid malignancies.

4. Conclusion

The results achieved from the tests within 5 days course of ITF and e.m. waves treatment of hamsters with experimental subcutaneous tumor are positive. Prolonged survival rate and decreased mortality between the experimental and control group, as well as lowered transplantability and slowed tumor growth were observed. The present results are the base for conducting further tests that aim to establish the optimum regimen of bioinfluence with regards to frequency and duration of the therapeutic procedures,

The mathematical model of blood serum solution of hamsters with cancer after the Drossinakis' influence gives significant information about the possible number of hydrogen bonds as a percent of H_2O molecules with different distribution of energy relative to the same number in the two control groups.

As a result of different energies of hydrogen bonds, the surface tension of the blood serum solution of cancer hamsters is increased after the treatment relative to the control samples. This effect is connected with the preservation and increase in the energy of the biochemical processes between water molecules and biomolecules.

The achieved results of hamsters from experimental bio-influence of Christos Drossinakis reveal their biological efficiency and can be subject of future studies. Extending the life of the hamsters is an indicator of improving immune status. The obtained results correspond to recent data from the medical scientific literature for the positive effect of the near infrared irradiation on the structure and function of erythrocyte membrane in normal and pathological conditions. The mitochondrial polarity in cancer cells was found to be lower than *that of normal cells. Drossinakis is increasing the* mitochondrial polarity.

The basic conclusion is that Drossinakis is able to increase the average energy of hydrogen bonds among water molecules in the blood of hamsters with cancer after treatment compared to the average energy of hydrogen bonds among water molecules in the blood of non-treated hamsters as control group.

In the report there are results with *DNA,* DNES spectrum of 1% solution of blood serum of hamsters with tumors with influence from e.m. fields, and control group of hamsters with tumors.

At the x-axis of Fig. 3 the values of energy (-E) of hydrogen bonds are reported . A portion of these bonds is in DNA. The function of distribution by energies for DNES df (E) в in eV^{-1} is given at the y-axis. The positive values of the spectrum indicate effects over the tumor cells. Biological studies reveal improvement of the life status of tumor cells compared to the condition of healthy ones. It comes as a result of the improved replication of DNA. After the influence the hydrogen bonds among oxygen (O) and hydrogen (H) in DNA helix have bigger energy.

During the study of physiological saline 5-times increase of hydrogen ions and a change in conductivity is observed. It is a proof for recovery of the ion balance. In the healthy cells the potential for transmission of hydrogen ions H^+ through the membrane is (-140 mV), and in the cancer cells it is (-70 mV). The increase of the number of hydrogen ions reveals a process of recovery in the potential of a cancer cell to a healthy condition.

The effect of bioinfluence of Christos Drossinakis over the values of pH of physiological saline can be considered as established (Ignatov et al., 2019).

Due to the 65 % of water content in the human body, it can be considered that its parameters irrespective of its consistency in the blood and internal organs, will be influenced from an external bioinfluence, which will affect their functioning, and hence the health condition of the body.

The potential of hydrogen ions in a healthy cell is (-140mV), and in a cancer cell (-70 mV). The increase of the number of hydrogen ions reveals a process of recovery in the potential of a cancer cell to a healthy condition (Ignatov et al., 2019).

References

Alberts et al. 1994 – *Alberts, B. et al.* (1994). Molecular Biology of the Cell 3rd ed.., Garland Publishing, New York and London.

Antonov, Galabova, 1992 – *Antonov, A., Galabova, T.* (1992). Ext. Abstr. of The 6th National Conference of Biomedical Physics and Engeneering, 60.

Antonov, 1995 – *Antonov, A.* (1995). Research of the Non-equilibrium Processes in the Area in Allocated Systems. Dissertation thesis for degree "Doctor of Physical Sciences", Blagoevgrad, Sofia.

Azab et al., 2013 – *Azab B. et al.* (2013). Pretreatment Neurophil/lymphocyte Ratio is Superior to Platelet/lymphocyte Ratio as a Predictor of Long-term Mortality in Breast Cancer Patients. *Med. Oncol.*, 30, 432.

Calvin et al., 2012 – *Calvin, Yu. et al.* (2012). The Potential of Terahertz Imaging for Cancer Diagnosis. A Review of Investigations to Date.

Drossinakis et al., 2019 – *Drossinakis, Ch., Toshkova, R., Zvetkova, E, Ignatov, I, Gluhchev, G.* (2019). Methods of Research in Vivo Research of Therapeutical Effect in Hamsters with Experimental Myeloid Tum or of *Graffi*, 8th World Congress on Immunology, Pulsus, London, 3, 21.

Drossinakis et al., 2019 – *Drossinakis, Ch., Ignatov, I., Toshkova, R., Zvetkova, E., Gluhchev, G.* (2019). Functional Changes of Cells and DNA by Electromagnetic Waves in the Case of Cancer. Cancer Stem Cell, Epidemiology and Surgery, Seoul, 23.

Drossinakis et al., 2019 – *Drossinakis, Ch., Toshkova, R., Zvetkova, E., Ignatov, I., Gluhchev, G.* (2019). Methods of Research in Vivo Research of Therapeutical Effect in Hamsters with Experimental Mieloid Tumor of Graffi. *Journal of Nursing Research and Practice*, 1-2.

Tang et al., 2018 – *Tang et al.* (2018). Detection of DNA Oligonucleotides with Base Mutations by Terahertz Spectroscopy and Microstructures, *PLoS ONE,* 13 (1): e0191515.

Gluhchev et al., 2015 – *Gluhchev, G., Ignatov, I., Karadzhov, S., Miloshev, G., Ivanov, N., Mosin, O.V.* (2015). Electrochemically Activited Water. Biophysical and Biological Effects of Anolyte and Catholyte as Types of Water. *Journal of Medicine, Physiology and Biophysics*, 10: 1-17.

Hoeijmakers, 2009 – *Hoeijmakers, J.H.* (2009). DNA Damage, Aging, and Cancer, 361(15): 1475-85.

Ignatov et al., 1998 – *Ignatov, A., Antonov, A., Galabova, T.* (1998). Medical Biophysics – Biophysical Fields of Man, Gea Libris, Sofia.

Ignatov, Mosin, 2013 – *Ignatov, I., Mosin, O.V.* (2013). Structural Mathematical Models Describing Water Clusters. *Journal of Mathematical Theory and Modeling*, 3 (11): 72-87.

Ignatov et al., 2014 – *Ignatov, I., Mosin, O. V., Niggli, H., Drossinakis, Ch.* (2014). Evaluating of Possible Methods and Approaches for Registering of Electromagnetic Waves Emitted from the Human Body. *Advances in Physics Theories and Applications*, 30: 15-33.

Ignatov et al., 2019 – *Ignatov, I., Toshkova, R., Gluhchev, G., Drossinakis, Ch.* (2019). Results of Blood Serum from Cancer Treated Hamsters with Infrared Thermal Field and Electromagnetic Fields. *Journal of Health, Medicine and Nursing*, 58: 101-112.

Ignatov, 2011 – *Ignatov, I.* (2011). Entropy and Time in Living Organisms. *Euromedica, Hanover*: 60-62.

Ignatov, Mosin, 2013 – *Ignatov I., Mosin O.V.* (2013). Possible Processes for Origin of Life and Living Matter with modeling of Physiological Processes of Bacterium Bacillus Subtilis in Heavy Water as Model System. *Journal of Natural Sciences Research*, 3(9): 65-76.

Ignatov, Mosin, 2013 – *Ignatov, I., Mosin, O.V.* (2013). Modeling of Possible Processes for Origin of Life and Living Matter in Hot Mineral and Seawater with Deuterium. *Journal of Environment and Earth Science*, 3 (14): 103-118.

Ignatov et al., 2019 – *Ignatov, I., Drossinakis, Ch., Toshkova,R., Zvetkova, E., Yaneva, I., Gluhchev, G.* (2019). Effects of Electromagnetic Fields over DNA of Hamsters with Implanted Graffi Tumor. *Journal of Health Medicine and Nursing,* 68: 34-40.

Toshkova, 1995 – *Toshkova, R.* (1995). Attempts for Immunomodulation in Hamsters with Transplanted Myeloid Tumor, Previously Induced by Graffi Virus, Bulgarian Academy of Sciences. PhD Dissertation, Sofia.

Toshkova et al., 2019 – *Toshkova, R., Ignatov, I., Zvetkova, E., Gluhchev, G.* (2019). Bioinfluence with Infrared Thermal and Electromagnetic Fields as a Therapeutic Approach of Hamsters with Experimental Graffi Myeloid Tumor. *Journal of Natural Sciences Research*, 9 (4): 1-11.

Toshkova et al., 2019 – *Toshkova, R., Ignatov, I., Zvetkova, E., Gluhchev, G., Drossinakis, Ch.* (2019). Beneficial Effects of *Drossinakis Bio-influence* (with Infrared Thermal and Electromagnetic Fields) on the Development of Experimental *Graffi* Myeloid Tumors in Hamsters. Hematological studies. *Journal of Medicine, Physiology and Biophysics*, 54: 13-17.

Toshkova, 2019 – *Toshkova, R., Ignatov, I., Zvetkova, E., Gluhchev, G.* (2019). Effects of Catholyte Water on the Development of Experimental Graffi Tumor on Hamsters. *Cells&Cellular Life Sciences Journal*, 4 (1): 000140.

Toshkova et al., 2019 – *Toshkova, R., Ignatov, I., Zvetkova, E., Gluhchev, G.* (2019). Effects of Catholyte Water on the Development of Experimental Graffi Tumor on Hamsters. *European Journal of Medicine,* 7(1): 45-56.

Zvetkova, 2006 – *Zvetkova E.* (2006). F.140. Quantitative Reduction in the RNP-Contents of Peripheral Blood Lymphocytes in Cancer Patients. Conference: 6th Annual Meeting of the Federation-of-Clinical-Immunology-Societies Location: San Francisco, CA Date: JUN 07-11. *Clinical Immunology*: 119: S100.

Zvetkova, Fuchs, 2017 – *Zvetkova, E., Fuchs, D.* (2017). Medical Significance of Simultaneous Application of Red Blood Cell Distribution Width (RDW) and Neopterin as Diagnostic Biomarkers in Clinical Practice, *Pteridines*, 28(3-4): 133-140.

Published in the Slovak Republic
European Journal of Medicine
Has been issued since 2013.
E-ISSN: 2310-3434
2019, 7(2): 99-105

DOI: 10.13187/ejm.2019.2.99
www.ejournal5.com

Research of Water Catholyte of Presence of Nascent (Atomic) Hydrogen (H*). Hydrogen and Nascent Hydrogen of the Reactions for Origin of Life in Hot Mineral Water

Ignat Ignatov [a, *], Dimitar Mehandjiev [b], Paunka Vassileva [b], Dimitrinka Voykova [b], Stoil Karadzhov [c], Georgi Gluhchev [b], Nikolai Ivanov [b]

[a] Scientific Research Center of Medical Biophysics (SRCMB), Sofia, Bulgaria
[b] Bulgarian Academy of Sciences (BAS), Sofia, Bulgaria
[c] Bulgarian Association of Activated Water, Sofia, Bulgaria

Abstract

A reaction is published for forming of nascent (atomic) hydrogen (H*) from hydronium ions (H_3O^+) in catholyte (Ignatov et al., 2015). It is also observed the production of nascent hydrogen in electrolysis in the transition to H_2 (Mehandjiev et al., 2017a, b). For checking of the theoretical suggestion experiments with potassium permanganate ($KMnO_4$) are conducted. Potassium permanganate is a strong oxidizing agent. In this compound, manganese is in the +7 oxidation state (Mn^{7+}). In reduction process the color of the aqueous solution of $KMnO_4$ is changed and thus the process could be examined spectrophotometrically Described is a reaction that proves the presence of nascent hydrogen in catholyte using potassium permanganate (Parn et al., 2012). In order to avoid the influence of salts contained in water from other sources, deionized water is used for production of catholyte/anolyte.

There is possibility nascent hydrogen to have been part of reaction for origin of life in hot mineral water in primary hydrosphere as result of contact with hydrogen from primary atmosphere with hydrogen and gas discharge (Ignatov, 2019).

Keywords: electrolysis, catholyte, anolyte, nascent hydrogen, reduction.

1. Introducion

The interest towards electrochemically activated water (ECAW) increases due to its applications. It is gained from electrolysis with direct current where the electrodes are separated with semipermeable membrane. The liquid surrounding the cathode is called catholyte, and the liquid surrounding the anode is called anolyte. It is observed a higher pH in catholyte (> 7.0) in comparison with the water before activation. Lower pH is observed in the anolyte (< 7.0) compared to the water before activation. The catholyte has reduction properties, and the anolyte oxidative. The catholyte has beneficial effect over the human health. The strong oxidative action of anolyte enables its use as an antibacterial tool for disinfection, in agriculture, and for purifying contaminated water.

For the science however, still remains open the question what determines these specific properties of ECAW. A large number of scientific investigations are conducted in this field, and certain physical properties of ECAW are established.

* Corresponding author
E-mail addresses: mbioph@dir.bg (I. Ignatov)

The following reactions are known:

$2H_2O + 2e^- \rightarrow H_2 + 2OH^-$ (1)

The hydrogen gas is separated and the water acquires alkaline reactivity. The catholyte has reduction properties, and it has increase in number of the electrons compared to the control sample, and a negative ORP.

The following reaction happens in the anode section

$2H_2O - 4e^- \rightarrow 4H^+ + O_2$ (2)

The anolyte has oxidative properties and there is reduction in number of the electrons in it, and a positive ORP, compared to the control sample.

The following is valid (Ignatov, Mosin et al., 2015).

The gaseous hydrogen is generated at the cathode while the oxygen is produced at the anode. Water also contains a certain amount of hydronium ions (H_3O^+) depolarizing at the cathode with formation of the atomic hydrogen:

$H_3O^+ + e^- \rightarrow H^* + H_2O$, (3)

In an alkaline environment a disruption of H_2O molecules, accompanied by formation of atomic hydrogen and hydroxide ion (OH^-) occurs:

$H_2O + e^- \rightarrow H^* + OH^-$, (4)

The reactive hydrogen atoms are adsorbed on the surface of the cathode, and molecular hydrogen H_2 released in the gaseous form after recombination is formed:

$H^* + H^* \rightarrow H_2$, (5)

At the same time atomic oxygen is released at the anode. In an acidic environment this process is accompanied by the destruction of H_2O molecules according to formula (2).

In an alkaline environment the OH^- ions moving from the cathode to the anode during the electrolysis are a source of oxygen:

$4OH^- \rightarrow O_2 + 2H_2O + 4e^-$, (6)

In a previous article (Mehandjiev et al., 2017a, b) was shown that the mechanism of activation in ECAW can occur with the following intermediate reaction taking place:

At cathode	$H^+ + e^- \rightarrow H^*$ (7)
	$2H^* \rightarrow H_2$ (8)
At anode	$O^{2-} - 2e^- \rightarrow O^*$ (9)
	$2O^* \rightarrow O_2$ (10)

In ECAW the mechanism includes two stages as it is for cathode and anode. At the first stage nascent hydrogen and nascent oxygen are released according to reactions (7) and (9). The gained products react with each other and produce a hydrogen molecule and an oxygen molecule respectively – reactions (8) and (10). Certain quantities of the nascent forms of hydrogen in catholyte, and oxygen in anolyte can be kept. Due to the strong reduction properties of the nascent hydrogen and the oxidative properties of the nascent oxygen, the obtained catholyte and anolyte have stronger reduction and oxidative abilities respectively. The experimental check of this statement defined the aim of the current scientific research.

The check of the reduction property of catholyte was performed through a chemical reaction with potassium permanganate as a reagent, and a strong oxidant. It is well known that potassium permanganate dissolves in water to give intensely pink or purple solutions. Therefore the content of manganese ions (Mn^{7+}) in the permanganate anion (MnO_4^-) can be controlled spectrophotometrically.

2. Materials and methods

The production of catholyte is performed by the means of device called “Activator 2”, developed in the Institute of Information and Communication Technologies, BAS. The electrochemical treatment of water is processed in a glass container inside of which two electrodes from platinized titanium are put. These are cathode and anode at a distance 3 cm of each other. The electrodes of size 17/3 cm and thickness of 0.5 mm are separated by a semipermeable membrane. Direct current of 220 V is used. The anode space contains 400 ml of water, and the cathode one 1500 ml. Time for activation is 6 minutes, which is sufficient to reach the saturation point of the pH curve.

Methodology is based on defining the concentration of potassium permanganate in the catholyte. For this purpose potassium permanganate ($KMnO_4$) from Merck (Germany) is used. Initial solution of $KMnO_4$ is prepared with a concentration of 1000 mg/L through dissolving the necessary amount of salt into the deionized water. In volumetric flasks of 50 ml solutions of $KMnO_4$ of concentrations 1, 2.5 and 5 mg/L are prepared through dilution of the starting solution with deionized water or catholyte.

The concentrations of solutions are measured spectrophotometrically using the apparatus Spekol 11 (Carl Zeiss Industrielle Messtechnik GmbH) via admeasurement of absorbance at λmax of 560 nm. The width of cuvettes is 1 cm. Standard line is built within the interval of concentrations of $KMnO_4$: from 0.2 to 50 mg/L (R^2 =09988). The concentrations of the working solutions are measured at different intervals of time – 1, 2, 3, 24 hours.

3. Experimental results and discussion

3.1. Experiments with potassium permanganate for presence of nascent hydrogen

On Fig. 1 are presented the results from the potassium permanganate concentration measurements at three initial concentrations of 1.0 mg/L; 2.5 mg/L; 5.0 mg/L, depending on the time. Over the course of time the concentration of potassium permanganate in the catholyte slightly decreases. This supports the supposition that active reduction forms are built in the catholyte, which reduce the manganese ions. In control study with the same deionized water but without electrolysis the concentration of potassium permanganate remains unchanged over a time period of 24 hours.

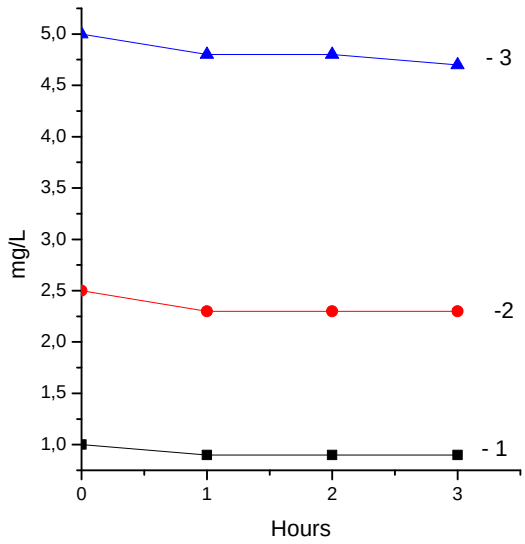

Fig. 1. Change of concentration of potassium permanganate in the catholyte over time depending on the initial concentration of 1.0 mg/L; 2.5 mg/L; 5.0 mg/L

From the conducted experiments we can conclude that during the electrolysis atoms of nascent hydrogen are created in the catholyte, according to the equations (3) and (7). Figure 1 shows that the activity of cations lasts for 24 hours with regards to the reduction process. We need to take into consideration that as per reaction (8) hydrogen molecules are also released into the solution, as they saturate it. In order to exclude the possibility that the observed reduction of concentration of permanganate ions is due to this hydrogen, trials were conducted under the same conditions using deionized water saturated with hydrogen at 20°C for a period of 30 minutes without electrochemical activation. The analysis of the contents of permanganate ions shows that their concentration is not diminished as a result of saturation of water with hydrogen. This proves that the observed reduction of concentration of these ions is due to the formation of nascent hydrogen during the electrochemical activation of deionized water.

In Table 1 the measurement results done 24 hours later are presented. The initial and residual concentration of permanganate ions, % of reduction, reduced Mn^{7+}- ions, and the quantity of nascent hydrogen for this reduction are also shown.

The content of nascent hydrogen remains the same for 24 hours even in the presence of a strong oxidizer such as the manganese ion (Mn^{7+}) in the permanganate anion (MnO_4^-). It can be concluded that the action of ECAW continues for at least 24 hours. From the Table 1 is also evident that with the increase of the initial concentration of potassium permanganate the quantity of reduced manganese ions increases. The explanation for this is that the probability for reacting in such low concentrations gets higher with the increase of the initial concentration of manganese ions.

Table 1. Initial and residual concentration of permanganate ions, % of reduction, reduced Mn^{7+}-ions, and the quantity of nascent hydrogen for this reduction

Initial concentration mg/L	Residual concentration mg/L	% of reduction	Reduced Mn^{7+} - ions mg/L	Nascent hydrogen mg/L 10^2
1.0	0.8±0.2	20.0	0.2	1.85
2.5	2.1 ±0.2	16.0	0.4	3.65
5.0	4.5±0.1	10.0	0.5	4.65

In the Table 1 is also calculated the quantity of nascent hydrogen contained in ECAW for up to 24 hours and acted as antioxidant agent. The amount of stabilized nascent hydrogen is low, in a range of $0.9.10^{-2}$ mg/L, but it has to be taken into account that these are only the kept after reactions (5) (8) and forming of molecular hydrogen quantities.

3.2. Reactions with hydrogen and nascent hydrogen in ancient hydrosphere and atmosphere

There were the following reactions for structuring of stromatolites in hot mineral water in ancient hydrosphere.

$CO_2 + OH^- \rightarrow HCO_3^-$ (11)

$2\ HCO_3^- + Ca^{2+} \rightarrow CaCO_3 + CO_2 + H_2O$ (12)

The following reaction (1) is valid in electrolysis. In the ancient atmosphere and hydrosphere there was increased gas discharge.

$2H_2O + 2\ e^- \rightarrow H_2 + 2OH^-$ (1)

The same reaction contributed for the formation of stromatolites as result of negative oxidation reduction potential in hot mineral water (Ignatov. 2019). Nowadays it is observed in elecrolyzer devices for waters catholyte and anolyte. In the ancient hydrosphere and land the charge had been negative and in the atmosphere positive. The conditions had been optimal for "nature" electrolysis. In these direction had been the experiments of Miller (Miller, 1953).

The reaction (14) is possible to structure nascent hydrogen H^* (Mehandjiev et al., 2019).

$H_2O + e^- \rightarrow H^* + OH^-$, (4)

The reaction (5) released in the gaseous form after recombination is formed:

$H^* + H^* \rightarrow H_2$ (5)

The nascent hydrogen is very active for chemical reactions in primary hydrosphere for origin of life and additional formation of H_2 makes alkalizing effect.

The allocation of H_2O molecule when a peptide chain is formed is important factor in reaction of condensation of two amino acid molecules into dipeptide. As reaction of polycondensation of amino acids is accompanied by dehydration, the H_2O removal from reaction mixture speeds up the reaction rate. This testifies that formation of early organic forms may have occured nearby active volcanoes, because at early periods of geological history volcanic activity occurred more actively than during subsequent geological times.

However, dehydratation accompanies not only amino acid polymerization, but also association of other small blocks into larger organic molecules, and also polymerization of nucleotides into nucleic acids. Such association is connected with the reaction of condensation, at which from one block a proton is removed, and from another – a hydroxyl group with the formation of H_2O molecule (Ignatov. Mosin, 2012)

4. Conclusion

The achieved results show that ECAW creates strong reducing agents in catholyte. The availability of free electrons contributes to the reduction properties of catholyte. Deionized water is used, as the reducing components in this case can be also based on hydrogen. These are atoms from nascent hydrogen (H*), which can be achieved from hydronium ions (H_3O^+) and from the electrolysis itself, as an intermediate reaction of $2H^* \rightarrow H_2$. The atoms of nascent hydrogen (H*) get stabilized within certain amounts in the catholyte, and by having strong reducing activity they define its antioxidant activity. The obtained results reveal that the mechanism of activation is also determined by nascent hydrogen in ECAW.

There has been possibility the nascent hydrogen to have took part of reaction for origin of life in hot mineral water in primary hydrosphere as result of contact with hydrogen from primary atmosphere with hydrogen and gas discharge (Ignatov, 2019).

References

Aider et al., 2012 – *Aider, M., Kastyuchik, A., Gnatko, E., Benali, M., Plutakhin, G.* (2012). Electro-activated Aqueous Solutions: Theory and Application in the Foodindustry and Biotechnology. *Innovative Food Science and Emerging Technologies,* 15: 38-49.

Bakhir et al., 2001 – *Bakhir, V.M., Zadorozhnii, Y.G., Leonov, V. I., Panicheva, S.A., Prilutsky, V.I.* (2001). Electrochemical Activation; Water Purification and Production of Useful Solutions. *Moscow: VNIIIMT*, 1: 100-176. [in Russian].

Bachir, Pogorelov, 2018 – *Bachir, V. M., Pogorelov, A.G.* (2018). Universal Electrochemical Technology for Environmental Protection. *International Journal of Pharmaceutical Research & Allied Sciences*, 7(1): 41-57.

Cha, Chun-Nam et al., 2016 – *Cha, Chun-Nam et al.* (2016). Virucidal Efficacy of a Fumigant Containing Orth-phenylphenol Against Classical Swine Fever Virus and Porcine Reproductive and Respiratory Syndrome Virus. *Korean Journal of Veterinary Service*, 39 (2): 117-124.

Fukuzaki, 2006 – *Fukuzaki, S.* (2006). Mechanisms of Actions of Sodium Hypochlorite in Cleaning and Disinfection Processes. *Biocontrol Sci.*, 11 (4): 147-57.

Gluhchev et al., 2015 – *Gluhchev, G., Ignatov, I., Karadzhov, S., Miloshev, G., Ivanov, N., Mosin, O.V.* (2015). Studying of Viruscidal and Biocidal Effects of Electrochemically Activated Anolyte and Catholyte Types of Water on Classical Swine. *Journal of Medicine, Physiology and Biophysics*, 13: 1-17.

Dube, Jain, 2018 – *Dube, K., Jain, P.* (2018). Electrolyzed Saline… an Alternative to Sodium Hypochlorite for Root Canal Irrigation. *Clujul Med*, 91(3): 322-327.

Ignatov et al., 2014 – *Ignatov, I., Karadzhov, S., Atanasov, A., Ivanova, E., Mosin, O.V.* (2014). Electrochemical Aqueous Sodium Chloride Solution (Anolyte and Catholyte) as Types of Water, Mathematical Models, Study of Effects of Anolyte on the Virus of Classical Swine Fever Virus. *Journal of Health, Medicine and Nursing*, 8: 1-28.

Ignatov et al., 2015 – *Ignatov, I., Gluhchev, G., Karadzhov, S., Miloshev, G., Ivanov, I., Mosin, O.V.* (2015). Preparation of Electrochemically Activated Water Solutions (Catholyte/Anolyte) and Studying of their Physical-Chemical Properties. *Journal of Medicine, Physiology and Biophysics*, 13: 18-38.

Ignatov et al., 2015 – *Ignatov, I., Mosin, O.V., Gluhchev, G., Karadzhov, S., Miloshev, G., Ivanov, N.* (2015). The Evaluation of Mathematical Model of Interaction of Electrochemically Activated Water Solutions (Anolyte and Catholyte) with Water. *European Reviews of Chemical Research*, 2 (4): 72-86.

Ignatov et al., 2018 – *Ignatov, I., Karadzhov, S., Gluhchev, G, Yakimov, I.* (2018). Electromagnetically Activated Water – Properties and Effects. *Bulgarian Journal of Public Health*, 10 (4): 63-69.

Ignatov, Mosin, 2013 – *Ignatov, I., Mosin, O.V.* (2013). Possible Processes for Origin of Life and Living Matter with modeling of Physiological Processes of Bacterium Bacillus Subtilis in Heavy Water as Model System. *Journal of Natural Sciences Research*, 3 (9): 65-76.

Ignatov, 2012 – *Ignatov, I.* (2012). Origin of Life and Living Matter in Hot Mineral Water. *Conference on the Physics, Chemistry and Biology of Water, Vermont Photonics, USA.*

Ignatov, Mosin, 2012 – *Ignatov, I., Mosin, O.V.* (2012). Isotopic Composition of Water and its Temperature in Modeling of Primordial Hydrosphere Experiments. *Euro-Eco, Hanover*, 62.

Ignatov, Mosin, 2013 – *Ignatov, I., Mosin, O.V.* (2013). Modeling of Possible Processes for Origin of Life and Living Matter in Hot Mineral and Seawater with Deuterium, *Journal of Environment and Earth Science*, 3 (14): 103-118.

Ignatov, Mosin, 2014 – *Ignatov, I., Mosin, O.V.* (2014). Modeling of Possible Conditions For Origin of First Organic Forms in Hot Mineral Water. *Journal of Medicine, Physiology and Biophysics*, 3, 1-14.

Ignatov, 2019 – *Ignatov, I.* (2019). Origin of Life in Hot Mineral Water from Hydrothermal Springs and Ponds. Effects of Hydrogen and Nascent Hydrogen. Analyses with Spectral Methods, pH and ORP. *European Reviews of Chemical Research*, 1.

Ignatov, Mosin, 2014 – *Ignatov, I., Mosin, O.V.* (2014). Coronal Gas Discharge Effect in Modeling of Non-Equilibrium Conditions with Gas Electric Discharge Simulating Primary Atmosphere and Hydrosphere for Origin of Life and Living Matter. *Journal of Medicine, Physiology and Biophysics*, 5, 47-70.

Ignatov, Mosin, 2014a – *Ignatov, I., Mosin, O.V.* (2014). Origin of Life and Living Matter in Primary Atmosphere and Hydrosphere. Modeling of Non-equilibrium Electric Gas Discharge Conditions. *Journal of Health, Medicine and Nursing*, 6, 25-49.

Ignatov, Mosin, 2014b – *Ignatov, I., Mosin, O.V.* (2014). Color Coronal Spectral Analysis in Modeling of Non-Equilibrium Conditions with Gas Electric Discharge Simulating Primary Atmosphere. *Biomedical Radioelectronic*, 2: 42-51.

Ignatov, Mosin, 2014c – *Ignatov, I., Mosin, O.V.* (2014). Coronal Effect in Modeling of Non-Equilibrium Conditions with the Gas Electric Discharge, Simulating Primary Atmosphere. *Nanotechnology Research and Practice,* Vol. 3, No. 3, pp. 127-140.

Ignatov, Mosin, 2013 – *Ignatov, I., Mosin, O.V.* (2013). Color Coronal Spectral Analysis for Modeling of Non-Equilibrium Conditions with the Gas Electric Discharge, Simulating Primary Atmosphere. *Nanoengineering*, 12: 41-51.

Ignatov, Mosin, 2015 – *Ignatov, I., Mosin, O.V.* (2015). Non-equilibrium Gas Discharge Conditions for Origin of Life and Living Matter. Experiments of Miller. Modeling of the Conditions with Gas Coronal Discharge Simulating Primary Atmosphere. *Journal of Medicine, Physiology and Biophysics*, 9: 27-50.

Ignatov, Mosin, 2015a – *Ignatov, I. Mosin, O.V.* (2015). S. Miller's Experiments in Modelling of Non-Equilibrium Conditions with Gas Electric Discharge Simulating Primary Atmosphere. *Journal of Medicine, Physiology and Biophysics*, 15: 61-76.

Ignatov, Mosin, 2016a – *Ignatov, I., Mosin, O.V.* (2016). Studying the Process of Formation of Precambrian Period Limestone Dolomite Fossils of Stromatolites in Hot Mineral Water Interacting with $CaCO_3$. *Journal of Medicine, Physiology and Biophysics*, 25: 29-44.

Ignatov, Mosin, 2016b – *Ignatov, I., Mosin, O.V.* (2016). Deuterium, Heavy Water and Origin of Life. LAP LAMBERT Academic Publishing, 1-500.

Ignatov, Mosin, 2016c – *Ignatov, I., Mosin, O.V.* (2016). Water and Origin of Life. *Altaspera Publishing & Literary Agency Inc*, 1-616.

Ignatov, Mosin, 2016d – *Ignatov, I.,Mosin, O.V.* (2016). Water and Origin of Life: Collection of Scientific Publications, Moscow, Berlin, Direct Media, 1-658.

Ignatov, Mosin, 2016e – *Ignatov, I., Mosin, O.V.* (2016). Studying the Process of Formation of Precambrian Period Limestone Fossils of Stromatolites in Hot Mineral Water with $CaCO_3$. *Russian Journal of Biological Research,* 8 (2): 48-68.

Inoe et al., 1997 – *Inoe, Y., Endo, S., Kondo, K., Ito, H., Omori, H., K. Saito* (1997). Trial of Electrolyzed Strong and Aqueous Solution Lavage in the Treatment of Peritonitis and Intraperitoneal Abscess. *Artificial Organs,* 21(1): 28-31.

Komatsu et al., 2001 – *Komatsu, T., Kabayama, S., Hayashida, A et al.* (2001). Suppressive effect of Electrolyzed Reduced Water on the Growth of Cancer Cells and Microorganisms. *Animal cell technology: From target to market, Kluwer Academic Publishers*, 220-223.

Kim et al., 2000 – *Kim, C., Hung, Y.C., Brackett, R.E.* (2000). Roles of Oxidation-reduction Potential in Electrolyzed Oxidizing and Chemically Modified Water for the Inactivation of Food-related Pathogens. *Journal of Food Protection,* 63: 19-24.

Kirkpatrick, 2009 – *Kirkpatrick, R.D.* (2009). The Mechanism of Antimicrobial Action of Electro-chemically Activated (ECA) water and its Healthcare Applications. Doctoral Thesis, University of Pretoria.

Lata et al., 2016 – *Lata, S. et al.* (2016). Anti bacterial Effectiveness of Electro-Chemically Activated (ECA) Water as a Root Canal Irrigant- An In-vitro Comparative Study. *Journal of Clinical and Diagnostic Research,* 10 (10): 138-142.

Lee et al., 2006 – *Lee, M-Y., Kim.-K., Ryoo, K.-K et al.* (2006). Electrolyzed-reduced Water Protects Against Oxidative Damage to DNA, RNA and Protein. *Applied Biochemistry and Biotechnology,* 135*:* 133-144.

Leonov et al., 1999 – *Leonov, I.B., Bakhir, V.M., Vtorenko, V.I.* (1999). Electrochemical Activation in the Practice of Medicine. *2nd Int. Symposium "Electrochemical Activation", Pros. Rep. and brief reperts*, 1: 15-23. [in Russian]

Mehandjiev et al., 2017a – *Mehandjiev, D., Ignatov, I., Karadzhov, I., Gluhchev, G., Atanasov, A.* (2017). On the Mechanism of Water Electrolysis. *Journal of Medicine, Physiology and Biophysics*, 31: 23-26.

Mehandjiev et al., 2017b – *Mehandjiev, D., Ignatov, I., Karadzhov, S., Gluhchev, G., Atanasov, A.* (2017). Processes in Catholyte and Anolyte as Result of Water Electrolysis. *European Journal of Molecular Biotechnology*, 5 (1): 23-29.

Miller, 1953 – *Miller, S.L.* (1953). A Production of Amino Acids Under Possible Primitive Earth Conditions. *Science*, 117(3046): 528-529.

Morita et al., 2000 – *Morita, C., Sano, K., Morimatsu, S., Kiura, H., Goto, T., Kohno, T.* (2000). Disinfection Potential of Electrolyzed Solutions Containing Chloride at Low Concentrations, *Journal of Virological Methods,* 85(2): 163-174.

Nguyễn Thị, Thanh Hải, 2018 – *Nguyễn Thị, Thanh Hải* (2018). Nghiên Cứu Cải Tiến Quy Trình Điều Chế Dung Dịch Siêu Oxy Hóa Và Ứng Dụng Trong Khử Trùng Nọước Thải Bệnh Viện, 1-161.

Pharn et al., 2012 – *Pharn, V.H. et al.* (2012). Chemical Reduction of an Aqueous Suspension of Graphene Oxide by Nascent Hydrogen. *Journal of Materials Chemistry*, 21: 1-5.

Prilutsky, Bakhir, 1997 – *Prilutsky, V.I., Bakhir, V.M.* (1997). Electrochemically Activated Water: Anomalous properties, Mechanism of biological action. *All Russian Scientific Research and Experimental Institute of Medical Engineering* (VNIIIMT), 1: 124. [in Russian]

Reinert et al., 1994 – *Reinert, F., Kumar, S., Steiner, P., Claessen, R., Hüfner, S.* (1994). The Electronic Structure of $KMnO_4$ Investigated by Photoemission and Electron-energy-loss Spectroscopy. *Zeitschrift für Physik B Condensed Matter*, 94 (4): 431-438.

Shirahata, 2002 – *Shirahata, S.* (2002). Reduced Water For Prevention of Diseases. *Animal Cell Technology: Challenges for the 21st Century*, pp. 25-30.

Shirahata et al., 1999 – *Shirahata, S., Murakami, E., Kusimoto, K.-I., et al.* (1999). Telomere Shortening in Cancercells by Electrolyzed-reduced Water. *Animal Cell Technology: Challenges for the 21st Century,* 355-359.

Tanaka et al., 1996 – *Tanaka, H., Y. Hirakata, M. Kaku, R. Yoshida, H. Takemura, Mizukane, R.* (1996). Antimicrobial Activity of Superoxidized Water. *Journal of Hospital Infection,* 34(1): 43-49.

Truong Nhu Ngoc Vo et al., 2018 – *Truong Nhu Ngoc Vo et al.* (2018). Efficacy of Electrochemically Activated Water Solution in Gingivitis Treatment. *Journal of Pharmaceutical Investigation*, 49: 323-329.

Vassileva et al., 2019 – *Vassileva, P., Voykova, D., Ignatov, I., Karadzhov, S., Gluhchev, S., Ivanov, N., Mehandjiev, D.* (2019). Results from the Research of Water Catholyte with Nascent (Atomic) Hydrogen. *Journal of Medicine, Physiology and Biophysics*, 52: 7-11.

Yahagi et al., 2000 – *Yahagi, N., Kono, M., Kitahara, M., Ohmura, A., Sumita, O., Hashimoto, T.* (2000). Effect of Electrolyzed Water on Wound Healing. *Artificial Organs,* 24 (12): 984-987.

Ye et al., 2008 – *Ye, J., Li, Y., Hamasaki, T., N., Komatsu, E. et al.* (2008). Inhibitory Effect of Electrolyzed Reduced Water on Tumor Angiogenesis. *Biological and Pharmaceutical Bulletin,* 31: 19-26.

Zhou, Endelberg, 2018 – *Zhou, Y., Endelberg, D.L.* (2018). Application of a Modified Bi-polar Electrochemistry Approach to Determine Pitting Corrosion Characteristics. *Electrochemistry Communications*, 93: 158-161.

Published in the Slovak Republic
European Journal of Medicine
Has been issued since 2013.
E-ISSN: 2310-3434
2019, 7(2): 106-113

DOI: 10.13187/ejm.2019.2.106
www.ejournal5.com

Drug Interactions of Dihydropyridine Calcium Channel Blockers (CCBs) involving CYP3A4 Enzymes

Naina Mohamed Pakkir Maideen [a, *]

[a] Dubai Health Authority, Dubai, United Arab Emirates

Abstract

Dihydropyridine Calcium Channel Blockers (CCBs) are widely used as first-line agents to treat hypertension in black patients and in patients aged more than 55 years. They have been identified as the substrates of intestinal and hepatic CYP3A4 enzymes and this review focuses on possible drug-drug interactions of dihydropyridine CCBs involving CYP3A4 enzymes. As object drugs, the dihydropyridine CCBs involved in drug-drug interactions with drugs such as Macrolide antibiotics, Azole antifungals, Protease inhibitors and fruit juices like Grapefruit juice and Seville orange juice and increase the plasma concentrations of dihydropyridine CCBs resulting in enhanced adverse effects. In addition, the drugs like Rifampicin, Phenytoin, and other antiepileptics including Carbamazepine and Phenobarbital decrease the bioavailability of dihydropyridine CCBs. Moreover, as precipitant drugs dihydropyridine CCBs increase the plasma concentrations of Statins and Cyclosporine and decrease the therapeutic efficacy of Clopidogrel. The prescribers and pharmacists are required to be aware of the adverse drug interactions of dihydropyridine CCBs to prevent adverse outcomes.

Keywords: Drug interactions, Dihydropyridine Calcium Channel Blockers, CYP3A4 enzymes, Nifedipine, Amlodipine, Felodipine.

1. Introduction

Calcium channel blockers (CCBs) include Dihydropyridines (DHPs) such as Nifedipine, Amlodipine, Felodipine, Nicardipine, and others and non-dihydropyridines (non-DHPs) like Verapamil and Diltiazem (Whyte et al., 2016). The first-generation DHPs include Nifedipine and Nicardipine, the second-generation agents include Benidipine and Efonidipine, the third-generation DHPs include Amlodipine and Azelnidipine and fourth-generation drugs include Lercanidipine and Lacidipine (Chandra et al., 2013). The dihydropyridine CCBs are approved to manage the patients with hypertension and angina (Elliott et al., 2011).

The National Institute for Health and Care Excellence (NICE) guideline on the diagnosis and treatment of high blood pressure (hypertension) recommends CCBs as initial therapy to treat hypertension in black patients and in patients aged more than 55 years (Krause et al., 2011). Moreover, the guidelines from Eighth Joint National Committee (JNC 8) and American College of Cardiology/American Heart Association task force recommend CCBs as first-line antihypertensive agents along with Thiazide diuretics, Angiotensin converting enzyme inhibitors (ACEIs), Angiotensin receptor blockers (ARBs). Thiazide diuretics are preferred as initial drug to treat hypertension irrespective of age and race and CCBs are a good alternative choice for

* Corresponding author
E-mail addresses: nmmaideen@dha.gov.ae (N. Mohamed Pakkir Maideen)

initial therapy when thiazide diuretics are not tolerated. Similar to thiazide diuretics, CCBs have been identified to reduce all Cardio vascular disease (CVD) events except Heart failure (HF) (James et al., 2014; Whelton et al., 2018).

The dihydropyridine CCBs bind to L-type calcium channels and block the entry of calcium in vascular smooth muscle, which leads to vasodilatation and reduction of blood pressure (BP) (Meredith et al., 2004). The rate of premature death and disability is higher among patients with hypertension due to cardiovascular disease (CVD) including coronary artery disease (CAD), peripheral artery disease (PAD), congestive heart failure (CHF), and stroke and chronic kidney disease (CKD) induced by high blood pressure. It has been estimated that 7.6 million premature deaths were attributed to hypertension, in 2001 and hypertension also found to be associated with 54 % of stroke and 47 % of ischaemic heart disease (Lawes et al., 2001). In 2010, it has been estimated that 1.39 billion of people across the globe are affected by hypertension and the numbers are increasing daily (Bloch, 2016).

Modification of effects of one drug by the concomitant administration of other drug(s), supplements, food or alcohol is known as Drug interaction (Maideen, 2019). The drug which induces the drug-drug interaction is termed "precipitant drug" while the drug affected by the drug-drug interaction is called "object drug" (Pakkir Maideen, 2018). It has been estimated that the prevalence of Adverse drug reactions (ADR)-related hospital admissions was about 3.3 % and drug interactions were accounted for 49 % of those admissions (Pedrós et al., 2016). To prevent the adverse outcomes, the prescribers and the pharmacists are required to be aware of the possible drug interactions of dihydropyridine CCBs.

2. Discussion

Dihydropyridine CCBs as Object drugs

The dihydropyridine CCBs have been identified as the substrates of cytochrome P450 3A4 (CYP3A4) enzymes and they are metabolised in the gut wall and liver by them (Zhu et al., 2014). The drugs inhibiting or inducing CYP3A4 enzyme may increase the risk of adverse drug reactions of dihydropyridine CCBs including hypotension and shock.

Macrolide antibiotics

Macrolide antibiotics help to treat respiratory tract, skin, and soft tissue infections, mainly. The macrolide antibiotics such as Erythromycin and Clarithromycin have been identified as moderate to potent inhibitors of intestinal and hepatic CYP3A4 enzymes (Pakkir Maideen NM, 2018).

Administration of Erythromycin 250mg four times a day, in healthy men taking Felodipine 10mg resulted in elevated plasma concentrations of Felodipine due to the inhibition of CYP3A4-mediated metabolism of Felodipine by Erythromycin (Bailey et al., 1996). Similarly, concomitant use of Erythromycin in a 43-year-old patient taking Felodipine lead to increased symptoms of palpitations, flushing, and ankle edema, which might have occurred due to the inhibition of CYP3A4-mediated metabolism of Felodipine by Erythromycin (Liedholm et al., 1991).

Vasodilatory shock and heart block were occurred in a 77-year-old patient receiving Clarithromycin along with Nifedipine, possibly due to the inhibition of CYP3A4-mediated metabolism of Nifedipine by Clarithromycin resulting in elevated plasma concentrations and toxicity of Nifedipine (Gerónimo-Pardo et al., 2005). The risk of hospitalizations with acute kidney injury found higher in patients taking a Calcium channel blocker and Clarithromycin, concurrently (Gandhi et al., 2013).

Erythromycin and Clarithromycin were attributed to increased risk of hypotension-associated hospitalizations of patients taking calcium-channel blockers (Wright et al., 2011). Azithromycin is a weak inhibitor of CYP3A4 enzyme and it may be preferred when the use of macrolide antibiotic is necessary for a patient receiving calcium channel blockers (Henneman et al., 2012).

Azole antifungals

Azole antifungals such as Fluconazole, Itraconazole, Posaconazole and Voriconazole are frequently used to prevent or treat systemic fungal infections and they have been identified as the inhibitors of CYP3A4 enzyme. Itraconazole and Posaconazole are found to be potent CYP3A4 inhibitors more than Fluconazole and Voriconazole (Brüggemann et al., 2009). Hence, the azole antifungals may inhibit the CYP3A4-mediated metabolism of dihydropyridine CCBs. Concomitant

use of Itraconazole and Felodipine in nine healthy individuals resulted in elevated plasma concentrations of Felodipine leading to decreased blood pressure and increased heart rate (Jalava et al., 1997).

Administration of Itraconazole in a patient receiving Nifedipine resulted in increased the serum concentrations of Nifedipine and ankle edema (Tailor et al., 1996). It is recommended to avoid the combination of azole antifungals and dihydropyridine CCBs and dosage adjustments are required if their concomitant use is necessary (Jalava et al., 1997).

Protease inhibitors

The protease inhibitors include Ritonavir, Saquinavir, Indinavir and others, which are used to treat the patients with human immunodeficiency virus (HIV). Ritonavir was found to be very potent CYP3A4 inhibitors while other protease inhibitors are also capable of inhibiting CYP3A4 enzyme (Eagling et al., 1997).

The plasma concentrations of Amlodipine was increased in healthy HIV- seronegative subjects when Indinavir-Ritonavir combination is administered to them (Glesby et al., 2005).

Administration of Nelfinavir in a 51- year-old man with HIV infection receiving extended-release Nifedipine developed symptomatic orthostasis and heart block. Recurrence of orthostatic symptoms noted, when he was switched to Ritonavir-Indinavir combination. The orthostatic symptoms have been managed by dosage reduction of Nifedipine (Rossi et al., 2002).

Concomitant use of Nifedipine and Lopinavir-Ritonavir in a 47-year-old man with HIV infection resulted in severe hypotension along with other symptoms such as malaise, oliguria, and progressive generalized edemas and the discontinuation of both the drugs brought the blood pressure back to normal (Baeza et al., 2007). The dihydropyridine CCBs should be initiated at low doses with careful monitoring, if the coadministration of CCBs and protease inhibitors is necessary (Glesby et al., 2005).

Grapefruit Juice

Furanocoumarins of grapefruit juice are potent inhibitors of CYP3A4 enzymes and it has been noted that CYP3A4-mediated metabolism of substrates could be inhibited by one whole grapefruit or 200 mL of grapefruit juice (Glesby et al., 2005).

The interaction between Felodipine and grapefruit juice was discovered accidentally, as the plasma concentrations of Felodipine was increased by the concomitant use of grapefruit juice in 10 healthy male subjects (Bailey et al., 2013). The plasma concentrations of Felodipine have been increased by the consumption of grapefruit juice (Bailey et al., 1989; Bailey et al., 1993) as well as unprocessed grapefruit (Dresser et al., 2000; Bailey et al., 2000).

Moreover, a single glass (250ml) of grapefruit juice was found sufficient to increase the plasma concentrations of Felodipine (Lundahl et al., 1998), Amlodipine (Josefsson et al., 1996) and Nimodipine (Fuhr et al., 1998). To prevent the adverse outcomes, the patients receiving dihydropyridine CCBs should be advised to avoid the consumption of grapefruit juice (Lim et al., 2003).

Seville orange juice

Seville orange inhibits intestinal CYP3A4 as it contains the furanocoumarins such as 6',7'-dihydroxybergamottin and bergamottin (Penzak et al., 2002). Administration of 10mg of Felodipine in healthy volunteers consuming 240 mL of Seville orange juice resulted in elevated plasma concentrations of Felodipine (Malhotra et al., 2001).

Rifampicin

Rifampicin is an antimycobacterial antibiotic extensively used to treat tuberculosis and leprosy and it has been identified as an inducer of CYP enzymes including CYP3A4 (Pakkir Maideen, 2018). The oral bioavailability of Nifedipine (Holtbecker et al., 1996) and Nilvadipine (Saima et al., 2002) were decreased in healthy volunteers taking Rifampicin due to the induction of intestinal CYP3A4-mediated metabolism of dihydropyridine CCBs. In addition, the blood pressure of the patients receiving Nisoldipine, Nifedipine, Barnidipine or Manidipine has been increased due to the initiation of Rifampicin in them the blood pressure fell once Rifampicin was withdrawn (Yoshimoto et al., 1996).

As the antihypertensive efficacy of dihydropyridine CCBs is expected to be diminished by Rifampicin, the blood pressure of the patients receiving this combination of drugs should be

monitored or other antihypertensive drugs which are not affected by Rifampicin should be employed in patients with hypertension as well as tuberculosis (Cordeanu et al., 2017).

Phenytoin

Phenytoin is an antiepileptic drug and it has been identified as a potent inducer of CYP enzymes including CYP3A4 (Hole et al., 2018). The plasma concentrations of Nisoldipine decreased in patients receiving Phenytoin concurrently, due to increased first-pass metabolism (Michelucci et al., 1996).

Other Antiepileptic Drugs

The antiepileptic drugs such as Carbamazepine and Phenobarbital have also been recognized as the inducers of CYP3A4 enzymes (Hole et al., 2018). Concomitant administration of Nimodipine in epileptic patients receiving antiepileptic drugs such as Carbamazepine and Phenobarbital resulted in decreased plasma concentrations of Nimodipine and the patients taking the combination of dihydropyridine CCBs and enzyme-inducing antiepileptic drugs may need to increase their doses of Nimodipine (Tartara et al., 1991).

Dihydropyridine CCBs as Precipitant drugs

The dihydropyridine CCBs are the possible inhibitors of CYP3A4 enzyme and Nicardipine found to be the strongest inhibitor of CYP3A4, followed by Lercanidipine, Cilnidipine, Nimodipine, and Amlodipine (Bernard et al., 2014). Coadministration of dihydropyridine CCBs and CYP3A4 substrates may increase the risk of toxicity of CYP3A4 substrates.

HMG-CoA reductase inhibitors (Statins)

Hydroxy methyl glutaryl-CoA (HMG-CoA) reductase inhibitors (Statins) are recommended primarily to treat atherosclerosis and to prevent myocardial infarction, and stroke (Davies et al., 2016). The risks of adverse effects such as acute kidney injury, hyperkalemia, acute myocardial infarction, and acute ischemic stroke increased due to combined therapy of CYP3A4-metabolized statins and CYP3A4-inhibiting CCBs (Wang et al., 2016).

The plasma concentrations of Simvastatin increased by the concomitant administration of Simvastatin and Amlodipine in patients with hypercholesterolemia and hypertension (Nishio et al., 2005). The probability of interaction between Simvastatin and Amlodipine may be decreased by non-concurrent dosing of them (Park et al., 2010).

Cyclosporine

Cyclosporine is an immunosuppressant drug and it is a substrate of CYP3A4 enzyme (Hu et al., 2007). The plasma concentrations of Cyclosporine increased in hypertensive renal transplant patients receiving Amlodipine (Pesavento et al., 1996; Cai et al., 2011) and Nicardipine (Guan et al., 1996).

Clopidogrel

Clopidogrel is an antiplatelet drug and it is useful to manage patients with acute coronary syndrome, ischemic stroke or peripheral vascular disease to prevent thrombotic events. It is a prodrug and it is metabolised to active form mainly by CYP2C19 and CYP3A4 enzymes (Tirkkonen et al., 2013). The antiplatelet efficacy of Clopidogrel found to be decreased in patients receiving dihydropyridine CCBs such as Amlodipine, Benidpine, Nifedipine and others (Seo et al., 2014; Gremmel et al., 2015).

3. Conclusion

Dihydropyridine Calcium Channel Blockers (CCBs) have been identified as the substrates of intestinal and hepatic CYP3A4 enzymes. The plasma concentrations of dihydropyridine CCBs could be increased by the concomitant administration of drugs such as Macrolide antibiotics, Azole antifungals, Protease inhibitors and juices like Grapefruit juice and Seville orange juice, which may result in enhanced adverse effects. In addition, the drugs like Rifampicin, Phenytoin, and other antiepileptics including Carbamazepine and Phenobarbital reported to reduce the bioavailability of dihydropyridine CCBs that could decrease the therapeutic efficacy.

Moreover, dihydropyridine CCBs increase the plasma concentrations of Statins and Cyclosporine and decrease the therapeutic efficacy of Clopidogrel. The prescribers and pharmacists are required to be aware of the adverse drug interactions of dihydropyridine CCBs to prevent adverse outcomes.

Conflicts of Interest
NIL

Funding
NIL

References

Baeza et al., 2007 – *Baeza, M.T, Merino, E, Boix, V, Climent, E.* (2007). Nifedipine–lopinavir/ritonavir severe interaction: a case report. *Aids*. 2Jan 2; 21(1): 119-20.

Bailey et al., 1989 – *Bailey, D.G., Spence J.D., Edgar, B., Bayliff, C.D., Arnold, J.M.* (1989). Ethanol enhances the hemodynamic effects of felodipine. Clinical and investigative medicine. Medecine clinique et experimentale. Dec; 12(6): 357-62.

Bailey et al., 1993 – *Bailey, D.G., Arnold, J.M., Munoz, C., Spence, J.D.* (1993). Grapefruit juice–felodipine interaction: mechanism, predictability, and effect of naringin. *Clinical Pharmacology & Therapeutics*. Jun 1; 53(6): 637-42.

Bailey et al., 1996 – *Bailey, DG, Bend, J.R., Arnold, J.M., Tran, L.T., Spence, J.D.* (1996). Erythromycin-felodipine interaction: magnitude, mechanism, and comparison with grapefruit juice. Clinical Pharmacology & Therapeutics. Jul 1; 60(1): 25-33.

Bailey et al., 2000 – *Bailey, D.G., Dresser, G.K., Kreeft, J.H., Munoz, C., Freeman, D.J., Bend, J.R.* (2000). Grapefruit-felodipine interaction: effect of unprocessed fruit and probable active ingredients. *Clinical Pharmacology & Therapeutics*. Nov; 68(5): 468-77.

Bailey et al., 2013 – *Bailey, D.G., Dresser, G., Arnold, J.M.* (2013). Grapefruit–medication interactions: Forbidden fruit or avoidable consequences? *Cmaj*. Mar 5; 185(4): 309-16.

Bernard et al., 2014 – *Bernard, E., Goutelle, S., Bertrand, Y., Bleyzac, N.* (2014). Pharmacokinetic drug-drug interaction of calcium channel blockers with cyclosporine in hematopoietic stem cell transplant children. *Annals of Pharmacotherapy*. Dec; 48(12): 1580-4.

Bloch, 2016 – *Bloch, M.J.* (2016). Worldwide prevalence of hypertension exceeds 1.3 billion. *Journal of the American Society of Hypertension: JASH*. Oct; 10(10): 753.

Brüggemann et al., 2009 – *Brüggemann, R.J., Alffenaar, J.W., Blijlevens, N.M., Billaud, E.M., Kosterink, J.G., Verweij, P.E., Burger, D.M., Saravolatz, L.D.* (2009). Clinical relevance of the pharmacokinetic interactions of azole antifungal drugs with other coadministered agents. *Clinical Infectious Diseases*. May 15; 48(10): 1441-58.

Cai et al., 2011 – *Cai, J., Huang, Z., Yang, G., Cheng, K., Ye, Q., Ming, Y., Zuo, X., Zhou, P., Yuan, H.* (2011). Comparing antihypertensive effect and plasma ciclosporin concentration between amlodipine and valsartan regimens in hypertensive renal transplant patients receiving ciclosporin therapy. *American Journal of Cardiovascular Drugs*. Dec 1; 11(6): 401-9.

Chandra et al., 2013 – *Chandra, K.S., Ramesh, G.* (2013). The fourth-generation Calcium channel blocker: cilnidipine. *Indian heart journal*. Dec 1;65(6): 691-5.

Cordeanu et al., 2017 – *Cordeanu, E.M., Gaertner, S., Faller, A., Mirea, C., Lessinger, J.M., Kemmel, V., Stephan, D.* (2017). Rifampicin reverses nicardipine effect inducing uncontrolled essential hypertension. *Fundamental & clinical pharmacology*. Oct; 31(5): 587-9.

Davies et al., 2016 – *Davies, J.T., Delfino, S.F., Feinberg, C.E., Johnson, M.F., Nappi, V.L., Olinge,r J.T, Schwab, A.P., Swanson, H.I.* (2016). Current and emerging uses of statins in clinical therapeutics: a review. *Lipid insights*. Jan; 9: LPI-S37450.

Dresser et al., 2000 – *Dresser, G.K., Bailey, D.G., Carruthers, S.G.* (2000). Grapefruit juice–felodipine interaction in the elderly. *Clinical Pharmacology & Therapeutics*. Jul 1; 68(1): 28-34.

Eagling et al., 1997 – Eagling, V.A., Back, D.J., Barry, M.G. (1997). Differential inhibition of cytochrome P450 isoforms by the protease inhibitors, ritonavir, saquinavir and indinavir. *British journal of clinical pharmacology*. Aug; 44(2): 190-4.

Elliott et al., 2011 – *Elliott, W.J., Ram, C.V.* (2011). Calcium channel blockers. *The journal of clinical hypertension*. Sep; 13(9): 687-9.

Fuhr et al., 1998 – *Fuhr, U., Maier-Brüggemann, A., Blume, H., Mück, W., Unger, S., Kuhlmann, J., Huschka, C., Zaigler, M., Rietbrock, S., Staib, A.H.* (1998). Grapefruit juice increases oral nimodipine bioavailability. *International journal of clinical pharmacology and therapeutics*. Mar; 36(3): 126-32.

Gandhi et al., 2013 – *Gandhi, S., Fleet, J.L., Bailey, D.G., McArthur, E., Wald, R., Rehman, F., Garg, A.X.* (2013). Calcium-channel blocker–clarithromycin drug interactions and acute kidney injury. *Jama*. Dec 18; 310(23): 2544-53.

Gerónimo-Pardo et al., 2005 – *Gerónimo-Pardo, M, Cuartero-del-Pozo, AB, Jiménez-Vizuete, J.M., Cortiñas-Sáez, M., Peyró-García, R.* (2005). Clarithromycin—Nifedipine Interaction as Possible Cause of Vasodilatory Shock. *Annals of Pharmacotherapy*. Mar; 39(3): 538-42.

Glesby et al., 2005 – *Glesby, M.J., Aberg, J.A., Kendall, M.A., Fichtenbaum, C.J., Hafner, R., Hall, S., Grosskopf, N., Zolopa, A.R., Gerber, J.G.* (2005). Pharmacokinetic interactions between indinavir plus ritonavir and calcium channel blockers. *Clinical Pharmacology & Therapeutics*. Aug 1; 78(2): 143-53.

Gremmel et al., 2015 – *Gremmel, T., Durstberger, M., Eichelberger, B., Koppensteiner, R., Panzer, S.* (2015). Calcium-Channel Blockers Attenuate the Antiplatelet Effect of Clopidogrel. *Cardiovascular therapeutics*. Oct; 33(5): 264-9.

Guan D et al., 1996 – *Guan, D., Wang, R., Lu, J., Wang, M., Xu, C.* (1996). Effects of nicardipine on blood cyclosporine levels in renal transplant patients. *Transplantation proceedings*. Jun. 28(3): 1311-1312.

Henneman et al., 2012 – *Henneman, A., Thornby, K.A.* (2012). Risk of hypotension with concomitant use of calcium-channel blockers and macrolide antibiotics. *American Journal of Health-System Pharmacy*. Jun 15; 69(12): 1038-43.

Hole et al., 2018 – *Hole, K., Wollmann, B.M., Nguyen, C., Haslemo, T., Molden, E.* (2018). Comparison of CYP3A4-inducing capacity of enzyme-inducing antiepileptic drugs using 4β-hydroxycholesterol as biomarker. *Therapeutic drug monitoring*. Aug 1; 40(4): 463-8.

Holtbecker et al., 1996 – *Holtbecker, N., Fromm, M.F, Kroemer, H.K., Ohnhaus, E.E., Heidemann, H.* (1996). The nifedipine-rifampin interaction. Evidence for induction of gut wall metabolism. *Drug Metabolism and Disposition*. Oct. 1; 24(10): 1121-3.

Hu et al., 2007 – *Hu, Y.F., Tu, J.H., Tan, Z.R., Liu, Z.Q., Zhou, G., He, J., Wang, D., Zhou, H.H.* (2007). Association of CYP3A4* 18B polymorphisms with the pharmacokinetics of cyclosporine in healthy subjects. *Xenobiotica*. Mar 1; 37(3): 315-27.

Jalava et al., 1997 – *Jalava, K.M., Olkkola, K.T., Neuvonen, P.J.* (1997). Itraconazole greatly increases plasma concentrations and effects of felodipine. *Clinical Pharmacology & Therapeutics*. Apr 1; 61(4): 410-5.

James et al., 2014 – *James, P.A., Oparil, S., Carter, B.L., Cushman, W.C., Dennison-Himmelfarb, C., Handler, J., Lackland, D.T., LeFevre, M.L., MacKenzie, T.D., Ogedegbe, O., Smith, S.C.* (2014). 2014 evidence-based guideline for the management of high blood pressure in adults: report from the panel members appointed to the Eighth Joint National Committee (JNC 8). *Jama*. Feb 5; 311(5): 507-20.

Josefsson et al., 1996 – *Josefsson, M., Zackrisson, A.L., Ahlner, J.* (1996). Effect of grapefruit juice on the pharmacokinetics of amlodipine in healthy volunteers. *European journal of clinical pharmacology*. Oct 1; 51(2): 189-93.

Krause et al., 2011 – *Krause, T., Lovibond, K., Caulfield, M., McCormack, T., Williams, B.* (2011). Management of hypertension: summary of NICE guidance. Bmj. Aug 25; 343: d4891.

Lawes et al., 2001 – *Lawes, C.M., Vander Hoorn, S., Rodgers, A.* (2001). Global burden of blood-pressure-related disease. *The Lancet*. May 3; 371(9623): 1513-8.

Liedholm et al., 1991 – *Liedholm, H., Nordin, G.* (1991). Erythromycin-felodipine interaction. *DICP*. Sep; 25(9): 1007-8.

Lim et al., 2003 – *Lim, G.E., Li, T., Buttar, H.S.* (2003). Interactions of grapefruit juice and cardiovascular medications: a potential risk of toxicity. *Experimental & Clinical Cardiology*. 2003; 8(2): 99.

Lundahl et al., 1998 – *Lundahl, J.U., Regårdh, C.G., Edgar, B., Johnsson, G.* (1998). The interaction effect of grapefruit juice is maximal after the first glass. *European journal of clinical pharmacology*. Apr 1; 54(1): 75-81.

Maideen, 2019 – *Maideen, N.M.* (2019). Tobacco smoking and its drug interactions with comedications involving CYP and UGT enzymes and nicotine. *World Journal of Pharmacology*. 30; 8(2): 14-25.

Malhotra et al., 2001 – *Malhotra, S., Bailey, D.G., Paine, M.F., Watkins, P.B.* (2001). Seville orange juice-felodipine interaction: comparison with dilute grapefruit juice and involvement of furocoumarins. *Clinical Pharmacology & Therapeutics*. Jan 1; 69(1): 14-23.

Meredith et al., 2004 – *Meredith, P.A., Elliott, H.L.* (2004). Dihydropyridine calcium channel blockers: basic pharmacological similarities but fundamental therapeutic differences. *Journal of hypertension*. Sep 1; 22(9): 1641-8.

Michelucci et al., 1996 – *Michelucci, R., Cipolla, G., Passarelli, D., Gatti, G., Ochan, M., Heinig, R., Tassinari, C.A., Perucca, E.* (1996). Reduced plasma nisoldipine concentrations in phenytoin-treated patients with epilepsy. *Epilepsia*. Nov; 37(11): 1107-10.

Nishio et al., 2005 – *Nishio, S., Watanabe, H., Kosuge, K., Uchida, S., Hayashi, H., Ohashi, K.* (2005). Interaction between amlodipine and simvastatin in patients with hypercholesterolemia and hypertension. *Hypertension research*. Mar; 28(3): 223.

Pakkir Maideen, 2018 – *Pakkir Maideen, N.M.* (2018). Thiazolidinediones and their Drug Interactions involving CYP enzymes. *American Journal of Physiology, Biochemistry and Pharmacology*, 8(2): 47-54.

Pakkir Maideen et al., 2018 – *Pakkir Maideen, N.M., Manavalan, G., Balasubramanian, K.* (2018). Drug interactions of meglitinide antidiabetics involving CYP enzymes and OATP1B1 transporter. *Therapeutic advances in endocrinology and metabolism*. Aug; 9(8): 259-68.

Park et al., 2010 – *Park, C.G., Lee, H., Choi, J.W., Lee, S.J., Kim, S.H., Lim, H.E.* (2010). Non-concurrent dosing attenuates the pharmacokinetic interaction between amlodipine and simvastatin. *Int J Clin Pharmacol Ther*. Aug 1; 48(8): 497-503.

Pedrós et al., 2016 – Pedrós, C., Formiga, F., Corbella, X., Arnau, J.M. (2016). Adverse drug reactions leading to urgent hospital admission in an elderly population: prevalence and main features. *European journal of clinical pharmacology*. Feb 1; 72(2): 219-26.

Penzak et al., 2002 – *Penzak, S.R., Acosta, E.P., Turner, M., Edwards, D.J., Hon, Y.Y., Desai, H.D., Jann, M.W.* (2002). Effect of Seville orange juice and grapefruit juice on indinavir pharmacokinetics. *The Journal of Clinical Pharmacology*. Oct; 42(10): 1165-70.

Pesavento et al., 1996 – *Pesavento, T.E., Jones, P.A., Julian, B.A., Curtis, J.J.* (1996). Amlodipine increases cyclosporine levels in hypertensive renal transplant patients: results of a prospective study. *Journal of the American Society of Nephrology*. Jun 1; 7(6): 831-5.

Rossi et al., 2002 – *Rossi, D.R., Rathbun, R.C., Slater, L.N.* (2002). Symptomatic orthostasis with extended-release nifedipine and protease inhibitors. *Pharmacotherapy: The Journal of Human Pharmacology and Drug Therapy*. Oct; 22(10): 1312-6.Saima et al., 2002 – Saima, S., Furuie, K., Yoshimoto, H., Fukuda, J., Hayashi, T., Echizen, H. (2002). The effects of rifampicin on the pharmacokinetics and pharmacodynamics of orally administered nilvadipine to healthy subjects. *British journal of clinical pharmacology*. Feb; 53(2): 203-6.

Tailor et al., 1996 – *Tailor, S.A., Gupta, A.K., Walker, S.E., Shear, N.H.* (1996). Peripheral edema due to nifedipine-itraconazole interaction: a case report. *Archives of dermatology*. Mar 1; 132(3): 350-2.

Tartara et al., 1991 – *Tartara, A., Galimberti, C.A., Manni, R., Parietti, L., Zucca, C., Baasch, H., Caresia, L., Muck, W., Barzaghi, N., Gatti, G.* (1991). Differential effects of valproic acid and enzyme-inducing anticonvulsants on nimodipine pharmacokinetics in epileptic patients. *British journal of clinical pharmacology*. Sep 1; 32(3): 335-40.

Tirkkonen et al., 2013 – *Tirkkonen, T., Heikkilä, P., Vahlberg, T., Huupponen, R., Laine, K.* (2013). Epidemiology of CYP3A4-Mediated Clopidogrel Drug–Drug Interactions and Their Clinical Consequences. Cardiovascular therapeutics. Dec 1; 31(6): 344-51.

Seo et al., 2014 – *Seo, K.D., Kim, Y.D., Yoon, Y.W., Kim, J.Y., Lee, K.Y.* (2014). Antiplatelet effect of clopidogrel can be reduced by calcium-channel blockers. *Yonsei medical journal*. May 1;55(3): 683-8.

Wang et al., 2016 – *Wang, Y.C., Hsieh, T.C., Chou, C.L., Wu, J.L., Fang, T.C.* (2016). Risks of adverse events following coprescription of statins and calcium channel blockers: a nationwide population-based study. *Medicine*. Jan; 95(2).

Whelton et al., 2017 – *Whelton, P.K., Carey, R.M., Aronow, W.S., Casey, D.E., Collins, K.J., Himmelfarb, C.D., DePalma, S.M., Gidding, S., Jamerson, K.A., Jones, D.W., MacLaughlin, E.J.* (2017). ACC/AHA/AAPA/ABC/ACPM/AGS/APhA/ASH/ASPC/NMA/PCNA guideline for the prevention, detection, evaluation, and management of high blood pressure in adults: a report of the

American College of Cardiology/American Heart Association Task Force on Clinical Practice Guidelines. *Journal of the American College of Cardiology*. May 7; 71(19): e127-248.

Whyte et al., 2016 – *Whyte, I., Buckley, N., Dawson, A.* (2016). Calcium channel blockers. Medicine. Mar 1; 44(3): 148-50.

Wright et al., 2011 – *Wright, A.J., Gomes, T., Mamdani, M.M., Horn, J.R., Juurlink, D.N.* (2011). The risk of hypotension following co-prescription of macrolide antibiotics and calcium-channel blockers. *CMAJ*. Feb 22; 183(3): 303-7.

Yoshimoto et al., 1996 – *Yoshimoto, H, Takahashi, M, Saima, S.* (1996). Influence of rifampicin on antihypertensive effects of dihydropiridine calcium-channel blockers in four elderly patients. Nihon Ronen Igakkai zasshi. *Japanese journal of geriatrics*. Sep; 33(9): 692-6.

Zhu et al., 2014 – *Zhu, Y, Wang, F, Li, Q, Zhu, M, Du, A, Tang, W, Chen, W.* (2014). Amlodipine metabolism in human liver microsomes and roles of CYP3A4/5 in the dihydropyridine dehydrogenation. *Drug Metabolism and Disposition*. Feb 1; 42(2): 245-9.

Published in the Slovak Republic
European Journal of Medicine
Has been issued since 2013.
E-ISSN: 2310-3434
2019, 7(2): 114-119

DOI: 10.13187/ejm.2019.2.114
www.ejournal5.com

Fibroblast Growth Factor 23 Can Serve as an Early Biomarker of Type 2 Diabetic Nephropathy Progression

Athena Myrou [a], Theodoros Aslanidis [b, *], Triantafyllos Didangelos [a], Christos Savopoulos [a], Apostolos Chatzitolios [a], Dimitrios Grekas [c]

[a] AHEPA University Hospital, Thessaloniki, Greece
[b] St. Paul General Hospital, Thessaloniki, Greece
[c] School of Medicine, Aristotle University, Thessaloniki, Greece

Abstract

Fibroblast growth Factors (FGFs) are multifunctional proteins with a wide variety of effects. (1) Aim: The aim of the present study was to examine FGF23 levels in patients with type II diabetic nephropathy (DN) and its correlation with bone metabolism biomarkers (2) Methods-material: Demographic, history, clinical examination and laboratory data were recorded from 80 patients with type II diabetes mellitus and diabetic nephropathy, 31 patients with type II diabetes mellitus and normal renal function and 31 healthy volunteers. (3) Results: GFR in negatively related to FGF23 levels, especially in the progression form early (I, II) to late stage (II, IV) of diabetic nephropathy, while a moderate relation between $1.25(OH)_2D_3$ and FGF23 was found only in stage III and IV of diabetic nephropathy. Weak or no correlation was noticed among other parameters. (4) Conclusions: FGF23 is related to early progression of diabetic nephropathy and to markers of bone metabolism in stage III and IV of DM related chronic renal disease. The latter is not valid for patients with DM with normal renal function. Future research is needed to clarify FGF 23 role as prognostic and therapeutic index.

Keywords: fibroblast growth factor 23, diabetic nephropathy.

1. Introduction

Fibroblast growth Factors (FGFs) are multifunctional proteins with a wide variety of effects. Today, FGFs (over 22) are classified as intracrine, paracrine, and endocrine FGFs by their action mechanisms (Itoh et al., 2015:154).

FGG23 belongs structurally to FGF family and specifically to endocrine FGFs which include FGF19, FGF21, and FGF23. The latter is a 32KD protein (251 amino acids), encoded in FGF23 gene, which in turn is located in chromosome 12p13 and composed by three exons. However, it is functionally included in a group of hormones that regulate phosphorus metabolism called phosphatonins (Amin, 2014).

Several tissues express FGF-23, such as bone tissue, bone marrow vessels, ventrolateral thalamic nucleus, thymus, and lymph nodes. Its principal target is kidney, where it regulates phosphate reabsorption and production of $1,25(OH)_2D_3$ (Liu et al., 2007:18)

In the past decade, FGF23 has emerged as a possible marker (both diagnostic and prognostic) and therapeutic target in several conditions: hereditary diseases such as a) syndromes

* Corresponding author
E-mail addresses: thaslan@hotmail.com (T. Aslanidis)

of FGF23 excess and syndromes of FGF23 deficiency; and b) hypophosphatemic and hyperhosphatemic disorders, acute renal failure and chronic kidney disease (CKD), stoke and subarachnoid hemorrhage, several types of neoplasm and psoriasis (Kendrick J ,2011;11).

High FGF23 levels in patients with CKD are related with progression to ESRD, cardiovascular disease, transfusion needs, infection susceptibility and death (Myrou et al.,2016:16; Tsai et al.,2016:95). In patients with diabetes mellitus (DM), FGF23 has been proposed as possible new marker for gestational DM (Tuzun et al. 2018:62) and has been positively related to resistin in patients with Type II DM (T2DM) (Nakashima et al.,2018:8; Reyes-Garcia ,2014:37, National Kidney Foundation. 2012:60). A previous report relates serum FGF23 to bone metabolic disease and preclinical vascular disease in Type II DM patients (Ketteler et al.2017:92).

The aim of the present study was to examine FGF23 levels in patients with type II diabetic nephropathy (DN) and its correlation with bone metabolism biomarkers [25(OH)D3, 1,25$(OH)_2D_3$, parathormone, calcium, phosphorus, alkaline phosphatase].

2. Materials and Methods

This prospective study was performed in the 1st Propaedeutic Clinic of Internal Medicine at "AHEPA" University Hospital, Thessaloniki, Greece. It was part of a thesis project (Reference No 3377/Academic Year 2017-2018, National Archive of PhD Theses No 44124), approved by AHEPA General University Hospital Research Committee.

In total, 140 persons were included. Eighty (80) patients with T2 DM and renal disease were divided into two groups, depending on the stage of the renal disease, i.e. Group 1 (n1=48): stage I and II DN and Group 2 (n2=32): stage III and IV DN. Another sixty-two (62) volunteers served as control groups: Group 3 (n3=31), patients with T2 DM and normal renal function; and Group 4 (n4=31), healthy individuals. Diagnosis and staging of CKD were in accordance with National Kidney Foundation Disease Outcome Quality Initiative guidelines12-13. All participants were informed about the study's goal and procedures.

Exclusion criteria were: other than T2 DM type of diabetes (e.g. Type 1 DM, drug-induced, pregnancy-related, pancreas diseases related, etc.),presence of acute renal failure, chronic renal failure in renal replacement therapy, hepatic failure, cardiac failure, malignancies, women in reproductive age, thyroid gland disease, systemic inflammatory disease or immunosuppression state.

Demographic, history and clinical examination data were recorded. Creatinine clearance was estimated via 24h urine collection and Glomerular Filtration Ration (GFR) measurement was performed via 51Cr-EDTA (ethylenediamine tetra acetic acid) method. Microalbuminuria (Microalb) level was considered as the average between two 24h urine measurements, collected 10day apart from each other. In case of large difference between the two results, a third urine collection was ordered. FGF23 examination was carried out with sandwich ELISA (Enzyme-linked Immunosorbent Assay) method (ELISA Kits, AMS Biotechnology Ltd®, UK) and the rest of parameters (parathyroid hormone-PTH, serum Phosphorus – P, calcitriol -1,25 $(OH)_2D_3$, calcifediol-25,$(OH)D_3$, alkaline phospatase- ALP and total serum Calcium – Ca) was performed in biochemistry analyst.

Data analysis was performed with SPSS v.21 (IBM® Corp. Armonk, NY, USA) and included initially descriptive statistics analysis, followed by Kolmogorov-Smirnov and Shapiro-Wilk normality tests. After that, multiple comparisons among the 4 groups was carried out via non-parametric Kruskal-Wallis technique; while in case of significant difference ($p<0.05$), further post-hoc analysis was performed. Finally, relation between parameters was examined.

3. Results

Main demographics parameters are displayed in Table 1, while descriptive statistics of the measured parameters are shown in Table 2.

Table 1. Selected demographic characteristics in the four groups. BMI – Body Mass Index, DN-Diabetic Nephropathy. (*p > 0.02)

	Sex (No of male/female)	Age* (mean/standard deviation)	BMI (mean/standard deviation)
Group I (DNI, DNII)	27/21	63 (7)	30(4)
Group II (DNIII, DNIV)	19/13	66.72(6.60)	27.9(4)
Group III (DM)	11/20	64.77(5.31)	31.31(6.25)
Group IV (Healthy)	13/18	60.68(6.11)	28.62(5.1)

Table 2. Descriptive statistics, in the form of mean (standard deviation), of the measured parameters

Parameter	Group I	Group II	Group III	Group IV
ClCr (ml/min)	92.33(23.93)	34.96(14.96)	123.01(14.93)	124.61(18.59)
Ca (mg/dl)	9.26(0.45)	8.66(0.54)	9.37(0.64)	9.42(0.47)
P (mg/dl)	3.92(0.43)	4.92(1.05)	3.64(0.5)	3.55(0.5)
ALP (IU/l)	77.46(25.78)	88.00(20.27)	68.71(16.07)	59.74(14.42)
PTH (pmol/l)	8.08(4.11)	18.41(8.15)	4.70(1.13)	3.99(1.41)
Microalb (mg/l)	1423.88 (2218.53)	4235.47 (2294.08)	9.29(5.85)	7.74(6.02)
$25(OH)D_3$ (ng/ml)	20.67(7.64)	11.86(3.6)	40.63(11.24)	50.98 (16.1)
$1.25(OH)_2D_3$ (pg/ml)	14.56(3.55)	9.51(3.33)	43.33(10.53)	52.45(10.31)
FGF23 (ng/ml)	1.00(0.27)	2.55(1.42)	0.49(0.08)	0.44(0.05)

Kruskal-Wallis test results for all measured parameters and age, revealed significance $p<0.05$, while the results (p) of the post analysis are displayed in Table 3*:*

Relation between change of parameters revealed weak negative relation between $25(OH)D_3$ and FGF23 (Kendall $\tau_b = -0.377$, $p < 0.01$) in Group I, a moderate relation between $1.25(OH)_2D_3$ and FGF23 ($\tau_b=-0.631$, $p < 0.01$) in Group II and a weak negative relation $1.25(OH)_2D_3$ and FGF23 ($\tau_b = -0.453$, $p < 0.01$) Group IV. The rest of the results were either non-significant or without correlation.

Table 3. Adjusted significance (p) in post-hoc comparisons among groups. Group I: DNI+DNII, Group II: DNIII+DNIV, Group II: DM and Group IV: Healthy volunteers.

Parameter	Group IV-Group I	Group IV-Group III	Group IV-Group II	Group I-Group III	Group I-Group II	Group III-Group II
Age	0.13	0.31	0.01	1.00	1.00	1.00
ClCr	<0.001	<0.001	<0.001	<0.001	<0.001	0.97
Ca	<0.001	<0.001	<0.001	1.00	1.00	1.00
P	1.00	0.055	<0.001	0.33	<0.001	<0.001
ALP	0.29	0.007	<0.001	1.00	0.005	0.06
PTH	1.00	<0.001	<0.001	<0.001	<0.001	<0.001
Microalb	1.00	<0.001	<0.001	<0.001	<0.001	0.004
$25(OH)D_3$	0.002	<0.001	<0.001	<0.001	<0.001	0.97
$1.25(OH)_2D_3$	0.006	<0.001	<0.001	<0.001	<0.001	0.89
FGF23	1.00	<0.001	<0.001	<0.001	<0.001	<0.001

Calculated Kendal τ_b between FGF23 and the others parameters in all Groups reveals a moderate relation with ClCr (τ_b = -0.584, $p < 0.001$), PTH (τ_b = 0.583, $p < 0.01$) , Microalb (τ_b = 0.653, $p < 0.01$), 25(OH)D_3 (τ_b = -0.667, $p < 0.01$) and 1.25$(OH)_2D_3$ (τ_b = -0.697, $p < 0.01$).

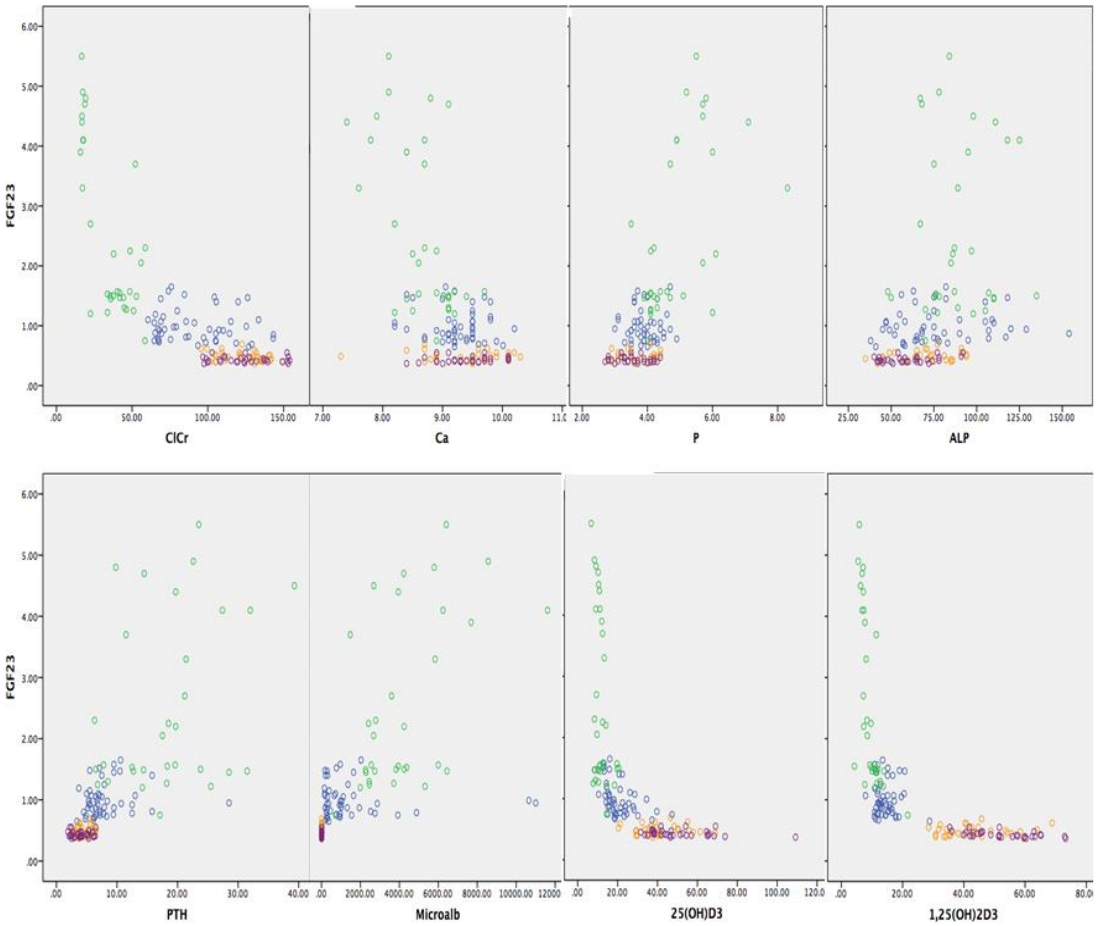

Fig. 1. Scatter plot of FGF23 and other parameters, in all four Groups (blue-Group I, green- Group II, orange-Group III, purple-Group IV)

4. Discussion

From the above as GFR decreases, FGF23 levels increase; the relation is increasingly expressed in stage III and IV DN. Moreover, in these two stages, there is also a weak positive relation between microalbuminuria and FG23. Previous reports have also supported that FGF-23 is a significant independent predictor of renal outcome in patients with macroalbuminuric DN (Titan et al., 2011: 6). The rest of the results seem also to agree with the available literature data.

Recently, there is ever growing research interest about the subject and new data, confirming the present study, are becoming available. In a similar study with 30 type II DM normoalbuminuric patients and 30 sex and age matched healthy individuals as a control group, negative correlation was found between FGF23 and GFR (El-Saeed et al., 2017: 24). Moreover, higher concentration of FGF-23 reduced the odds of early nephropathy in patients with type 2 DM, in comparison with those in more advanced nephropathy (Farías-Basulto et al., 2018: 49).On the contrary, a recent report suggests that other biomarkers, such as tumor necrosis factor receptor 1 (TNFR1), kidney injury molecule-1 (KIM-1) and 3) urinary markers: albumin/creatinine ratio (ACR) may be better indices of renal function decline (Nowak et al., 2018: 93).

Positive correlation was recorded between FGF21 and FGF23 and between each of them and other biochemical parameters, such as cholesterol, triglycerides, LDL cholesterol, creatinine, and urinary albumin excretion (Farías-Basulto et al.,2018: 49). Other studies report strong positive correlation was found between soluble Klotho (s-Klotho) levels and FGF23 levels in DN (Nowak et al., 2018: 93; Inci et al., 2016: 20; Inci et al., 2016: 64). In the same type of patients (DN) FGF23

levels is related also to diastolic dysfunction (Dogan et al., 2016: 48). However, there is no data of which FGF23 increase could predict the presence of diastolic dysfunction (Silva et al., 2019: 20). Also, there is no direct feedback loop between volume status and FGF-23 in hypertension or DN (Humalda et al., 2016: 95); even though that in early stages of CKD, FGF23, as well as lower magnesium levels were significantly and independently associated with higher pulse pressure levels, an established biomarker of cardiovascular morbidity and mortality (Fragoso et al., 2014: 7).

In the present study we did not asses the time course of the markers in interest. Previous studies reported that in the absence of CKD, parathyroid hormone increases earlier than FGF23 when the estimated GFR decreases. The increase in FGF23 is closely associated with a decrease in $1.25(OH)_2D_3$ (Dhayat et al., 2016:20). In early DN though, we cannot claim weather this is also valid.

Finally, the present study did not asses the effect of therapy to FGF23. Yet, there are data that support the negative relation between the former and angiotensin-II receptor blocker therapy (Nowak et al., 2018:93).

5. Conclusion

FGF23 is related to early progression of diabetic nephropathy and to biomarkers of bone metabolism in stage III and IV of DM related chronic renal disease. The latter is not valid for patients with DM with normal renal function. FGF23 levels increase in diabetic nephropathy stage I and II DN, thus serving as a possible prognostic biomarker. However, since DN progression is a multifactorial process further research is needed to clarify its role as independent or as embedded in a prognostic model marker and as a therapeutic target.

6. Acknowledgments

The authors would like to thank Prof. Michalis Karamouzis, Director of Biochemistry Laboratory at AHEPA University Hospital for its help during this project.

7. Conflicts of Interest

The authors declare no conflict of interest.

Author Contributions: Conceptualization, A.M.,T.D and D.G..; methodology, A.M,T.D,C.S,A.C..; formal analysis, T.A; investigation, A.M,T.A.; resources, A.M,T.A..; data curation, T.A..; writing—original draft preparation, T.A.,A.M..; writing—review and editing, T.A..; visualization, T.A; supervision, A.C.,C.S.,T.D, D.G.; project administration, A.C.

Funding: This research received no external funding.

References

Amin, 2014 – *Amin, R.* (2014). Renal Klotho and mineral metabolism, Department of Clinical Science, Intervention and Technology, Division of Renal Medicine, Karolinska Institutet, Stockholm, Sweden. [Electronic resource]. URL: https://openarchive.ki.se/xmlui/bitstream/handle/10616/41939/Thesis_Risul_Amin.pdf?sequence=1 (accessed 10/08/2016).

Dhayat et al., 2016 – *Dhayat, N.A., Ackermann, D., Pruijm, M., Ponte, B., Ehret, G., Guessous, I, Leichtle, A.B., Paccaud, F., Mohaupt, M., Fiedler, G.M., Devuyst, O., Pechère-Bertschi, A., Burnier, M., Martin, P.Y., Bochud, M., Vogt, B., Fuster, D.G.* (2016). Fibroblast growth factor 23 and markers of mineral metabolism in individuals with preserved renal function. *Kidney International*, 90(3): 648-657.

Dogan et al., 2016 – *Dogan, B, Arikan, I.H., Guler, D., Keles, N., Isbilen, B., Isman, F., Oguz, A.* (2016). Fibroblast growth factor-23 but not sKlotho levels are related to diastolic dysfunction in type 1 diabetic patients with early diabetic nephropathy. *International journal of Urology and Nephrology,* 48(3): 399-407.

El-Saeed et al., 2017 – *El-Saeed, A.M., El-Mohasseb, G.F. (2017).* Circulating Fibroblast Growth Factors 21 and 23 as Biomarkers of Progression in Diabetic Nephropathy in Type 2 Diabetes with Normoalbuminuria. *Egyptian Journal of Immunology,* 24(2): 93-99.

Farias-Basulto et al., 2018 – *Farías-Basulto, A., Martínez-Ramírez, H.R., Gómez-García, E.F., Cueto-Manzano, A.M., Cortés-Sanabria, L., Hernández-Ramos, L.E., Ramírez-López, G., Mendoza-Carrera, F.* (2018). Circulating Levels of Soluble Klotho and Fibroblast

Growth Factor 23 in Diabetic Patients and Its Association with Early Nephropathy. *Archives of Medical Research,* 49(7): 451-455.

Fragoso et al., 2014 – *Fragoso, A, Silva, A.P., Gundlach, K., Büchel, J., Neves, P.L.* (2014). Magnesium and FGF-23 are independent predictors of pulse pressure in pre-dialysis diabetic chronic kidney disease patients. *Clinical Kidney Journal,* 7(2): 161-166.

Humalda et al., 2016 – *Humalda, J.K., Seiler-Muler, S., Kwakernaak, A.J., Vervloet, M.G., Navis, G., Fliser, D., Heine, G.H., de Borst, M.H.* (2016). Response of fibroblast growth factor 23 to volume interventions in arterial hypertension and diabetic nephropathy. *Medicine (Baltimore),* 95(46): e5003.

Inci et al., 2016 – *Inci, A, Sari, F, Coban, M, Olmaz, R, Dolu, S, Sarıkaya, M, Yılmaz, N.* (2016). Soluble Klotho and fibroblast growth factor 23 levels in diabetic nephropathy with different stages of albuminuria. *Journal of Investigational Medicine,* 64(6): 1128-1133.

Inci et al., 2016 – *Inci, A., Sari, F., Olmaz, R., Coban, M., Dolu, S., Sarikaya, M., Ellidag, H.Y.* (2016). Soluble Klotho levels in diabetic nephropathy: relationship with arterial stiffness. *European Review in Medical Pharmacology Science*, 20(15): 3230-3237.

Itoh et al., 2015 – *Itoh, N., Ohta, H., Konishi, M.* (2015). Endocrine FGFs: physiology, evolution, pathophysiology and pharmacotherapy. *Frontiers in Endocrinology (Lausanne),* 29(6): 154.

Kendrick et al., 2011 – *Kendrick, J., Cheung, A.K., Kaufman, J.S., Greene, T., Roberts, W.L., Smits, G., Chonchol, M., HOST Investigators* (2011). FGF-23 associates with death, cardiovascular events, and initiation of chronic dialysis. *Journal of American Society of Nephrology*, 22(10): 1913-1922.

Ketteler et al., 2017 – *Ketteler, M., Block, G.A., Evenepoel, P., Fukagawa, M., Herzog, C.A., McCann, L. et al.* (2017). Executive Summary of the KIDOQI Chronic Kidney Disease – Mineral and Bone Disorder guideline update: what's changed, and why it matters. *Kidney International,* 92(1): 26-36.

Liu et al., 2007 – *Liu, S., Quarles, L.D.* (2018). How fibroblast growth factor 23 works. *Journal of American Society of Nephrology*, *18:* 1637-1647.

Myrou et al.,2016 – *Myrou, A., Aslanidis, T., Grekas, D.* (2016). Fibroblast Growth Factor 23: Review of its role in clinical medicine. *European Journal of Medicine,* 14(4): 91-99.

Nakashima et al., 2018 – *Nakashima, A., Yokoyama, K., Kawanami, D., Ohkido, I., Urashima, M., Utsunomiya, K., Yokoo, T.* (2018). Association between resistin and fibroblast growth factor 23 in patients with type 2 diabetes mellitus. *Scientific Reports*, 8(1): 13999.

National Kidney Foundation, 2012 – National Kidney Foundation (2012). KDOQI Clinical Practice Guideline for Diabetes and CKD: 2012. *American Journal of Kidney Disease,* 60(5): 850-886.

Nowak et al.,2018 – *Nowak, N., Skupien, J., Smiles, A.M., Yamanouchi, M., Niewczas, M.A., Galecki, A.T., Duffin, K.L., Breyer, M.D., Pullen, N., Bonventre, J.V., Krolewski, A.S.* (2018). Markers of early progressive renal decline in type 2 diabetes suggest different implications for etiological studies and prognostic tests development. *Kidney International,* 93(5): 1198-1206.

Reyes-Garcia et al., 2014 – *Reyes-Garcia, R, Garcia-Martín, A, García-Fontana, B, Morales-Santana, S, Rozas-Moreno, P., Muñoz-Torres, M.* (2014) FGF23 in type 2 diabetic patients: relationship with bone metabolism and vascular disease. *Diabetes Care,* 37(5): e89-90.

Silva et al.,2019 – *Silva, A.P., Mendes, F., Carias, E., Gonçalves, R.B., Fragoso, A., Dias, C., Tavares, N., Café, H.M., Santos, N., Rato, F., Leão Neves, P., Almeida, E.* (2019). Plasmatic Klotho and FGF23 Levels as Biomarkers of CKD-Associated Cardiac Disease in Type 2 Diabetic Patients. *International Journal of Molecular Science,* 20(7), pii: E1536.

Titan et al., 2011 –*Titan, S.M., Zatz, R., Graciolli, F.G., dos Reis, L.M., Barros, R.T., Jorgetti, V., Moysés, R.M.* (2011). FGF23 as a predictor of renal outcome in diabetic nephropathy. *Clinical Journal of American Society of Nephrolology,* 6: 241-247.

Tsai et al., 2016 –*Tsai, M.H., Leu, J.G., Fang, Y.W., Liou, H.H.* (2016). High Fibroblast Growth Factor 23 Levels Associated with Low Hemoglobin Levels in Patients with Chronic Kidney Disease Stages 3 and 4. *Medicine (Baltimore),* 95(11): e3049.

Tuzun et al., 2018 – *Tuzun, D., Oguz, A., Aydin, M.N., Kurutas, E.B., Ercan, O., Sahin, M., Ünsal, V., Ceren, I., Akçay, A., Gul, K.* (2018). Is FGF-23 an early indicator of atherosclerosis and cardiac dysfunction in patients with gestational diabetes? *Archives of Endocrinology and Metabolism,* 62(5): 506-513.

Published in the Slovak Republic
European Journal of Medicine
Has been issued since 2013.
E-ISSN: 2310-3434
2019, 7(2): 120-130

DOI: 10.13187/ejm.2019.2.120
www.ejournal5.com

Physicochemical and Microbiological Characteristics of Thermal Healing Spring Waters in the Districts of Varna and Burgas, Black Sea Region, Bulgaria

Nedyalka Valcheva [a, *]

[a] Trakia University, Stara Zagora, Bulgaria

Abstract

Defined are the physicochemical properties of healing thermal spring waters in the area of Burgas District. It is shown that according to 18 controlled parameters included in the research, the thermal healing spring water village of Shivarovo, thermal healing spring water village of Polyanovo, fulfill the required conditions for drinking water.

The spring waters from the given four water sources are characterized by microbiological indicators, as the pathogenic micro-organisms are defined by the membrane method. It is established that thermal healing spring water Burgas Mineral baths, thermal healing spring water village of Shivarovo, thermal healing spring water of village of Polyanovo, fulfill the standard requirements. The healing water of village Judge, District ofBurgas does not conform to the physicochemical indicators given for fluorides, and microbiological indicators with regards to coliform bacteria, *Escherichia coli* and enterococci.

Defined are the physicochemical properties of healing thermal and non-thermal spring waters in the area of Varna District. It is shown that according to 18 controlled parameters included in the research, the thermal healing spring water drilling №P-83xKK "Saints Constantine and Helena", thermal healing spring water P-1x "Aquarium", thermal healing spring water P-106 x "Dom Mladost", thermal healing spring water P-161x Varna at "Primorski" swimming pool, fulfill the required conditions for drinking water.

The spring waters from the given four water sources are characterized by microbiological indicators, as the pathogenic micro-organisms are defined by the membrane method. It is established that thermal healing spring water drilling №P-83xKK "Saints Constantine and Helena", thermal healing spring water P-1x "Aquarium", thermal healing spring water P-106 x "Dom Mladost", thermal healing spring water P-161x Varna at "Primorski" swimming pool, fulfill the standard requirements. "The healing water" of village Goren Chiflik, District of Varna does not conform with the physicochemical indicators given for nitrates, and microbiological indicators with regards to coliform bacteria and enterococci.

Keywords: spring water, drinking water, physicochemical properties, microbiological indicators.

1. Introduction

Bulgaria is one of the richest in mineral springs countries in Europe. It takes second place after Iceland. Their total number is around 225.

[*] Corresponding author
E-mail addresses: neli_naneva@abv.bg (N. Valcheva)

In Bulgaria there are mineral and spring waters, which are not subjected to physicochemical and microbiological control by the Regional Health Inspectorate and microbiological control byt they are the most use springs for drinking from the population. Similar springs are located in the territory of Haskovo District, Stara Zagora District, Varna District (Valcheva et al., 2013).

Many of these sources do not carry out physicochemical and microbiological studies bu are used for drinking and household needs.

Although water is an unfavorable environment for the development of microorganisms and for the development of microorganisms, studies by many authors including heir, own, that microorganisms with valuable properties (enzymes, antibiotics, thermopile can acidophilic strains) are in mineral and non – thermal spring waters. This was proved by the results obtained from the experimental work carried out to determinal the microflora of medicinal and spring waters in Haskovo , Stara Zagora, Plovdiv (Tumbarski et al., 2014) and Varna region (Valcheva, Ignatov, 2019).

Isolated bacteria from the healing and spring regions have been identified by *Bacillus subtilis, Bacillus cereus, Bacillus thuringiensis, Bacillus methylotrophicus, Aeromonashydrophila.*

The isolated bacteria from the healing and spring waters in the Plovdiv region have been identified by molecular genetic methods suchas *Aeromonassobria, Klebsiellaoxytoca, Bacillus amyloliquefacienssubsp. plantarum, Bacillus thuringiensis, Bacillus cereus* (Valcheva et al., 2013, 2014).

Strains with high proteolytic, lipolytic and amylolytic activity were selected (Valcheva et al., 2013, 2014).

Antimicrobial activity of the strains of *Bacillus* sp., against the saprophytic and pathogenic microorganisms was detected: *Penicillium sp., Fusariummoliniforme, Rhizopus sp., Aspergillusniger, Aspergillusoryzae, Aspergillusawamori, Mucorsp. Enterococcus faecalis*, in the process of development and growt of the four *Bacillus – Bacillus cereus, Bacillus thuringiensis, Bacillus subtilis, Bacillus methylotrophicus*are the the most active strains – *Bacillus* methylotrophicus PY5, *Bacillus cereus LH1*, *Bacillus cereus WIF15* и *Bacillus thuringiensis B62* (Valcheva et al., 2013, 2014).

Pathogenic bacteria exhibit resistance and 4 retain their vitality in the process of develop pment and interaction between them and the strains of *Bacillus sp.* and at 37C°.

A relatively low bactericidal effect was demonstrated against the (Gr+) bacterium *Enterococcus faecalis*. The isolated strains are likely to have a higher inhibitory ability agains(Gr -) bacteria compared to (Gr+) bacteria (Valcheva et al., 2013, 2014).

The yeasts used in the genus *Candida* exhibit a simulating effect of two of *Bacillus sp. – Bacillus methylotrophicus PY5*, and *Bacillus cereus LH1*. This indicates that synergism has occurred between these microorganisms (Valcheva et al., 2013, 2014).

Based on their location are observed certain specifics. The ones to the north of Balkan are with lower temperatures, and are reached usually via drilling. Their total number is almost half the amount of the ones to the south of Old Mountain. There are around 148 known springs from Southern Bulgaria. Predominant in them are the ones with natural origin and higher temperature of the water. The causes for that lie in the combination between hydrological conditions of the continuing tectonic processes in the Earth's crust (Ignatov et al., 2012). By their nature the springs can be separated in cold, warm and hot springs. The first group includes the ones with temperature up to 37°C, the second one ranges between 37°C and 60°C, and the third one with over 60°C. The hottest mineral spring in Bulgaria is the one at Sapareva Banya with temperature of 101,4°C. The springing waters have different mineralogical characteristics. Their content is defined by the ones of the rocks, where the water has been flowing through, and the solubility of the minerals within them (Ignatov et al., 2012).

Mineral springs of Burgas

Burgas is the second largest seaside town in Bulgaria, located on the Southern Black Sea coast. In addition to the beautiful sea and spa – pious beaches, Burgas offers great opportunities for balneological treatment with mineral water, characteristic sea mud and lye.

This is one of the oldest balneological centers in Bulgaria. Mineral water is suitable for the treatment and prevention of diseases of the musculoskeletal system, peripheral nervous system, chronic gastritis and pyelonephritis infertility, gout.

Water is also beneficial for strengthening the general state of the body.

Mineral spring of District Sudievo

Sudievo is a village in southeastern Bulgaria. It is located in Aytos municipality. Water helps diseases of urinary system, disorders of locomotory system, endocrine diseases. It is suitable for daily use as drinking water. This water in Sudievo is hydrocarbonate, sodium, but contains fluoride. According to the requirements for drinking water, not mineral water, water should contains not more than 1.5 milligrams per liter of fluoride. The water in Sudievo contains much more in quantity than this chemical element.What those who consume this water need to know is that excessive ingestion of this fluoride per day can accordingly damage tooth enamel in young children.In the northern part of Aytosko Polje there are several mineral springs along the fault line: the "Smelly Fountain" near the village of Shivarovo and those near the villages of Cherry, Yabulchevo and Saedinenie. Geothermal water with a flow rate of 30 L/s and a temperature of 51 °C emerges from deep drilling in the village of Polyanovo, which flows freely without being used. Analyses show that the sources have extremely good healing properties.

Medicinal properties of water: in diseases of the locomotory system, gastrointestinal, liver-bile and renal diseases.

Mineral springs of Varna district

Health resort "Saints Constantine and Helena" is the first Bulgarian resort at Black Sea. One of the most important conditions for the resort development is the availability of 7 mineral springs with no analogue in Europe. They are calcium-magnesium, with low mineralization and come from depth of 1800 to 2050 meters under the ground with total flow rate of 175 l/sec. The temperature of the water varies between 40 and 60 degrees centigrade, it can heal successfully cardiovascular diseases, the endocrine system, illnesses of the musculoskeletal system and the functional nervous system, myocardial infarction.

Thermal healing spring, city of Varna 2 (P-1x "Aquarium")

Healing prophylactic properties of the mineral water-the drinking thermal cure has positive influence over gastro-intestinal tract, biliary liver system and kidney excretory system. The presence of calcium proves to be suitable for application of mineral water for treatment of dental caries, as well as osteoporosis of any kind.

Thermal healing spring Varna (P-106 x "Dom Mladost")

The water comes via drilling with depth 1980 m, and it is thermal with temperature of 47°C. It cures conditions of cardiovascular system, of peripheral nervous system, digestive system, gynaecological diseases and post-traumatic stress disorders.

Non-thermal healing spring "Healing water", village of Goren Chiflik

Healing water that can be ignited and can burn, it springs up in the locality Botevo near Dolni Chiflik. That is due to the methane contained within it. The water comes up years ago after drilling for natural gas. The phenomenal liquid springs up like a geyser from 600 meters depth. Research shows that the water contains around 30% iodine and helps for gastro-intestinal conditions, arthritis, skin and eye diseases.

2. Materials and methods

In the work are used thermal healing waters from the district of Burgas – thermal healing spring Burgas Mineral baths with water temperature of 41°C, thermal healing spring village of Shivarovo with water temperature of 47°C, thermal healing spring village of Polyanovo with water temperature of 51°C, thermal healing spring village of Judge with water temperature of 51°C.

Nutrient media

Nutrientagar (MPA) with contents (in %) – meat water, peptone – 1 %, agar –agar – 2 % . Endo's Medium (for defining of *Escherichia coli*and coliform bacteria) with contents (g/dm^3) – peptone– 5,0 ; triptone– 5,0 ; lactose – 10,0 ; Na_2SO_3 – 1,4 ; K_2HPO_4– 3,0 ; fuchsine– 0,14 ; agar – agar– 12,0 pH 7,5 – 7,7 .

Nutrient gelatine (MPD) (for defining of *Pseudomonas aeruginosa*) with contents (in %) – Peptic digest of animal tissue; 25 % gelatin ; pH = 7, 0 – 7, 2.

Medium for defining of enterococci (esculin – bile agar).

Medium for defining of sulphite reducing bacteria (Iron Sulfite Modified Agar).

Wilson-Bleer medium (for defining of sulphite reducing spore anaerobes (*Clostridium perfringens*) with contents(g/dm^3) – 3% Nutrient agar; 100 cm^{3}20% solution Na_2SO_3 ; 50 cm^3 20 % glucose solution; 10 cm^3 8% solution ofFe_2SO_4.

Methods for analysis

Methods for physicochemical analysis

Method for determination of color according to Rublyovska Scale – method by Bulgarian State Standard (BDS) 8451: 1977;

Method for determination of smell at 20°C — method BDS 8451 : 1977 technical device – glass mercury thermometer, conditions № 21;

Method for determination of turbidity - EN ISO 7027, technical device turbidimeter type TURB 355 IR ID № 200807088;

Method for determination of pH – BDS 3424 : 1981, technical device pH meter type UB10 ID № UB10128148;

Method for determination of oxidisability – BDS 3413 : 1981;

Method for determination of chlorides – BDS 3414 : 1980;

Method for determination of nitrates – Validated Laboratory Method (VLM) – NO_3 – № 2, technical device photometer ,, NOVA 60 A " ID № 08450505;

Method for determination of nitrites – VLM NO_3 –№ 3, technical device photometer ,, NOVA 60 A " ID № 08450505;

Method for determination of ammonium ions – VLM - NH_4 – № 1, technical device photometer ,, NOVA 60 A " ID № 08450505;

Method for determination of general hardness – BDS ISO 6058;

Method for determination of sulphates – VLM - SO_4 – № 4, technical device photometer ,, NOVA 60 A " ID № 08450505;

Method for determination of calcium – BDS ISO 6058;

Method for determination of magnesium – BDS 7211: 1982;

Method for determination of phosphates – VLM - PO_4 – № 5, technical device photometer ,, NOVA 60 A " ID № 08450505;

Method for determination of manganese – VLM – Mn – № 7, technical device photometer ,, NOVA 60 A " ID № 08450505;

Method for determination of iron – VLM – Fe – № 6, technical device photometer ,, NOVA 60 A " ID № 08450505;

Method for determination of fluorides – VLM – F – № 8, technical device photometer, NOVA 60 A " ID № 08450505;

Method for determination of electrical conductivity – BDS EN 27888, technical device – conductivity meter inoLabcond 720 ID № 11081137.

Methods for determination of microbiological indicators

Methods for evaluation of microbiological indicators according to Ordinance № 9/2001, Official State Gazette, issue 30, and decree № 178/23.07.2004 about the quality of water, intended for drinking purposes.

Method for determination of *Escherichia coli* and coliform bacteria –BDSEN ISO 9308 – 1: 2004;

Method for determination of enterococci – BDS EN ISO 7899 – 2;

Method for determination of sulphite reducing spore anaerobes – BDS EN 26461 – 2: 2004;

Method for determination of total number of aerobic and facultative anaerobic bacteria – BDS EN ISO 6222: 2002;

Method for determination of *Pseudomonas aeruginosa* – BDS EN ISO 16266: 2008.

Determination of coli – titre by fermentation method – Ginchev's method

Determination of coli – bacteria over Endo's medium – membrane method.

Determination of sulphite reducing anaerobic bacteria (*Clostridium perfringens*) – membrane method.

3. Results and discussion

3.1. Results of mineral springs in Burgas region

It is done a comparative physicochemical analysis of mineral spring waters at the territory of Burgas District by the main indicators (colour according to Rublyovska Scale, smell at 20°C,

turbidity, pH, oxidisability, chlorides, nitrates, nitrites, ammonium ions, general hardness, sulphates, calcium, magnesium, phosphates, manganese, iron, fluorides, electrical conductivity). The results from these examinations are given in Table 1.

The trial data reveal that thermal healing spring water village of Shivarovo, thermal healing spring water village of Polyanovo swimming pool are in compliance with the controlled parameters set out in Ordinance № 9/2001, Official State Gazette, issue 30, and decree № 178 / 23.07.2004 about the quality of water, intended for drinking purposes(RZI (Regional Health Inspection) – Burgas).

Table 1. Comparison of the examined spring waters in Burgas District by physicochemical properties

Controlled parameter	Measuring unit	Maximum Limit Value	Result Burgas Mineral baths	Result Shivarovo	Result Polyanovo	Result Judge
1. Color according to Rublyovska Scale	Chromaticity Values	Acceptable to consumers	Acceptable to consumers	Acceptable to consumers	Acceptable to consumers	Acceptable to consumers
2. Smell at 20°C	Rating	Acceptable to consumers	Acceptable to consumers	Acceptable to consumers	Acceptable to consumers	Acceptable to consumers
3. Turbidity	NTU	Acceptable to consumers	Acceptable to consumers	Acceptable to consumers	Acceptable to consumers	Acceptable to consumers
4. pH indicator	pH values	≥ 6,5 и ≤ 9,5	9,95	9	9,11	9,1
5. Oxidisability	mgO_2/dm^3	5,0	0,50	0,4	0,5	0,5
6. Chlorides	mg/ dm^3	250	30,7	26,3	26,3	26,0
7. Nitrates	mg/ dm^3	50	0,2	2,10	0,1	0,15
8. Nitrites	mg/ dm^3	0,50	0,007	0,00	0,006	0,005
9. Ammonium ions	mg/ dm^3	0,50	0,111	0,150	0,154	0,158
10. General hardness	$mgekv/ dm^3$	12	0,4	0,4	0,4	0,4
11. Sulphates	mg/ dm^3	250	37	34	35	36
12. Calcium	mg/ dm^3	150	120	118	116	117
13. Magnesium	mg/ dm^3	80	68	66	67	66
14. Phosphates	mg/ dm^3	0,5	0,015	0,016	0,016	1,018
15. Manganese	mg/ dm^3	50	0,0005	0,0008	0,0007	0,0009
16. Iron	$\mu g/ dm^3$	200	0,0016	0,0020	0,0022	0,0037
17. Fluorides	mg/ dm^3	1,5	7,73	0,4	1,48	5,5
18. Electrical conductivity	$\mu S/ dm^3$	2000	633	620	612	615

For the same spring waters are determined their microbiological indicators by the membrane method. In Table 2 are shown the experimental studies from the determination of total number of mesophilic aerobic and facultative anaerobic bacteria.

Table 2. Determination of total number of mesophilic aerobic and facultative anaerobic bacteria

Examined water source	Indicator, cfu/cm^3
1. Thermal healing spring Burgas Mineral baths with water temperature of 41°C	6 ± 1
2. Thermal Healing Spring village of Shivarovo with water temperature of 41 °C	11 - 17
3. Thermal Healing Springvillage of Polyanovo with water temperature of 51°C	5 - 8
4. Thermal Healing Springvillage of Judge with water temperature of 51 °C	120-150

According to the standard requirements from the examined water samples from the four springs, the water is clean.

The presence of coliforms and *Escherichia coli* is determined by the membrane method, and according to Ginchev's method. The trial results (Table 3 and Table 4) reveal that thermal healing spring Burgas Mineral baths with water temperature of 41°C, thermal healing spring village of Shivarovo with water temperature of 41°C, thermal healing spring village of Polyanovo with water temperature of 51°C swimming pool, are in compliance with the requirements for presence of coli bacteria. Thermal healing spring village of Polyanovo does not comply with the requirements for presence of coliform bacteria and enterococci. The given results are also confirmed by the analyses via the membrane method (Table 4). All the remaining indicators are determined by the membrane method.

Table 3. Coli – titre of thermal healing spring waters

Name of water source	Coli - titre	Culture volumes 50 cm³	Culture volumes 10 cm³	Culture volumes 10 cm³	Culture volumes 10 cm³	Culture volumes 10 cm³	Culture volumes 10 cm³
1. Thermal healing spring Burgas Mineral baths with water temperature of 41°C	> 100	–	–	–	–	–	–
2. Thermal Healing Spring village of Shivarovo with water temperature of 41 °C	> 100	–	–	–	–	–	–
3. Thermal Healing Springvillage of Polyanovo with water temperature of 51°C	> 100	–	–	–	–	–	–
4. Thermal Healing Spring village of Judge with water temperature of 51 °C	80	+ Acid	+ Acid	+ Acid and gas	+ Acid and gas	+ Acid and gas	–

Table 4. Microbiological indicators of spring waters in Burgas District

Indicators	Measuring unit	Thermal healing spring Burgas Mineral baths with water temperature of 41°C	Thermal healing springvillage of Shivarovo with water temperature of 41 °C	Thermal healing spring village of Polyanovo with watertemperature of 51 °C	Thermal healing springvillage of Judge with water temperature of 51 °C
Coliforms	cfu/cm³	0/100	0/100	0/100	10/100
Escherichiacoli	cfu/cm³	0/100	0/100	0/100	10/100
Enterococci	cfu/cm³	0/100	8/100	0/100	8/100

Sulphite reducing anaerobic bacteria*(Clostridium perfringens)*	cfu/cm³	0/100	0/100	0/100	0/100
Pseudomonas aeruginosa	cfu/cm³	0/250	0/250	0/250	0/250

Based on the conducted physicochemical and microbiological evaluations it is established that from the four examined springs at the territory of Burgas District by physicochemical parameters only thermal healing spring water village of Shivarovo, thermal healing spring water village of Polyanovo swimming pool correspond to all controlled parameters according to Ordinance № 9 / 2001, Official State Gazette, issue 30, and decree № 178 / 23.07.2004 about the quality of water, intended for drinking purposes. With regards to microbiological parameters thermal healing water Burgas Mineral baths, thermal healing spring village of Shivarovo, thermal healing spring water village of Polyanovo swimming pool are in compliance with the requirements for drinking water.

3.2. Results of mineral springs in Varna region

It is done a comparative physicochemical analysis of mineral spring waters at the territory of Varna District by the main indicators (colour according to Rublyovska Scale, smell at 20°C, turbidity, pH, oxidisability, chlorides, nitrates, nitrites, ammonium ions, general hardness, sulphates, calcium, magnesium, phosphates, manganese, iron, fluorides, electrical conductivity). The results from these examinations are given in Table 5.

The trial data reveal that thermal healing spring water drilling №P-83xКК "Saints Constantine and Helena", thermal healing spring water P-1x "Aquarium", thermal healing spring water P-106 x "Dom Mladost", thermal healing spring water P-161x at "Primorski" swimming pool are in compliance with the controlled parameters set out in Ordinance № 9 / 2001, Official State Gazette, issue 30, and decree № 178/23.07.2004 about the quality of water, intended for drinking purposes. The "Healing water", village of Goren Chiflik, District of Varna is not in compliance with regards to nitrates – higher than 130 milligrams per liter (RZI (Regional Health Inspection) – Varna).

Table 5. Comparison of the examined spring waters in Varna District by physicochemical properties

Controlled parameter	Measuring unit	Maximum Limit Value	Result Varna 1 (drilling №P-83xКК „Saints Constantine and Helena")	Result Varna 2 (P-1x "Aquarium")	Rsult Varna 3 (P-106 x „Dom Mladost")	Result Varna 4 (P-161x Varna "Primorski" swimming pool)
1. Colour according to Rublyovska Scale	Chromaticity Values	Acceptable to consumers	Acceptable to consumers	Acceptable to consumers	Acceptable to consumers	Acceptable to consumers
2. Smell at 20°C	Rating	Acceptable to consumers	Acceptable to consumers	Acceptable to consumers	Acceptable to consumers	Acceptable to consumers
3. Turbidity	NTU	Acceptable to consumers	Acceptable to consumers	Acceptable to consumers	Acceptable to consumers	Acceptable to consumers
4. pH	pH единици	≥ 6,5 и ≤ 9,5	7,79	7,6	9,48	9,46
5. Oxidisability	mgO_2/dm^3	5,0	2,1	1,6	1,9	1,2
6. Chlorides	mg/ dm³	250	64,41	104	130	96
7. Nitrates	mg/ dm³	50	0,9	2,9	2,1	4,9
8. Nitrites	mg/ dm³	0,50	0,04	0,04	0,00	0,004
9. Ammonium ions	mg/ dm³	0,50	0,04	0,29	0,21	0,85
10. General hardness	mgekv/ dm³	12	4	3,9	11,5	11,5

11. Sulphates	mg/ dm3	250	36,21	77	62	76
12. Calcium	mg/ dm3	150	53,11	43	118	120
13. Magnesium	mg/ dm3	80	32,83	27	68	67
14. Phosphates	mg/ dm3	0,5	0,02	0,03	0,02	0,02
15. Manganese	mg/ dm3	50	0,01	0,001	0,009	0,05
16. Iron	µg/ dm3	200	0,05	59	481	<5
17. Fluorides	mg/ dm3	1,5	0,43	0,71	0,55	0,62
18. Electrical conductivity	µS/ dm3	2000	694	768	350	350

For the same spring waters are determined their microbiological indicators by the membrane method. In Table 6 are shown the experimental studies from the determination of total number of mesophilic aerobic and facultative anaerobic bacteria.

Table 6. Determination of total number of mesophilic aerobic and facultative anaerobic bacteria

Examined water source	Indicator, cfu/cm3
1. Thermal healing spring Varna 1 (drilling №P-83x Health Resort „Saints Constantine and Helena") with water temperature of 48 °C	4± 1
2. Thermal Healing Spring Varna 2 P-1x "Aquarium") with water temperature of 47 °C	5 - 7
3. Thermal Healing Spring P-106 x „Dom Mladost" with water temperature of 40 °C	5 ± 1
4. Thermal Healing Spring P-161x Varna at "Primorski" swimming pool with water temperature of 50 °C	5-8
5. Healing spring „Healing water" village of Goren Chiflik	170-180

According to the standard requirements from the examined water samples from the four springs, the water is clean (Murgov, Denkova, 2010).

The presence of coliforms and *Escherichia coli* is determined by the membrane method, and according to Ginchev's method. The trial results (Table 7 and Table 8) reveal that thermal healing spring drilling №P-83x Health Resort "Saints Constantine and Helena" with water temperature of 48°C, thermal healing spring P-1x "Aquarium" with water temperature of 47°C, thermal healing spring P-106 x "Dom Mladost" with water temperature of 40°C, thermal healing spring P-161x Varna ate "Primorski" swimming pool, are in compliance with the requirements for presence of coli bacteria. Non-thermal healing spring "Healing water" village of Goren Chiflik does not comply with the requirements for presence of coliform bacteria and enterococci. The given results are also confirmed by the analyses via the membrane method (Table 4). All the remaining indicators are determined by the membrane method.

Table 7. Coli – titre of thermal healing spring waters

Name of water source	Coli – titre	Culture volumes 50cm3	Culture volumes 10cm3	Culture volumes 10cm3	Culture volumes 10cm3	Culture volumes 10cm3	Culture volumes 10cm3
1. Thermal healing spring Varna 1 (drilling №P-83x Health Resort„Saints Constantine nd Helena") with water temperature of 48°C	> 100	–	–	–	–	–	–

2. Thermal Healing Spring Varna 2 P-1x "Aquarium“) with water temperature of 47°C	> 100	–	–	–	–	–	–
3. Thermal healing spring P-106 x „Dom Mladost“ with water temperature of 40°C	> 100	–	–	–	–	–	–
4. Thermal healing spring P-161x Varna at "Primorski" swimming pool with water temperature of 50°C	> 100	–	–	–	–	–	–
5. Non-thermal healing spring „Healing water“ village of Goren Chiflik	70	+ Acid	+ Acid	+ Acid and gas	+ Acid and gas	+ Acid and gas	+ Acid and gas

Table 8. Microbiological indicators of spring waters in Varna District

Indicators	Measuring unit	Thermal healing spring Varna 1 (drilling №P-83x Health Resort „Saints Constantine and Helena”) with water temperature of 48 °C	Thermal healing spring Varna 2 P-1x "Aquarium“) with water temperature of 47 °C	Thermal healing spring P-106 x „Dom Mladost“ with water temperature of 40 °C	Thermal healing spring P-161x Varna at ”Primorski" swimming pool with water temperature of 50 °C	Non-thermal healing spring „Heling watera“ village of Goren Chiflik
Coliforms	cfu/cm³	0/100	0/100	0/100	0/100	15/100
Escherichia coli	cfu/cm³	0/100	0/100	0/100	0/100	15/100
Enterococci	cfu/cm³	0/100	0/100	0/100	0/100	10/100
Sulphite reducing anaerobic bacteria *(Clostridium perfringens)*	cfu/cm³	0/100	0/100	0/100	0/100	0/100
Pseudomonas aeruginosa	cfu/cm³	0/250	0/250	0/250	0/250	0/250

Based on the conducted physicochemical and microbiological evaluations it is established that from the five examined springs at the territory of Varna District only thermal spring water, drilling №P-83xKK “Saints Constantine and Helena”, thermal healing spring water P-1x "Aquarium“, thermal healing spring water P-106 x “Dom Mladost”, thermal healing spring water

P-161x Varna at “Primorski” swimming pool correspond to all controlled parameters according to Ordinance № 9/2001, Official State Gazette, issue 30, and decree № 178/23.07.2004 about the quality of water, intended for drinking purposes, and with regards to microbiological parameters thermal healing water, drilling №P-83xKK “Saints Constantine and Helena”, thermal healing spring water P-1x "Aquarium“, thermal healing spring water P-106 x “Dom Mladost”, thermal healing spring water P-161x at “Primorski” swimming pool are in compliance with the requirements for drinking water.

“Healing water” village of Goren Chiflik, Varna District does not comply with physicochemical indicators given for nitrates – them being higher than 130 milligrams per litre (Regional Health Inspection (RZI) – Varna), and with regards to microbiological indicators it is not in compliance with the requirements for presence of coliform bacteria and enterococci. According to Ordinance № 9/2001, Official State Gazette, issue 30, and decree № 178/23.07.2004 about the quality of water, intended for drinking purposes, it is not suitable for drinking.

4. Conclusion

The research shows the effects of hot mineral water from Burgas and Varna Districts, Bulgaria. There are the results with:

- Comparison of the examined spring waters in Burgas and Varna Districts by physicochemical properties;
- Determination of total number of mesophilic aerobic and facultative anaerobic bacteria;
- Coli – titre of thermal healing spring waters;
- Microbiological indicators of spring waters in Burgas and Varna Districts.

References

Gluhchev et al., 2015 – *Gluhchev, G., Ignatov, I., Karadzhov, S., Miloshev, G., Ivanov, N., Mosin, O.V.* (2015). Electrochemically Activited Water. Biophysical and Biological Effects of Anolyte and Catholyte as Types of Water. *Journal of Medicine, Physiology and Biophysics*, 10: 1-17.

Ignatov, Mosin, 2013 – *Ignatov, I., Mosin, O.V.* (2013). Structural Mathematical Models Describing Water Clusters. *Journal of Mathematical Theory and Modeling,* 3 (11): 72-87.

Ignatov et al., 2019 – *Ignatov, I., Toshkova, R., Gluhchev, G., Drossinakis, Ch.* (2019). Results of Blood Serum from Cancer Treated Hamsters with Infrared Thermal Field and Electromagnetic Fields. *Journal of Health, Medicine and Nursing*, 58: 101-112.

Ignatov, 2011 – *Ignatov, I.* (2011). Entropy and Time in Living Organisms. *Euromedica, Hanover*, 60-62.

Ignatov, Mosin, 2013 – *Ignatov I., Mosin O.V.* (2013). Possible Processes for Origin of Life and Living Matter with modeling of Physiological Processes of Bacterium Bacillus Subtilis in Heavy Water as Model System. *Journal of Natural Sciences Research*, 3 (9): 65-76.

Ignatov, Mosin, 2013a – *Ignatov, I., Mosin, O.V.* (2013). Modeling of Possible Processes for Origin of Life and Living Matter in Hot Mineral and Seawater with Deuterium. *Journal of Environment and Earth Science*, 3 (14): 103-118.

Ignatov, Mosin, 2013b – *Ignatov, I., Mosin, O.V.* (2013). Structural Mathematical Models Describing Water Clusters. *Journal of Mathematical Theory and Modeling*, 3 (11): 72-87.

Ignatov et al., 2014 – *Ignatov, I., Mosin, O. V., Velikov, B., Bauer, E. Tyminski, G.* (2014). Longevity Factors and Mountain Water as Factor. Research in Mountain and Fields Areas in Bulgaria. *Civil and Environmental Research*, 30 (4): 51-60.

Tumbarski et al., 2014 – *Tumbarski, T., Valcheva, N. Denkova, Z., Koleva, I.* (2014). Antimicrobial Activity against Some Saprophytic and Pathogenic Microorganisms of Bacillus species Strains Isolated from Natural Sping Waters in Bulgaria. *British Microbiology Research Journal* 4(12): 1353-1369.

Valcheva et al., 2013 – *Valcheva, N., Denkova, Z., Denkova, R.* (2013). Physicochemical and microbiological characteristics of spring waters in Haskovo. *Journal of Food and Packaging Science Technique and Technologies,* № 2: 21-25.

Valcheva et al., 2014 – *Valcheva, N., Denkova, Z., Nikolova, R., Denkova, R.* (2014) Physiological, Biochemical, and Molecular – Genetic Characterization of Bacterial Strains Isolated From Sping and Healing Waters in Region of Haskovo. *Food, Sciense, Engineering and technologiest, Plovdiv, LX*: 940-946.

Valcheva et al., 2013a – *Valcheva, N., Denkova, Z. Nikolova, Denkova, R.* (2013). Physiological – Biochemical and Molecular - Genetic Characteristics of Bacterial Strains Isolated from Spring and Healing Waters in the Haskovo Region, *N.T. at UCT, Volume LX*.

Valcheva et al., 2014 – *Valcheva, N., Denkova, Z., Denkova, R., Nikolova, R.* (2014). Characterization of bacterial strains isolated from a thermal spring in Pavel Banya, Stara Zagora Region, *N.T. at UCT, Volume LXI*.

Valcheva, 2014 – *Valcheva, N.* (2014). The Microflora of Medicinal and Spring Waters in Haskovo and Stara Zagora Region. Dissertation, University of Food Technology, 1: 142.

Valcheva, Ignatov, 2019 – *Valcheva, N., Ignatov, I.* (2019). Physicochemical and Microbiological Characteristics of Thermal Healing Spring Waters in the District of Varna. *Journal of Medicine, Physilogy and Biophysics*, 59: 10-16.

Valcheva, 2019 – *Valcheva, N.* (2014). Physicochemical and Microbiological Characteristics of Thermal Healing Spring Waters in the District of Burgas. *European Reviews of Chemistry,* 2.

Standards

Ordinance №9/2001, Official State Gazette,issue 30.

Decree № 178/23.07.2004 about the quality of water, intended for drinking purposes.

BDS8451: 1977 – defining of colour according to Rublyovska Scale, determination of smell at 20 °C.

EN ISO 7027 –determination of turbidity.

BDS3424: 1981 – determination ofpH.

BDS3413: 1981 –determination of oxidisability.

BDS3414: 1980 –determination of chlorides.

BDS ISO 6058 – determination of calcium, determination of general hardness.

BDS EN 27888 – determination of electrical conductivity.

VLM – NH_4 – № 1 –determination of ammonium ions.

VLM –NO_3 – № 2 –determination of nitrates.

VLM – NO_2 – № 3 – determination of nitrites.

VLM– SO_4 – № 4 –determination of sulphates.

VLM– PO_4 – № 5 – determination of phosphates.

VLM– Fe – № 6 – determination of iron.

VLM–Mn– № 7 – determination of manganese.

VLM– F – № 8 – determination of fluorides.

BDS 7211: 1982 – determination of magnesium.

BDSEN ISO 7899 – 2 –determination of nitrates.

BDSEN ISO 9308 – 1: 2004 – determination of*Escherichia coli*andcoliformbacteria.

BDSEN26461 – 2: 2004 – determination of sulphite reducing anaerobic bacteria*(Clostridiumperfringens)*.

BDSEN ISO 16266 – determination of*Pseudomonas aeruginosa*.

BDSEN ISO 7899 – 2 – determination of eneterococci.

BDS EN ISO 6222: 2002 – determination of total number of aerobic and facultative anaerobic bacteria.

Published in the Slovak Republic
European Journal of Medicine
Has been issued since 2013.
E-ISSN: 2310-3434
2019, 7(2): 131-135

DOI: 10.13187/ejm.2019.2.131
www.ejournal5.com

Sensitive Periods in the Ontogenesis of a Person

Yuri M. Kabanov [a], Dina A. Venskovich [a, *], Vladimir V. Trushchenko [a], Nikolai T. Stanski [a], Valentina A. Koloshkina [a], Inna M. Dudareva [a]

[a] Vitebsk State University named after P.M. Masherov, Belarus

Abstract

The article considers issues related to the development of motor abilities of a person in the process of ontogenesis. The author presents the analysis of the manifestation of sensitive (critical) periods in the development of motor abilities of individuals of different sex and age, which makes it possible to develop certain functions of the organism of a person purposefully and efficiently as well as to form stable motor skills. The article considers age and sex transformations of morphological characteristics: total body measurements, body mass, chest size and lungs volume as well as sex differentiations in the manifestation of sensitive periods. Dynamics of the quantity of the manifestation of sensitive periods in the development of motor abilities of both males and females within the range of 2 to 22 years old is studied. Motor abilities, which must be developed at every age period, are listed.

Keywords: motor abilities, age dynamics, sensitive (critical) periods.

1. Introduction

While considering the issue of age-related changes in the development of motor abilities, the following most important points should be noted. In a number of experimental studies (Alabyshev, 1980, Balsevich, 2000, Balsevich, 1996, Volkov, 1984) it was established that in the process of growth and development of the human body, there are special periods of its increased sensitivity to environmental influences. During these periods certain functions effectively develop and motor skills are forming. Such sensitive periods in the development of an individual in the process of ontogenesis are called “critical” or sensitive (Balsevich, 2000). During these periods, the body is much better adapted to the action of negative environmental factors, which is associated with its increased sensitivity to external influences. Knowing the limits of the “critical periods” and the optimal dose of exposure, one can purposefully control the individual program of a person’s physical development by identifying the leading factors of development for each stage of ontogenesis (Volkov, 1984).

The purpose of the work is to study the age dynamics in the number of manifestations of sensitive, or "critical", periods in the range from 2 to 22 years for both sexes based on the analysis of a generalized material of research on the age characteristics of the development of human motor abilities.

* Corresponding author
E-mail addresses: Venskovich.Dina@mail.ru (D.A. Venskovich), koloshkinava@mail.ru (V.A. Koloshkina)

2. Methods and organization of research

The authors for the first time carried out an analytical analysis of research materials (Alabyshev, 1980, Balsevich, 2000, Balsevich, 1996, Volkov, 1984, Guzhalovskiy, 1978, Guzhalovskiy, 1984, Gladysheva, 1976, Balsevich, 2000, Balsevich, 1996,Volkov, 1984, Guzhalovskiy, 1978, Guzhalovskiy, 1984) by belarusian and russian scientists in the field of theory and methods of physical culture, with the result that a new interpretation of data on issues related to the manifestations of sensitive periods in the development of human motor abilities was obtained.

3. Results and its discussion

Analysis of the dynamics of manifestation of sensitive periods for a person (pic.) of two, three years of sensitive periods for both sexes are synchronized. At this age, develop speed-power abilities, coordination of moving during movement and running, the ability to maintain body balance, flexibility and also a person gains weight.

At the age of 4, both boys and girls have the fast improvement of jogging abilities, static strength, general endurance, general coordination, coordination while running and throwing an object. There are changes in morphological characteristics: the circumference of the chest. At this age, gender differences appear in the manifestation of sensitive periods. In addition to these, boys have growth of overall strength, general and static endurance.

At the age of 5, all these children have different indicators of speed and flexibility, development of strength, spatial and temporal differentiation. As at the age of 4 boys have the growth of total strength, as well as dynamic strength.

At the age of 6, girls and boys continue to have fast growth of speed, dynamic and general characteristics, spatial and temporal characteristics. Boys have the improvement of dynamic strength; girls have the improvement of coordination during run-up in long jumps. From 6 to 9 years, there is a growth in the chest cells.

The seven-year age is the beginning of a fast rise in the increase in the number of sensitive periods in the development of motor abilities for girls and boys, besides girls exceeds the indicators of boys (10 to 6). This dynamic continues up to 11 years for girls and 12 years for boys, the beginning of periods when a marked reduction in the number of sensitive periods in the development of motor abilities for both sexes begins. For seven-years-old girls there is an increase in coordination indices is observed during the run-up in long jumps and height while throwing the ball, rhythm of movements, balance, flexibility. Synchronous increase of indicators for boys and girls occurs with the development of various types of speed, frequency of movements, coordination while running. In addition, the boys in the period from 7 to 11 years have an accelerated growth of coordination abilities in such a specific form of athletics as a hurdle race.

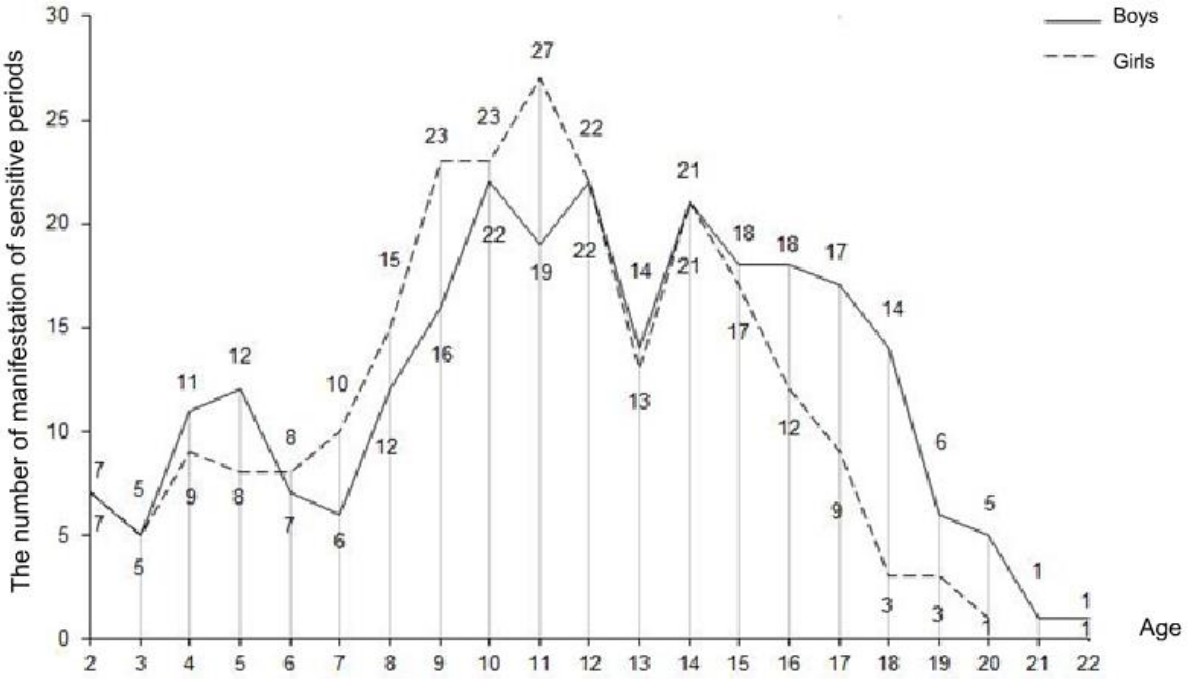

Fig. 1. The dynamics of the manifestations of sensitive periods in the development of motor abilities in individuals of different sexes and age

The period of 8 years old for girls is characterized by an increase in the indices of speed, static endurance, coordination during a run-up in long and high jumps, a rhythm of movements, coordination while throwing the ball, and the development of spatial and temporal differentiations. Boys have growth of speed-power indicators. Both girls and boys have growth of speed in the frequency of movements, the latent period of the motor response, general and coordination while running, rhythm of movements, body balance, flexibility, control of the duration of muscle tension.

At the age of 9, sensitive periods for girls are observed in terms of speed in the speed of a movement, total strength, endurance, manifested in static and dynamic modes, coordination while jumping and throwing, body weight increases. Boys develop coordination in gymnastic and acrobatic exercises, improve performance in swimming and hurdle race. The representatives of both sexes have growth of various types of speed, indicators of frequency of movements, speed-power abilities, general endurance, general coordination of running, rhythm of movements and body balance, control of the duration of muscular tension, spatial and temporal differentiation, flexibility; also increases the circumference of the chest.

At the age of 10, girls experience an increase of speed (movement frequency), endurance of static and dynamic modes, coordination of jumps and throws, coordination abilities, lung volume increases; boys experience endurance indicators in a zone of high intensity, coordination while a run-up in long jumps, gymnastic and acrobatic exercises, swimming, cycling, football, hurdle race, rhythm of movements, spatial and temporal differentiation. Both girls and boys have indicators of different types of speed, speed of a movement, latent time of motor reaction, speed-strength abilities, general endurance, coordination in running, balance, accuracy of movements, flexibility, duration of muscle stresses; increases the circumference of the chest.

At the age of 11, girls have the number of manifestations of sensitive periods reaches the highest value (27), after which they decrease until the age of 13. Moreover, for girls this process is clearly pronounced due to the processes of puberty, which is typical during these age periods. For boys from 10 to 12 years, there is a wavy dynamic in the quantitative manifestation of sensitive periods, but it is weakly expressed.

Thus, for girls of 11 years old, there are sensitive periods in terms of speed in the frequency of movements, endurance of static and dynamic (in the submaximal intensity zone) modes, coordination of jumping and throwing, swimming, coordination abilities of general, flexibility; total body size increases; for boys these sensitive periods are expressed in terms of speeds manifested in different types and in speed of a movement, coordination during a run-up in long jumps, while

throwing the ball into the basket, cycling and football; for both sexes it is expressed in terms of speed in the latent time of the motor response, total strength, speed-strength abilities, total endurance and endurance, manifested in a dynamic mode in areas of moderate and high intensity, coordination while running, balance and accuracy of movements; there is an increase of body weight, chest circumference, lung volume.

At the age of 12, sensitive periods in the development of motor abilities of girls are observed in terms of endurance in a static mode, coordination during run-up in long jumps and throwing the ball, rhythm of movements, and body balance; this period for boys is characterized by developing of indicators of speed in the frequency of movements and latent time of the motor reaction, coordination in acrobatic jumps and throwing the ball into the basket, cycling, football; for both boys and girls it is expressed in developing of terms of overall strength and endurance, speed-strength abilities, endurance in a dynamic mode in areas of high and submaximal intensity, coordination while running, swimming, spatial orientation, flexibility; also lung volume increases.

At the age of thirteen, girls experience an increase in indicators of speed, rhythm of movements, body balance, increasing muscle mass; there is a development of indicators of speed in the frequency of movements, general strength, speed-strength abilities, coordination while cycling, football, general coordination for boys; they also have increase of lung volume as girls. Both boys and girls have development of indicators of overall strength, speed-strength abilities, general endurance and endurance, manifested in a dynamic mode, coordination while running, swimming, flexibility; body weight increases.

Girls and boys from 12 to 14 years have the same number of manifestations of sensitive periods in the development of motor abilities. From 13 to 14 years, both girls and boys have another increase (peak of rise) in the number of sensitive periods in the development of motor abilities. Moreover, from the age of 15, this number for boys begins to exceed girl's indicators. This dynamic will persist throughout subsequent age periods (up to 22 years). From the age of 14, a gradual decrease in the number of sensitive periods for both sexes starts.

At the age of 14, sensitive periods for girls are observed in terms of speed in the frequency of movements, endurance in the zone of maximum intensity, coordination during a run-up in long jumps and jumps with a change in direction of movement, swimming, rhythm of movements, coordination abilities; an increase of total body size and muscle mass occurs. For young men this period is characterized by increasing of different types of speed, dynamic endurance in zones of moderate and submaximal intensity, coordination of acrobatic jumps and while throwing the ball into the basket, cycling, football, and body balance; lung volume increases. Boys and girls have increase of of overall strength, speed-strength abilities, general endurance and endurance of a dynamic mode in a zone of high intensity, coordination during a run-up in long jumps, while throwing the ball, spatial orientation, flexibility; increases the circumference of the chest.

At the age of 15, girls experience an increase in speed indicators in the frequency of movements, endurance, manifested in areas of high and maximum intensity, coordination during a run-up in long jumps and jumps with a change in direction of movement, complex coordination, accuracy of movements; total body size and muscle mass increase. Young men experience increase of different types of speed, speed of a movement, coordination while acrobatic jumps, while throwing the ball and throwing the ball into the basket, swimming and soccer, balance; body weight increases. Both boys and girls have increase of overall strength, speed-strength abilities, general endurance and endurance in static and dynamic modes, coordination during a run-up in jumps, spatial orientation, flexibility; increases the circumference of the chest.

At the age of 16, girls at an accelerated pace have observed an increase in the indices of endurance, manifested in a static mode and in zones of large, submaximal and maximum intensity, coordination during exercises with changing direction of movement, complex coordination, accuracy of movements; for young men there are indicators of speed in different types and speeds of a movement, general endurance and endurance, manifested in a dynamic mode, coordination while running and a run-up in jumps, acrobatic jumps, while throwing the ball and throwing the ball into the basket, swimming, general coordination; total body size and muscle mass increase; girls and boys have indicators of overall strength and speed-strength abilities, spatial orientation, flexibility; increases the circumference of the chest.

At age 17, girls have sensitive periods in the development of motor abilities in terms of endurance in areas of high and submaximal intensity, coordination while a run-up in long jumps

and jumps with a change in direction of movement, flexibility; for young men this period is characterized by speed improvement of movement while swimming, speed-strength abilities, endurance in the zone of moderate intensity, coordination during the run-up in jumps, acrobatic jumps and while throwing the ball, complex coordination, balance, accuracy of movements, spatial orientation; total body size and muscle mass increase; boys and girls experience development of overall strength, endurance in a static mode and a zone of maximum intensity.

At the age of 18, girls improve coordination wile a run-up in long jumps; boys have an increase in strength, manifested in swimming, endurance in static and dynamic modes, as well as in the zone of moderate, large, submaximal and maximum intensity, complex coordination, accuracy of movements; total body size, chest circumference, muscle mass increase; girls and boys have indicators of total strength.

At age of 19, girls experience gains in speed-power abilities; young men have indicators of endurance in all zones of intensity; both boys and girls experience development of coordination while running, general coordination. At 20, young men have indicators of endurance in a dynamic mode and in areas of high and submaximal intensity, coordination in acrobatic jumps, both boys and girls have improvement of overall coordination. At the age of 21, young men experience development of coordination of acrobatic jumps, at 22, young men and woman have improvement of their speed-strength abilities.

4. Conclusion

The dynamics of manifestations of sensitive periods in the development of motor abilities shows that at the age of 2 and 3 sensitive periods for both sexes is synchronized not only by quantitative indicators, but also by morphofunctional characteristics. From the age of 4, sexual morphofunctional differences appear in the manifestation of sensitive periods. The age of 7 is the beginning of an increase in the number of sensitive periods in the development of motor abilities for girls and boys, and this number for girls exceeds the boy's indicators, and this dynamic continues up to 11 years for girls and 12 years for boys, the beginning of decline the number of sensitive periods for both sexes. The age of 11 for girls is characterized by reaching a maximum value in number of manifestations of sensitive periods, after which they are markedly reduced to 13 years, which may be due to the processes of puberty. For boys from 10 to 12 years, there is a wavy dynamic in the quantitative manifestation of sensitive periods, but it is weakly expressed. In the period from 12 to 14 years, both sexes have the same number of manifestations of sensitive periods. From 13 to 14 years, girls and boys have another increase in this number. Moreover, from the age of 15 these indicators for boys begin to exceed girl's indicators. From the age of 14, a gradual decrease in the number of sensitive periods for both sexes starts. This dynamic will persist throughout subsequent age periods up to 22 years.

References

Alabyshev, 1980 – *Alabyshev, A.P.* (1980). Dynamics of morphofunctionalparameters of boy – gymnasium students aged 7-12. Ways of managing technical training of athletes, Omsk, 3-5.

Balsevich, 1996 – *Balsevich, V.K.* (1996). Enhancing of physical development of children aged 4-5. Physical culture: education, teaching, training, Moscow,5-6.

Balsevich, 2000 – *Balsevich, V.K.* (2000). Human ontokinesiology. Theory and practice of physical culture, 275.

Gladysheva, 1976 – *Gladysheva, A.A.* (1976). Age-related changes of somatometricindicators of young sportsmen. Problems of physical education, Moscow, 104.

Guzhalovskiy, 1978 – *Guzhalovskiy, A.A.* (1978). Development of motor skills of school children, Minsk, 88.

Guzhalovskiy, 1984 – *Guzhalovskiy, A.A.* (1984). The problem of «critical» periods of onto Genesis in its meaning for theory and practice of physical education. Essays on the theory of physical culture, Moscow, 211-224.

Karpeev, 1998 – *Karpeev, A.G.* (1998). Human motor coordination in sports exercise of ballistic type, Omsk, 322.

Kravchuk, 1980 – *Kravchuk, A.I.* (1980). Study of the ability of children aged 4-7 to control their movements taking into account their age, gender and motor preparedness. Ways of managing technical training of athletes, Omsk, 14-15.

Matveev, Nepopalov, 1995 – *Matveev, L.P., Nepopalov, V.N.* (1995). Physical culture: physical culture and human development. Theory and practice of physical culture, 2-5.

Popova, 1997 – *Popova, E.V.* (1997). Diagnostics of ballistic speed and power coordination abilities of girls aged 7-17: autoabstract dis. of candidate of pedagogical: 13.00.04, Saint-Petersburg, 16.

Salnikova, 1969 – *Salnikova, G.P.* (1969). Physical development of children and adolescents. Fundamentals of morphology and physiology of children and adolescents, Moscow, 554-570.

Volkov, 1984 – *Volkov, L.V.* (1984). The system of directed development of physical abilities in different age periods: autoabstractdis. Of Dr. Of pedagogical science: 13. 00. 04, Moscow, 40.